ΕΘΝΙΚΟ ΚΑΙ ΚΑΠΟΔΙΣΤΡΙΑΚΟ ΠΑΝΕΠΙΣΤΗΜΙΟ ΑΘΗΝΩΝ

ΣΧΟΛΗ ΘΕΤΙΚΩΝ ΕΠΙΣΤΗΜΩΝ

Δ.Π.Μ.Σ ΩΚΕΑΝΟΓΡΑΦΙΑ ΚΑΙ ΔΙΑΧΕΙΡΙΣΗ ΘΑΛΑΣΣΙΟΥ ΠΕΡΙΒΑΛΛΟΝΤΟΣ

ΜΕΤΑΠΤΥΧΙΑΚΗ ΕΡΓΑΣΙΑ ΕΙΔΙΚΕΥΣΗΣ

"THE WATER BUDGET OF MEDITERRANEAN AND BLACK SEAS ON A SCALE OF MAJOR AND SECONDARY MARINE REGIONS"

ΑΘΑΝΑΣΙΟΣ ΕΥΓΕΝΙΚΟΣ

ΑΜ: 215020

ΑΘΗΝΑ 2020

ΕΘΝΙΚΟ ΚΑΙ ΚΑΠΟΔΙΣΤΡΙΑΚΟ ΠΑΝΕΠΙΣΤΗΜΙΟ ΑΘΗΝΩΝ

ΣΧΟΛΗ ΘΕΤΙΚΩΝ ΕΠΙΣΤΗΜΩΝ

Δ.Π.Μ.Σ ΩΚΕΑΝΟΓΡΑΦΙΑ ΚΑΙ ΔΙΑΧΕΙΡΙΣΗ ΘΑΛΑΣΣΙΟΥ ΠΕΡΙΒΑΛΛΟΝΤΟΣ

ΜΕΤΑΠΤΥΧΙΑΚΗ ΕΡΓΑΣΙΑ ΕΙΔΙΚΕΥΣΗΣ

"ΤΟ ΥΔΡΟΛΟΓΙΚΟ ΙΣΟΖΥΓΙΟ ΤΗΣ ΜΕΣΟΓΕΙΟΥ ΚΑΙ ΤΗΣ ΜΑΥΡΗΣ ΘΑΛΑΣΣΑΣ ΣΕ ΚΛΙΜΑΚΑ ΚΥΡΙΩΝ ΚΑΙ ΔΕΥΤΕΡΕΥΟΥΣΩΝ ΛΕΚΑΝΩΝ"

"THE WATER BUDGET OF MEDITERRANEAN AND BLACK SEAS ON A SCALE OF MAJOR AND SECONDARY MARINE REGIONS"

ΑΘΑΝΑΣΙΟΣ ΕΥΓΕΝΙΚΟΣ

ΑΜ: 215020

Τριμελής Επιβλέπουσα Επιτροπή:

ΧΑΤΖΑΚΗ ΜΑΡΙΑ, ΕΠΙΚΟΥΡΗ ΚΑΘΗΓΗΤΡΙΑ (Επιβλέπουσα)

ΠΟΥΛΟΣ ΣΕΡΑΦΕΙΜ, ΚΑΘΗΓΗΤΗΣ

ΣΟΦΙΑΝΟΣ ΣΑΡΑΝΤΗΣ, ΕΠΙΚΟΥΡΟΣ ΚΑΘΗΓΗΤΗΣ

ΑΘΗΝΑ 2020

ΠΡΟΛΟΓΟΣ

Η παρούσα διπλωματική εργασία με τίτλο: «Το Υδρολογικό Ισοζύγιο της Μεσογείου και της Μαύρης Θάλασσας σε κλίμακα κύριων και δευτερεύουσων λεκανών» εκπονήθηκε στο πλαίσιο του Διιδρυματικού Μεταπτυχιακού Προγράμματος Σπουδών (ΔΠΜΣ) «Ωκεανογραφία και Διαχείριση Θαλάσσιου Περιβάλλοντος» της Σχολής Θετικών Επιστημών του Εθνικού και Καποδιστριακού Πανεπιστημίου Αθηνών (ΕΚΠΑ). Τα μέλη της τριμελούς συμβουλευτικής/εξεταστικής επιτροπής είναι: η Επίκουρη Καθηγήτρια Χατζάκη Μαρία ως Επιβλέπουσα, ο Καθηγητής Πούλος Σεραφείμ και ο Επίκουρος Καθηγητής Σοφιανός Σαράντης.

ΕΥΧΑΡΙΣΤΙΕΣ

Με την ολοκλήρωση της παρούσας μεταπτυχιακής διπλωματικής εργασίας μου, θα ήθελα να εκφράσω τις θερμές ευχαριστίες μου στην επιβλέπουσα Επίκουρη Καθηγήτρια κα. Χατζάκη Μαρία για την καθοδήγηση της, τη συμβολή της στη συλλογή, διάθεση και επεξεργασία του μεγάλου όγκου των κλιματολογικών δεδομένων, τις εποικοδομητικές υποδείξεις της και για τη συνολική της βοήθεια.

Θα ήθελα να ευχαριστήσω τον Καθηγητή κ. Πούλο Σεραφείμ για την εμπιστοσύνη και τη συμπαράσταση που μου έδειξε εξαρχής, το αμείωτο ενδιαφέρον του καθώς και για τη συμβολή του στη διάθεση και επεξεργασία των δεδομένων της Ποτάμιας Απορροής και των Υποθαλάσσιων Υπογείων Υδάτων.

Να ευχαριστήσω συγχρόνως τον Επίκουρο Καθηγητή κ. Σοφιανό Σαράντη για την υποστήριξή του, τη συνολική καθοδήγηση του και για τις γνώσεις που αποκόμισα καθ' όλη τη διάρκεια των σπουδών μου στον τομέα της Φυσικής Ωκεανογραφίας.

Θα ήθελα επίσης να ευχαριστήσω τον κ. Κοτίνα Βασίλειο για τη βοήθεια του στην ανάλυση και επεξεργασία των κλιματολογικών δεδομένων.

Τέλος, θα ήθελα να εκφράσω την απόλυτη ευγνωμοσύνη μου στην οικογένεια μου για την ηθική υποστήριξη, συμπαράσταση και κατανόηση κατά τη διάρκεια των σπουδών μου.

ABSTRACT

The Water Budget of the Mediterranean and Black Sea system (MBS) and its 11 sub-basins during the period 1979-2018 has been studied and presented using recent atmospheric ECMWF's reanalysis datasets of Evaporation (E) and Precipitation (P) along with quantitative assessments of Riverine Discharge (RD) and Submarine Groundwater Discharge (SGD). The analysis focused on climatology and inter-monthly to inter-annual variability. Due to uncertainties, sparse spatial-temporal resolution and lack of in-situ available data of RD and SGD, the compatible approach was to apply the Water Budget Equation for studying the variabilities of the MBS water budget. The analysis of all Water Budget Equation components from various data sets showed that the intense Evaporation, which exceeds the sum of Precipitation, RD and SGD in the Mediterranean and Black Sea system, clearly causes an annual Water Budget deficit in the MBS over the period from 1979 to 2018. In the sub-basins of Alboran (ALB), CentralMED (CEN), WestMED (WEST), Tyrrhenian (TYR), Levantine (LEV), Aegean (AEG), Ionian (ION), the results of Water Budget Equation indicate a water deficit. As for the Adriatic (ADR), Marmara (MAR), Black Sea (BLA) and Azov (AZO) sub-basins of MBS, the results of Water Budget Equation indicate a water surplus. The Total Water Budget of Black Sea System, Marmara and Adriatic sub-basins is positive, while for the remaining sub-basins, the Total Water Budget is negative. Combined together, the Total Water Budget for the Mediterranean and Black Sea System (MBS) is negative, with the Black Sea not being able to countercheck the excessive water loss of Mediterranean Sea, characterizing it as an Evaporation (concentration) basin. On inter-monthly to inter-annual timescales, the Atlantic water influx through the Strait of Gibraltar adjusts to counterbalance the enhanced MBS water budget deficit, playing a major role in the Mediterranean Sea circulation.

Keywords: Water Cycle, Mediterranean Sea, Black Sea, Sub-basins, Evaporation, Precipitation, Riverine Discharge, Submarine Groundwater Discharge, ECMWF ERA5, Total Water Budget.

ΠΕΡΙΛΗΨΗ

Το Υδρολογικό Ισοζύγιο του συστήματος της Μεσογείου και της Μαύρης Θάλασσας, καθώς και των 11 επιμέρους υπο-λεκανών του κατά την περίοδο 1979-2018 μελετήθηκε και παρουσιάστηκε, χρησιμοποιώντας πρόσφατα δεδομένα ατμοσφαιρικής επανανάλυσης της Εξάτμισης και της Βροχόπτωσης από το Ευρωπαϊκό Κέντρο Μεσοπρόθεσμων Προγνώσεων μαζί με ποσοτικές εκτιμήσεις της Ποτάμιας Απορροής και των Υποθαλάσσιων Υπογείων Υδάτων. Η ανάλυση επικεντρώθηκε στην κλιματολογία και στις ενδοετήσιες και υπερετήσιες διακυμάνσεις. Λόγω των αβεβαιοτήτων, της σποραδικής χωροχρονικής ανάλυσης και της έλλειψης διαθέσιμων επιτόπιων δεδομένων της Ποτάμιας Απορροής και των Υποθαλάσσιων Υπογείων Υδάτων, η συμβατή προσέγγιση ήταν η εφαρμογή της Εξίσωσης Υδάτινου Ισοζυγίου για τη μελέτη των διακυμάνσεων του υδρολογικού ισοζυγίου του συστήματος. Η ανάλυση όλων των συνιστωσών της Εξίσωσης Υδάτινου Ισοζυγίου από διάφορα σύνολα δεδομένων έδειξε ότι η τόσο έντονη Εξάτμιση, αφού ξεπερνάει ακόμα και την Βροχόπτωση, την Ποτάμια Απορροή και τα Υποβρύχια Υπόγεια Ύδατα όλα προστιθέμενα μαζί, προκαλεί ξεκάθαρα ένα ετήσιο έλλειμμα στο Υδρολογικό Ισοζύγιο του συστήματος της Μεσογείου και της Μαύρης Θάλασσας. Στις επιμέρους λεκάνες των ALB, CEN, WEST, TYR, LEV, AEG, ION, τα αποτελέσματα της Εξίσωσης Υδάτινου Ισοζυγίου δείχνουν έλλειμμα νερού. Όσον αφορά τις υπολεκάνες ADR, MAR, BLA και AZO του συστήματος, τα αποτελέσματα της Εξίσωσης Υδάτινου Ισοζυγίου δείχνουν πλεόνασμα νερού. Επομένως, το Συνολικό Υδρολογικό Ισοζύγιο του συστήματος της Μαύρης Θάλασσας, των υπολεκανών του Μαρμαρά και της Αδριατικής είναι θετικό, ενώ ως προς τις υπόλοιπες υπολεκάνες, το Συνολικό Υδρολογικό Ισοζύγιο είναι αρνητικό. Το Συνολικό Υδρολογικό Ισοζύγιο του συστήματος της Μεσογείου και της Μαύρης Θάλασσας (MBS) είναι αρνητικό, καθώς η Μαύρη Θάλασσα δεν είναι σε θέση να αντισταθμίσει την υπερβολική απώλεια νερού της Μεσογείου Θάλασσας, χαρακτηρίζοντάς τη Μεσόγειο ως λεκάνη εξάτμισης (συγκέντρωσης). Σε ενδοετήσιες και υπερετήσιες χρονικές κλίμακες, η εισροή του Ατλαντικού νερού μέσω του στενού του Γιβραλτάρ προσαρμόζεται για να αντισταθμίσει το ενισχυμένο έλλειμμα του Υδρολογικού Ισοζυγίου του συστήματος, παίζοντας σημαντικό ρόλο στην κυκλοφορία της Μεσογείου.

Λέξεις κλειδιά: Υδρολογικός Κύκλος, Μεσόγειος Θάλασσα, Μαύρη Θάλασσα, Υπολεκάνες, Εξάτμιση, Βροχόπτωση, Ποτάμια Απορροή, Υποθαλάσσια Υπόγεια Ύδατα, Ευρωπαϊκό Κέντρο Μεσοπρόθεσμων Προγνώσεων ERA5, Συνολικό Υδρολογικό Ισοζύγιο.

PREFACE

In this dissertation, we study the water cycle in the sensitive Mediterranean region and the Mediterranean and Black Sea water budget focusing on climatology and inter-monthly to inter-annual variability, exploiting recent progress in data availability. We use 40-yr European Centre for Medium-Range Weather Forecasts (ECMWF) Re-Analysis ("ECMWF ReAnalysis 5th generation" i.e. ERA5) datasets of Evaporation (E) and Precipitation (P), in conjunction with quantitative datasets of Riverine Discharge (RD) and Submarine Groundwater Discharge (SGD), to focus on the Mediterranean and Black Sea regions and their sub-basins. The approach will be based on the application of the water budget equation in Mediterranean and Black Sea System and their sub-basins.

A longstanding challenge is to provide a reliable estimate of the annual mean of the Mediterranean and Black Sea water budget. A goal for our research is to put together a much more integrated and complete picture of all of the water budget of the different marine regions of the Mediterranean and Black Sea marine system (MBMS), exploiting many different datasets and trying to take advantage of their merits, while overcoming their deficiencies.

This study is organized as follows: In chapter 1, the theoretical background is presented synoptically; in chapter 2, the geography, climatology, hydrology and circulation of Mediterranean Sea and Black Sea is given; while in section 2.4. an estimate of the current and future evolution of the different components of the MBS's water budget; in chapter 3, the different datasets and the applicable methodology is described; in chapter 4, the results and their discussion are given, with the analyses of precipitation, evaporation, riverine discharge and submarine groundwater discharge in section 4.1. while in section 4.2., the total water budget of each sub-basin and the total water budget of Mediterranean and Black Sea System (MBS) are analyzed in sub-sections 4.2.1 and 4.2.2 respectively. Finally, in chapter 5, a synthesis and the concluding remarks are provided.

CONTENTS

CHAPTER 1 : THEORETICAL BACKGROUND

1.1. WATER CYCLE

Earth's water is always in motion, and the natural water cycle, also known as the hydrologic cycle, describes the existence and continuous movement of water on, above, and below the surface of the Earth. Earth's water is always in movement and is always changing states between liquid, vapor, and ice, with these processes happening in the blink of an eye. The water cycle has been working for billions of years and all life on Earth depends on its continuing work. Earth would be a pretty stale place without it.

Ancient, earliest Earth was an incandescent globe made of magma, but all magmas contain water. Water set free by magma began to cool down the Earth's atmosphere and eventually, the environment became cool enough so water could stay on the surface as a liquid. Volcanic activity kept and still keeps introducing water into the atmosphere, thus, increasing the surface-water and groundwater volume of the Earth.

The United States Geological Survey (U.S.G.S) defined 16 components of the Water Cycle (considering the ocean as a starting point): 1) Atmosphere, 2) Condensation, 3) Evaporation, 4) Evapotranspiration, 5) Freshwater lakes and rivers, 6) Groundwater flow, 7) Groundwater storage, 8) Ice and snow, 9) Infiltration, 10) Oceans, 11) Precipitation, 12) Snowmelt, 13) Springs, 14) Streamflow, 15) Sublimation and 16) Surface runoff (Figure 1.1).

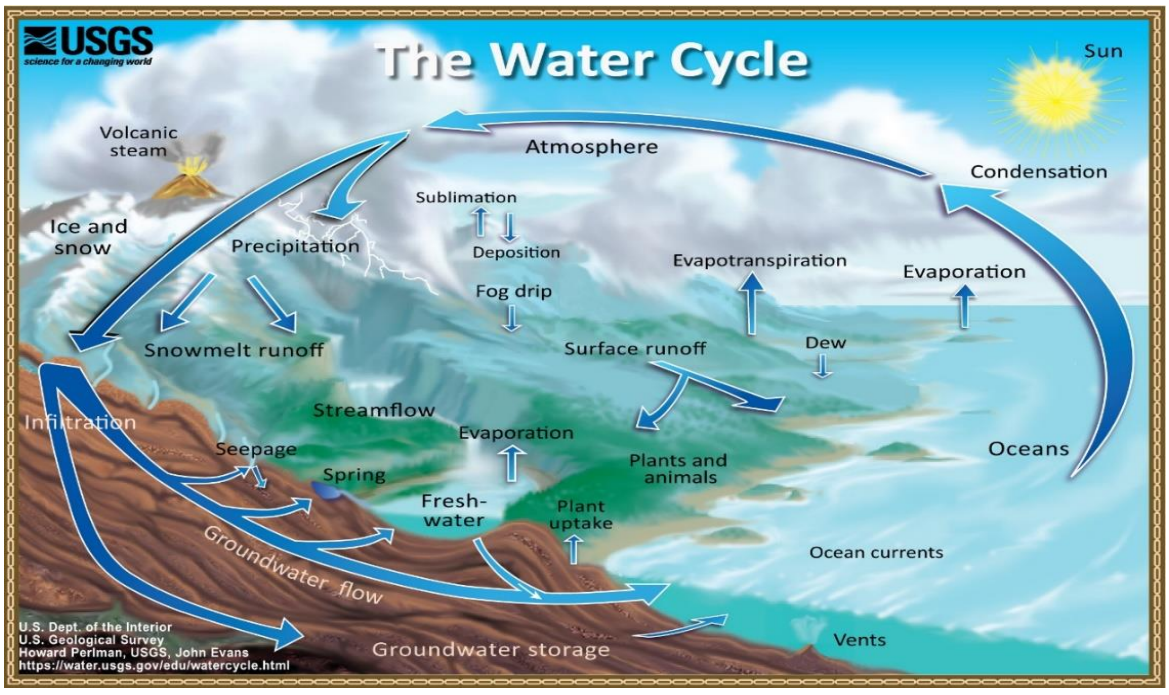

Figure 1.1. Natural water cycle (Howard Perlman; USGS and John Evans; USGS).

The water cycle has no real starting point. The starting point can be considered the oceans, since that is where most of Earth's water exists. The Sun, which drives the water cycle, heats water in the oceans. Some of it evaporates as vapor into the air. Ice and snow can sublimate directly into water vapor. Rising air currents take the vapor up into the atmosphere, along with water from evapotranspiration, which is water transpired from plants and evaporated from the soil. The vapor rises into the air where cooler temperatures cause it to condense into clouds. Air currents move clouds around the globe, cloud particles collide, grow, and fall out of the sky as precipitation. Some precipitation falls as snow and can accumulate as ice caps and glaciers, which can store frozen water for thousands of years. Snow packs in warmer climates often thaw and melt when spring arrives, and the melted water flows overland as snowmelt.

Most precipitation falls back into the oceans or onto land, where, due to gravity, the precipitation flows over the ground as surface runoff. A portion of runoff enters rivers in valleys in the landscape, with streamflow moving water towards the oceans. Runoff, and groundwater seepage, accumulate and are stored as freshwater in lakes. Not all runoff flows into rivers, though. Much of it soaks into the ground as infiltration. Some water infiltrates deep into the ground and replenishes aquifers (saturated subsurface rock), which store huge amounts of freshwater for long time periods. Some infiltration stays close to the land surface and can seep back into surface-water bodies (and the ocean) as groundwater discharge, and some groundwater finds openings in the land surface and emerges as freshwater springs. Over time, though, all of this water keeps moving, some to re-enter the ocean, where the water cycle restarts.

Over 96% of the world's total water supply of about 1,386 million km^3 of water, is saline. Over 68% of the total freshwater is locked up in ice and glaciers. Another 30% of freshwater is in the ground. Fresh surface water sources, such as rivers and lakes, only constitute about 93,100 km^3, which is about 0.007% of total water. Yet, rivers and lakes are the sources of most of the water people use every day (Figure 1.2).

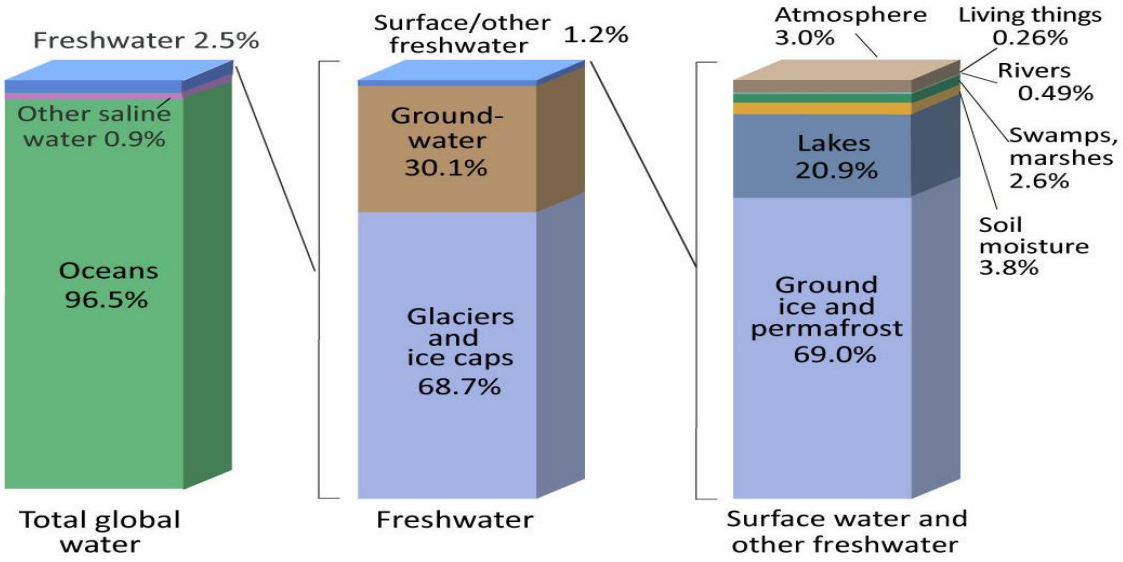

Figure 1.2. Estimated presence of Earth's water at a single point in time (Shiklomanov 1993).

1.2. WATER CYCLE AND CLIMATE CHANGE EFFECTS

Driven mainly by solar heating, water is evaporated from ocean and land surfaces, transported by winds, and condensed to form clouds and precipitation that falls to land and oceans. Precipitation over land may be stored temporarily as snow or soil moisture, while excess rainfall runs off and forms streams and rivers, which discharge the freshwater into the oceans, thereby completing the global water cycle (Figure 1.3). Associated with this water cycle, energy, salt within the oceans, and nutrients and minerals over land are all transported and redistributed within the earth climate system (Chahine 1992; Schlesinger 1997). Thus, water plays a crucial role in earth's climate and environment.

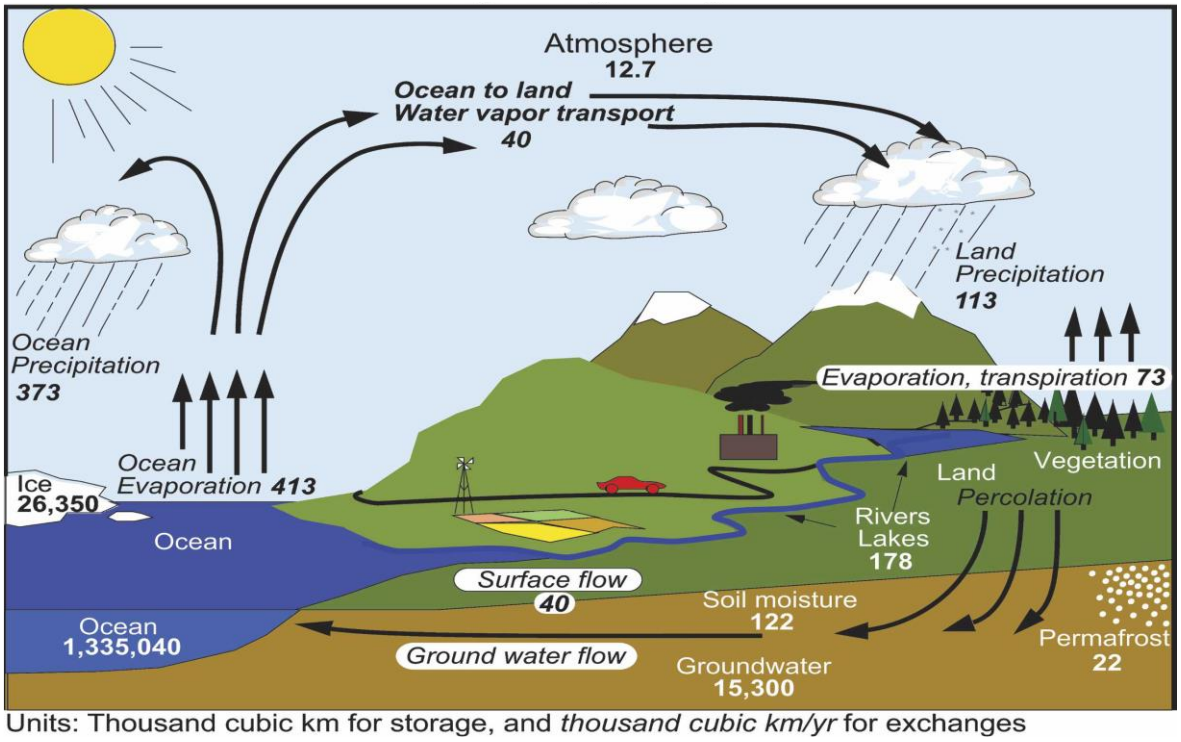

Figure 1.3. The hydrological cycle. Estimates of the main water reservoirs, given in plain font in 10^3 km^3/year, and the flow of moisture through the system, given in slant font (10^3 km^3/year) (Trenberth et al. 2006).

Water vapor is the dominant greenhouse gas (Kiehl and Trenberth 1997) and is responsible for the dominant feedback in the climate system (Karl and Trenberth 2003). However, it also provides the main resource for clouds and storms to produce precipitation, and most precipitation comes from moisture already in the atmosphere at the time a storm forms (Trenberth 1998, 1999; Trenberth et al. 2003). Hence, as global warming progresses, temperatures in the troposphere increase (Karl and Trenberth 2003) along with the water-holding capacity (governed by the Clausius–Clapeyron equation), and so do actual water vapor amounts (Trenberth et al. 2005; Soden et al. 2005). The strong relationships with sea surface temperatures (SSTs) allow estimates of column water vapor amounts since 1970 to

be made and results indicate increases of about 4% over the global oceans, suggesting that water vapor feedback has led to a radiative effect of about 1.5 W m^{-2} (Fasullo and Sun 2001), comparable to the radiative forcing of carbon dioxide increases (Houghton et al. 2001). This provides direct evidence for strong water vapor feedback in climate change.

The observed increase in atmospheric moisture in turn increases moisture convergence into storms (given the same low-level atmospheric convergence), and, thus, increases intensity of precipitation, as observed (Trenberth 1998; Trenberth et al. 2003), while frequency and duration are apt to decrease, exacerbating drought. This comes about because the total precipitation amount is constrained by the available surface energy and how much goes into evaporation. Hence, enhanced intensity implies reduced frequency or duration if the amount is the same. Drought appears to have increased substantially globally since the 1970s (Dai et al. 2004) in part because of decreased precipitation over land (mainly in the Tropics and subtropics), but also because of warming and increased atmospheric demand for moisture. Drought has increased especially throughout Africa and the Mediterranean region (both southern Europe and northern Africa), while precipitation has increased at higher latitudes in Europe (Dai et al. 2004) in part because higher temperatures increase water-holding capacity and more precipitation falls as rain instead of snow (Trenberth and Shea 2005; Trenberth et al. 2006).

The strength of the hydrological cycle and its changes over time are of considerable interest, especially as the climate changes. The essence of the overall hydrological cycle is the evaporation of moisture in one place and the precipitation in other places. In particular, evaporation exceeds precipitation over the oceans, which allows moisture to be transported by the atmosphere onto land where precipitation exceeds evapotranspiration, and the runoff flows into streams and rivers and discharges into the ocean, completing the cycle. Changes in moisture storage on land can be significant in the short term, especially in winter in the form of snow, but changes in atmospheric storage are fairly small.

The global energy cycle is also of considerable interest as it fundamentally changes with increasing greenhouse gases, changes in aerosols, and associated feedbacks. The water cycle is a key part of the energy cycle through the evaporative cooling at the surface and latent heating of the atmosphere, as atmospheric systems play a primary role in moving heat upward. The constraints in the energy budgets at the top of atmosphere, at the surface, and for the atmosphere itself can be used to provide a commentary on accuracy of observational estimates, as in Trenberth et al. (2009). Changes in atmospheric storage of energy are limited and the top of atmosphere and surface imbalances are therefore very similar, with most of the energy going into or out of the oceans in the form of heat (Trenberth 2009; Trenberth et al. 2011).

Effects of global warming on water cycle have been documented and many more are under investigation (NOAA 2013). Water cycle can be affected because the water molecule's movement through the cycle is temperature-dependent. The dynamic relationship between global warming and water cycle can be seen in the redistribution of

global water supply and the accelerated water movement between reservoirs. Water-related variables, such as precipitation, humidity, streamflow could be affected as a result of rising global temperature (Gordon 2012). Severe decrease in precipitation can potentially lead to drought, which is majorly attributed to global warming.

1.3. MEDITERRANEAN SEA WATER CYCLE

The Mediterranean region is considered to be one of the most vulnerable regions to climate change as water scarcity is expected to be exacerbated (Schewe et al. 2004 and Vargas-Amelin et al. 2014). The renewable water resources are predicted to decrease with climate change as a result of increasing temperature and reduced rainfall (García-Ruiz et al. 2011). These changes are particularly important for this region with already scarce water resources and increasing demands for water for domestic, industrial, irrigation, and tourism activities (Romanou et al. 2010*)*. According to the United Nations World Water Development Report (Unesco (ed.) Wastewater 2017*)*, the Mediterranean is a region, which includes catchments where water consumption exceeds the locally renewable water resources by a factor of two.

The renewable water resources can be characterized by the flow from the continents to the oceans, as it is the residual of the water exchanges between the continent and the atmosphere. Water discharge from the continents also plays an important role for the Mediterranean Sea as it provides a large fraction of the freshwater (Jordü et al. 2017) and most nutrients (Ludwig et al. 2010). Because of the semi-enclosed nature of this sea, these fluxes drive in large part the oceanic circulation patterns and the marine productivity (Bouraoui et al. 2010). The impact of climate change and human water usage on the quantity and quality of the flux from the continents will induce changes in salinity, thermohaline circulations (Skliris et al. 2007 and Verri et al. 2018), biological productivity and the ecological state of the sea (Bosc et al. 2004 and Smith et al. 2006).

Thus, the quantification of the water flux with its space and time variability will help monitor water availability over the continental catchments and the main drivers of the marine productivity. The complex morphology of the Mediterranean Sea with sharp orographic features and a tortuous coastline (Lionello et al. 2006) lead to a large number of small unmonitored catchments which are not well taken into account in these estimates. Furthermore, the Mediterranean is one of the regions of the world with the most karstic submarine and brackish coastal springs along the coasts (Fleury et al. 2007; Bakalowicz et al. 2015; Wang et al. 2019).

Located between the mid-latitude storm rainband and the Sahara Desert, the Mediterranean region experiences a profound seasonal cycle, with wet-cold winters and dry-warm summers (Peixoto et al. 1982). The hydrological cycle is especially sensitive to the timing and the location of the winter storms as they move into the region. Inter-annual

climate variability is closely related to the variability in the Atlantic sector such as the North Atlantic Oscillation (NAO) (Hurrell 1995, 1996; Rodo et al. 1997; Eshel and Farrel 2000). Past and future global climate changes affecting, for example, storm track characteristics (Arpe and Roeckner 1999), as well as changes in the land surface conditions (Reale and Shukla 2000), may be linked to significant changes of the hydrological cycle in the Mediterranean region (Bethoux and Gentili 1999). These in turn may potentially impact the Atlantic thermohaline circulation by changing the characteristics of the water flux at the Gibraltar Strait (Reid 1979; Hecht et al. 1997; Johnson 1997). Mediterranean Sea is also an important source of atmospheric moisture and the characteristics of the local water budget influence the amount of moisture that flows into northeast Africa and the Middle East (Peixoto et al. 1982; Ward 1998). Consequently, an improved knowledge of the Mediterranean water cycle and its variability could yield important socioeconomic benefits to these areas.

1.4. WATER BUDGET

Water Budget comprises the quantitative assessment of the water cycle components. Water Budget is essential for understanding and managing the water resources of a geographic area and the natural and cultural systems that connect them, including types of vegetation, land uses, water supplies, ground water recharge, streams and wetlands (Ferguson 1992, 1996; Mather 1978). Thorough understanding of the impact of global warming on water cycle helps policy makers to make informed decision on the best way of risk management (IUCN 2008). Besides engineered infrastructure such as dams and reservoirs, the environment itself such as intact river basins, wetlands and floodplains can reduce vulnerability of water source to climate change to mitigate the effect of global warming on water supply management.

Large-scale water budget studies have been conducted for various continental regions (Rasmusson 1968; Roads et al. 1994). Recent atmospheric re-analysis efforts offer the opportunity for new investigations providing a more stable platform for the analysis of long-term variability (e.g., Zeng 1999). A number of studies have dealt with the Mediterranean water budget (Bethoux 1979; Peixoto et al. 1982; Bryden and Kinder 1991; Harzallah et al. 1993; Gilman and Garrett 1994; Castellari et al. 1998; Angelucci et al. 1998; Bethoux and Gentili 1999; Boukthir and Barnier 2000) and results can vary significantly among authors according to the specific methodology applied. Their discrepancies reflect the uncertainties still more generally associated with the estimates of the air–sea fluxes and indicate that further work is necessary to obtain the climatological picture of the Mediterranean Sea water budget, useful among other things for validating global analyses and calibrating parameterizations.

The semi-enclosed nature of the Mediterranean Sea makes it an excellent place to test data sets and standard formulae used to estimate the heat flux into the world's oceans

(Gilman and Garrett 1994). Moreover, the Mediterranean basin offers the opportunity of calibrating the air-sea physics parameterizations in order to give a known steady-state surface heat balance (Castellari et al. 1998). Most importantly, few studies concerning the Mediterranean have focused on the long-term variability of air-sea fluxes. Bethoux et al. (1998) have discussed the observed changes in the salinity of the Mediterranean Deep Water since the 1940s and suggest that a decrease in precipitation and an increase in evaporation over the whole sea, possibly in relation to global warming, could be responsible for up to 50% of the observed salinity changes. Tsimplis and Baker (2000) suggest that the sea level drop observed in the Mediterranean Sea since 1960 could be partly related to the influence of NAO on the air-sea water fluxes. The availability of the atmospheric re-analyses in recent years have provided a new opportunity to study not only the climatology, but also the variability of the air-sea water fluxes at different timescales (Mariotti et al. 2001).

Determining the water balance for a country or a region is a complex undertaking because of a great variety of factors that influence supply of and demands for water. On the supply side, there are weather and climatic factors, which cause variation from season to season or year to year. On the demand side, the price and subsidy levels greatly influence consumption and economic use of water. Additionally, estimates of water balances depend on bureaucratic efficiency, in particular the quality and frequency of statistical data collection. Last, but not least, there are political factors, such as national boundaries on the map that do not coincide with natural watersheds, or strategic security concerns of neighboring countries which give rise to conflict rather than cooperation between them (Mehmet 1999).

While Water Budget comprises the quantitative assessment of the water cycle components, unfortunately, when trying to calculate it, several major problems start to spring up such as the lack of reliable data for sea surface evaporation, oceanic precipitation and terrestrial runoff (Zika et al. 2015; Trenberth et al. 2007; Schanze et al. 2010; Trenberth et al. 2006). Atmospheric reanalysis is another product that has generated interest increasingly in the recent decade. Reanalyses combine a wide array of measured and remotely sensed information within a dynamical-physical coupled numerical model. They use the analysis part of a weather forecasting model, in which data assimilation forces the model toward the closest possible current state of the atmosphere. A reanalysis is a retrospective analysis of past historical data making use of the ever increasing computational resources and more recent versions of numerical models and assimilation schemes. Reanalyses have the advantage of generating a large number of variables not only at the land surface, but also at various vertical atmospheric levels. Data assimilated in a reanalysis consist mostly of atmospheric and ocean data and do not typically rely on surface data, such as measured by weather stations. Reanalysis outputs are therefore not directly dependent on the density of surface observational networks and have the potential to provide surface variables in areas with little to no surface coverage.

In March 2019, European Centre for Medium-Range Weather Forecasts (ECMWF) released the 5th generation of its reanalysis (ERA5) over the 1979-2018 period (Hersbach and Dee, 2016), incorporating several improvements over ERA-Interim (4th generation). ERA5 should definitely be considered as a high-potential dataset for hydrological modelling and forecasting applications in regions where observations are lacking either in number or in quality. It is important to state that the replacement of observed data from weather stations by products such as reanalysis is not advocated, nor the current trend of decommissioning additional stations should be justified and pursued. Weather stations will continue to provide the best estimate of surface weather data at the local and regional scales and there are many fundamental reasons to keep on supporting a strong network of quality weather stations. However, atmospheric reanalysis have likely reached the point where they can reliably complement observations from weather stations, and provide reliable proxies in regions with less dense station networks (Tarek et al. 2019).

The Mediterranean region is well known for its pleasant climate with its wet-cold winters and dry-warm summers. Water is still one of the most vulnerable aspects of life in the region, now supporting an increased local population. Under a suite of global climate change scenarios, the 4th Assessment Report of the Intergovernmental Panel on Climate Change (IPCC-AR4 2007) projects major changes in the Mediterranean Sea region, in particular as a 'Hot Spot' in hydrological change with significant impacts on both mean precipitation and variability (Gibelin and Deque 2003, Giorgi 2006, Ulbrich et al. 2006, Giorgi and Lionello 2008, Sheffield and Wood 2008). However, the combined effects of future precipitation decrease and increasing surface temperature on Mediterranean water cycle, and in particular the impact on Mediterranean Sea water budget, are less well known (Mariotti et al. 2008).

CHAPTER 2 : STUDY AREA

2.1. MEDITERRANEAN SEA

2.1.1. Physical Geography

The Mediterranean Sea is surrounded by three continents and it is connected to the Atlantic Ocean by the Strait of Gibraltar in the west and to the Sea of Marmara and the Black Sea, by the Straits of the Dardanelles and the Bosporus respectively, in the east. The Sea of Marmara (Dardanelles) is often considered a part of the Mediterranean Sea, whereas the Black Sea is generally not. The 163 km long artificial Suez Canal in the southeast connects the Mediterranean Sea to the Red Sea (Vella 1985). It covers an area of about 2.5 million km^2, representing 0.7% of the global ocean surface, but its connection to the Atlantic via the Strait of Gibraltar -the narrow strait that connects the Atlantic Ocean to the Mediterranean Sea and separates Spain in Europe from Morocco in Africa- is only 14 km wide. In oceanography, it is sometimes called the Eurafrican Mediterranean Sea or the European Mediterranean Sea to distinguish it from Mediterranean seas elsewhere (Taupier-Letage et al. 2010).

Figure 2.1. Physico-geographic map of the Mediterranean and Black seas (www.grida.no/resources/5931).

The Mediterranean is a landlocked, semi-enclosed marginal sea that spans a maximum of 3,860 km in the west–east direction, and a maximum of ~1,600 km in the north–south direction. Along its roughly 46,000 km of coastline, the basin is enclosed by mountainous terrain, except for a part of the North African margin to the east of Tunisia. The Mediterranean Sea contains very deep basins, more than 4 km, and has an average depth of approximately 1,500 m. Its only natural connection with the open (Atlantic) ocean is through the narrow Strait of Gibraltar, which contains a 284 m deep sill (at a width of~ 30 km), and reaches a minimum width of only 14 km (at a depth of 880 m) (Bryden and Kinder 1991). The Strait of Sicily subdivides the Mediterranean Sea into a western and an eastern basin. This strait is relatively wide (about 130 km) and contains a topographically complex sill-structure with an estimated average depth of 330 m (Wust 1961), reaching 365 and 430 m in the two major channels (Garzoli and Maillard 1979).

The Mediterranean Sea has an average depth of 1,500 m and the deepest recorded point is 5,267 m in the Calypso Deep in the Ionian Sea. It lies between latitudes 30° and 46° N and longitudes 6° W and 36° E. Its west-east length, from the Strait of Gibraltar to the Gulf of Iskenderun, on the southwestern coast of Turkey, is about 4,000 km. The coastline extends for 46,000 km. A shallow submarine ridge (the Strait of Sicily) between the island of Sicily and the coast of Tunisia divides the sea in 2 main sub-regions: the Western Mediterranean, with an area of about 850,000 km^2; and the Eastern Mediterranean, of about 1.65 million km^2. Coastal areas have submarine karst springs (vruljas), which discharge pressurized groundwater into the water from below the surface; the discharge water is usually fresh, and sometimes may be thermal (LaMoreaux 2001; Žumer 2004).

2.1.2. Hydrology

The general vertical structure of the whole basin is characterized by the presence of different water masses, which are clearly distinguishable in the different layers. In the Mediterranean, 3 main water masses may be identified (Lionello et al. 2012) (Figure 2.2):

Atlantic Water (AW), entering the Mediterranean at the Gibraltar Strait, which circulates through the whole basin increasing its temperature and salinity from west to east; it occupies a surface layer of approximately 100–200 m, with salinities in the range between 36.6 psu in the Alboran sub-basin, 38.6 psu in the Ionian sub-basin, and 38.9 psu in the Levantine sub-basin; its temperature is mainly influenced by seasonal fluctuations.

Levantine Intermediate Water (LIW) is formed in the northeastern Levantine sub-basin in the eastern Mediterranean and occupies the whole basin at intermediate depths (300–800 m); it is characterized by a relative maximum in temperature (15–16°C in the Levantine sub-basin, 14–15°C in the Ionian sub-basin, >13°C in the Alboran sub-basin) and an absolute maximum in salinity (39–39.2 psu in the Levantine sub-basin, >38.8 psu in the

Ionian sub-basin, >38.5 psu in the Alboran sub-basin), both properties decreasing from east to west.

Deep Water (DW), which occupies the deep layer, is relatively colder and less salty than the intermediate water, originates during winter convection in the western Mediterranean (western Mediterranean deep water (WMDW), 12.7–12.9°C and 38.4 psu) and in the eastern Mediterranean (eastern Mediterranean deep water (EMDW), presently at 13.5°C and 38.7 psu). The EMDW formation shifted in the late 1980s/early 1990s from the Adriatic to the Aegean Sea characterizing the EMT.

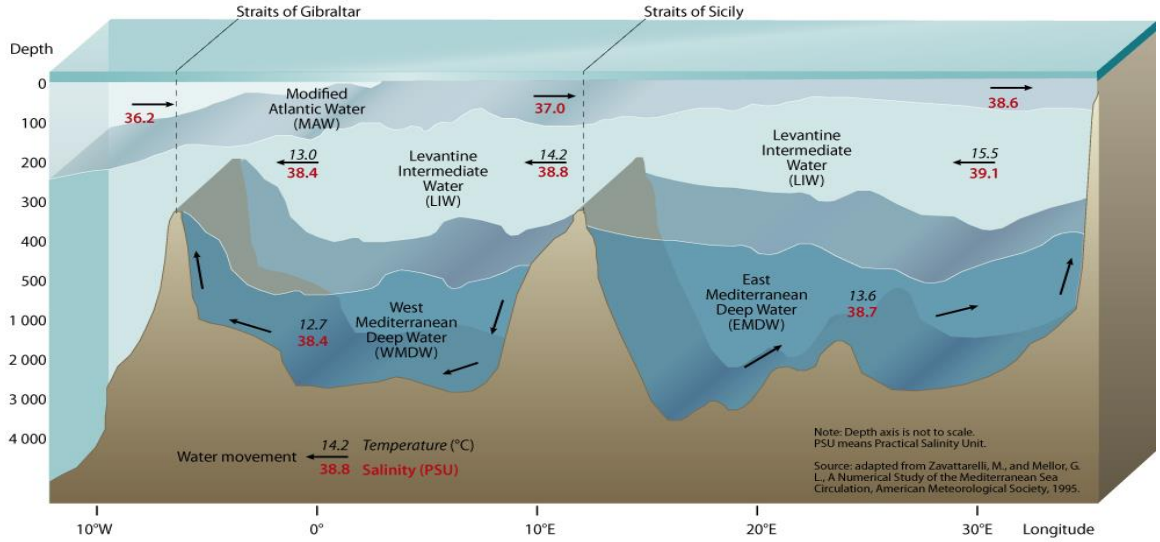

Figure 2.2. Mediterranean Sea water masses: vertical distribution (www.grida.no/resources/5885).

2.1.3. General Circulation

The Mediterranean circulation is forced by water exchange through the various straits, by wind stress, and by buoyancy flux at the surface due to freshwater and heat fluxes (Robinson et al. 2001). The high evaporation and intense air-sea interactions occurring in the Mediterranean Sea play an important role not only in Mediterranean deep-water formation and thermohaline circulation but also on an oceanic global scale. Mediterranean outflow is a key player in preconditioning the deep convection cells of the polar Atlantic, where it arrives through direct pathways or indirect mixing processes (Artale et al. 2006).

Mediterranean Sea deep water forms in the winter because of evaporation and heat losses. The Adriatic, Aegean, and Levantine sub-basins are the significant sources of EMB deep water (Malanotte-Rizzoli et al. 1999). The enhanced negative water balance in the EMB leads to increased deep-water formation, most pronounced in the Aegean Sea (Zervakis et al. 2000). Since 1969, there has been clear inter-annual variability in deep-water formation in the Gulf of Lion (Mertens and Schott 1997), which is the main deep

water formation area in the WMB (Bethoux et al. 2002). Of the few other deep-water formation areas in the WMB, the main ones are in the Balearic (Salat and Font 1987) and Ligurian (Sparnocchia et al. 1995) seas.

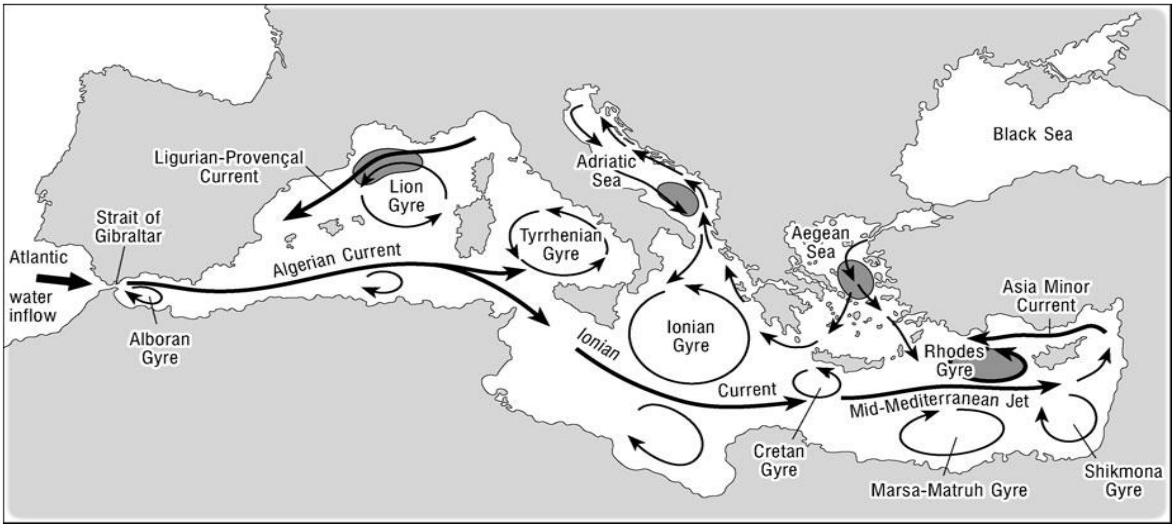

Figure 2.3. Surface water circulation in the Mediterranean Sea (modified from Vergnaud-Grazzini et al. 1988; Roussenov et al. 1995). Shaded areas indicate intermediate and deep water formation (Woodward 2009).

The Mediterranean thermohaline circulation is strongly affected by 2 key circulatory constrictions: (1) the Gibraltar Strait, 14 km wide and 300 m deep and the only connection between the Mediterranean Sea and the oceans and (2) the Sicily Channel, 140 km wide and 500 m deep, separating the Mediterranean Sea as 2 sub-basins: the Western Mediterranean Sea (West Med) and the East Mediterranean (East Med) (Figure 2.2).

Atlantic surface water flowing in through the upper layer of the Strait of Gibraltar is traceable through the Strait of Sicily into the eastern Mediterranean, although its salinity increases steadily towards the east (e.g. Wust 1961; Malanotte-Rizzoli and Hecht 1988; Malanotte-Rizzoli and Bergamasco 1989; Pinardi and Masetti 2000) (Figures 2.2 and 2.4). The eastward salinity increase culminates in values around 39.2 psu (up to an extreme of 39.5 psu, Wust 1960) in the eastern Levantine sector of the Mediterranean, compared with 36.1–36.2 psu for the Atlantic inflow at Gibraltar. The high Levantine salinities are associated with high temperatures in summer, but strong winter cooling (especially between Cyprus and Rhodes) causes surface waters to attain high enough densities to sink and spread at intermediate depths (150–600 m). This forms the 'Levantine Intermediate Water (LIW)'. This water mass spreads westward from its formation area throughout the entire Mediterranean Sea. Admixtures of regional winter mixed-layer waters slightly reduce the LIW salinity as it spreads, transforming this water mass into what has become known as 'Mediterranean Intermediate Water (MIW)'. There are also contributions of Eastern Mediterranean Deep Water (EMDW) and Western Mediterranean Deep Water (WMDW) to the MIW upon its passage through the Strait of Sicily and the Strait of Gibraltar.

In most parts of the eastern Mediterranean, MIW salinities are between 38.8 and 39.1 psu, while values in the western Mediterranean are between 38.5 and 38.8 psu. The subsurface outflow from the Mediterranean through the Strait of Gibraltar has a salinity of 38.2–38.4 psu (Wust 1960, 1961; Garzoli and Maillard 1979; Gascard and Richez 1985; Bryden et al. 1994).

EMDW and WMDW are found below about 1 km depth in the eastern and western Mediterranean basins, respectively, separated by the sill in the Strait of Sicily. Between about 600 and about 1,000 m, a transitional water mass is found between the deep waters and MIW. WMDW is formed in the northern sector of the western Mediterranean, notably in the Gulf of Lions, due to strong winter cooling caused by cold continental air outbreaks that are orographically channelled towards the basin via the Rhone valley (the 'Mistral'). EMDW is formed in two separate regions, namely the Adriatic Sea and the Aegean Sea. Both areas are subject to orographically channelled continental air outbursts in winter, the 'Bora' over the Adriatic, and the 'Vardar' over the Aegean Sea (Woodward 2009).

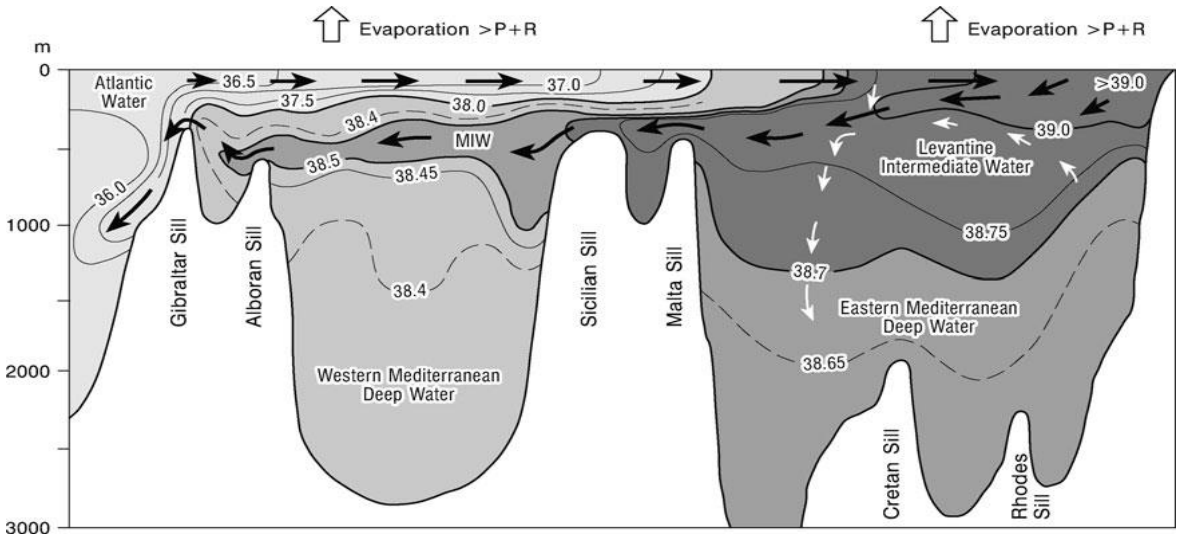

Figure 2.4. Longitudinal cross-section showing water mass circulation in the Mediterranean Sea during the present-day winter (modified from Wust 1961). Isolines indicate salinity values in psu (practical salinity units) and arrows indicate the direction of water circulation in the Mediterranean Sea (Woodward 2009).

2.1.4. Climatology

The Mediterranean climate is known for its particular regional characteristics: large seasonal contrast for temperature and rainfall, strong wind systems, intense precipitation, and Mediterranean cyclones. The Mediterranean Sea is a marginal sea, surrounded by lands and complex mountains. There are various sub-basins with shallow and narrow straits. Oceanic processes at different spatiotemporal scales, all together, participate in the formation and circulation of the complex water-mass system. The only connection of the Mediterranean Sea to the Atlantic and then the global ocean is the Strait of Gibraltar, in

which there are warm (15.4°C) and fresh (36.2psu) waters that enter the Mediterranean Sea at the surface and cold (13°C) and salty (38.4psu) waters that quit the Mediterranean Sea in sublayers. The Mediterranean Sea is a concentration basin with an evaporation rate much faster than the precipitation rate and the runoff, which constitutes the fundamental reason that the Mediterranean Sea forms deep waters and then has an overturning circulation. The Mediterranean Sea is a source of water vapor and energy for the atmosphere and has a strong impact on the nearby climate, even climate in remote regions (Rowell 2003; Li 2006). It is also sensitive to global-scale climate variation.

The climate of the MBS (in both the marine and coastal sectors), due to its geographical location (from 30° N to 46° N), belongs to the temperate zone of the northern hemisphere (Figure 2.5). However, the climatic conditions fluctuate substantially within the MBMS drainage basin, which covers an area expanding from 2° S to 56° N. According to the Koppen-Geiger classification (Geiger 1961) the climatic zones vary from hot desert (BWh) in Africa to humid continental (Dfb) in northern Europe, whilst in some mountainous areas (for example in Pontides) the climate is continental with dry and hot summers (Dsa), and humid continental with cool summers (Dfc) and/or even tundra (ET) in localised areas in the Carpathians, Balkanides and Alps. Moreover, within the Nile River catchment, south of the northern hot desert zone (BWh), the climate type of hot steppe (BSh), the tropical types of rainforest (Af), monsoon (Am) and savanna (Aw), and those of dry-winter humid subtropical (Cwa) and dry-winter temperate maritime (Cwb) are also present.

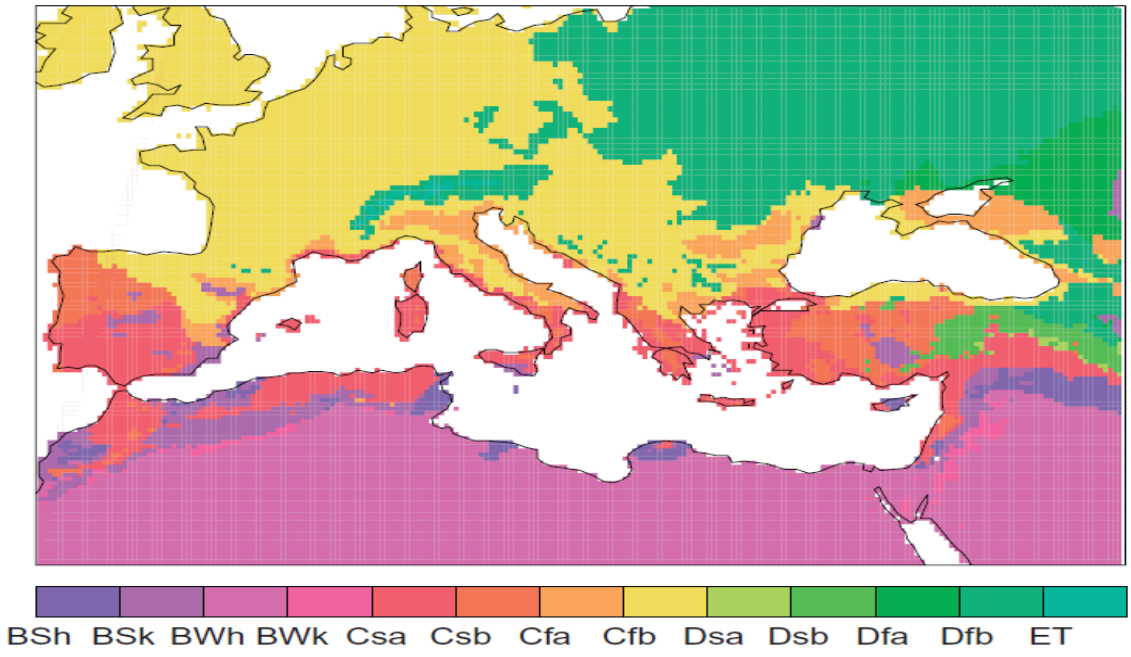

Figure 2.5. Köppen-Geiger climate types in the Mediterranean and Black Sea region: subtropical steppe (BSh), midlatitude steppe (BSk), subtropical desert (BWh), midlatitude desert (BWk), Mediterranean climate with hot/warm summer (Csa/b), humid subtropical with no dry season (Cfa), maritime temperate (Cfb), humid continental with hot/warm summer (Dfa/b), continental with dry hot/warm summer (Dsa/b), and tundra (ET). Figure is based on Climatic Research Unit (CRU) temperature and precipitation gridded data (New et al. 2000).

Strong contrasts among different areas are present, deriving from the complicated morphology of the Mediterranean region and its location between the subtropical zone to the south and the temperate zone to the north. According to the traditional climate classification (Köppen 1900), the Mediterranean climate is defined as a mid-latitude temperate climate with a dry summer season, which can be either warm or hot (these two types are labeled Csa and Csb, respectively, in the Köppen classification). However, the Csa and Csb classifications apply only to a fraction of the Mediterranean region (Figure 2.5). The distance between most parts of this region and the sea is only a couple hundred kilometers; however, other temperate, arid, and snow climate types are present. The contrasts are large: There are permanent glaciers in the humid alpine area north of the Mediterranean Sea and hot subtropical desert areas at the southern African coast, a temperate maritime climate at the north Iberian coast west of the Mediterranean Sea and truly Mediterranean areas, and steppe in the Middle East regions at the eastern coast. Note also the large areas with mid-latitude temperate climate and with no dry summer (Cfa and Cfb) in the northern parts of the Mediterranean.

The location of the Mediterranean region in a transitional zone between subtropical and mid-latitude regimes (Lionello et al. 2006a; Alpert et al. 2006a; Trigo et al. 2006) is another important factor of space and time variability. In general terms, there is a difference between the northwestern and southeastern areas, though this cannot be considered a rigorous distinction. The northern part of the region is strongly linked to the mid-latitude variability, characterized by the NAO (North Atlantic Oscillation) and other mid-latitude teleconnection patterns (Xoplaki 2002; Dünkeloh and Jacobeit 2003; Xoplaki et al. 2003, 2004; Lionello and Galati 2008). Different from areas in northern Europe or along the European Atlantic coast, many northern hemisphere teleconnection patterns besides the NAO exert a comparable influence on regional variables, such as the Scandinavian Pattern, the East Atlantic, and the East Atlantic/northern Russia pattern (Xoplaki 2002; Lionello and Galati 2008). The consequence is that many patterns need to be included for describing a significant fraction of climate variability. The southern part of the region is under the influence of the descending branch of the Hadley cell for a large part of the year and is exposed to the Asian monsoon in summer. The effect of the El Niño Southern Oscillation (ENSO) has been detected mainly on precipitation, and it is variable in time but not negligible (Mariotti et al. 2002a; Alpert et al. 2006a). This northwest (mid-latitude influences) versus southeast (subtropical influences) separation allows for many exceptions, such as the effect of ENSO on autumn precipitation in the northwestern Mediterranean region (Knippertz et al. 2003) and the effect of northern hemisphere patterns such as NAO on Middle East precipitation (Alpert et al. 2006b). The complicated land–sea pattern with many islands of various sizes and peninsulas dividing the Mediterranean Sea into many sub-basins connected by narrow straits and the presence of steep mountain ridges close to the coast helps to explain the spatial heterogeneity of climate in the Mediterranean region (Lionello et al. 2012) (as shown in Figure 2.1).

2.1.5. Water Exchange Flows

The water exchange through the Gibraltar Strait is considered a two-layer water flow, surface Atlantic water inflowing to the WMB above a lower outflow from the WMB. This exchange is affected by several factors, such as tides, atmospheric pressure, the steric effect, the geostrophic effect across the Strait, strait bathymetry, and wind (Bormans and Garrett 1989a,b; Delgado et al. 2001; Menemenlis et al. 2007; Tsimplis and Josey 2001). Tsimplis and Bryden (2000) estimated the average Atlantic inflow to the Mediterranean basin to be 0.78 x 10^6 m^3/s. Garcia-Lafuente et al. (2002) demonstrated that the surface Atlantic flow through the Gibraltar Strait was slightly smaller, i.e., 0.72 x 10^6 m^3/s. Soto-Navarro et al. (2010) calculated the surface Atlantic inflow to the Mediterranean Sea through the Gibraltar Strait using observations to be 0.81 x 10^6 m^3/s. Finally, Dubois et al. (2012) presented the results of calculating the Atlantic surface flow through Gibraltar strait over the 1961—1990 period using several models, i.e., the CNRM (Météo-France, Centre National de Recherches Météorologiques), MPI (Max Planck Institute for Meteorology), INGV (Istituto Nazionale di Geofisica e Vulcanologia), LMD (Laboratoire de Météorologie Dynamique), and ENEA (Italian National Agency for New Technologies, Energy and the Environment) models, to be 0.73, 0.75, 0.78, 0.91, and 1.06 x 10^6 m^3/s, respectively.

The water exchange through the Sicily Channel can be considered as a two-layer baroclinic exchange modified by sea-level variations (Pierini and Rubino 2001). This exchange has been investigated using CTD data (Astraldi et al. 1999; Stansfield et al. 2002), numerical modelling (Bèranger et al. 2002; Molcard et al. 2002), and sea surface height altimetry data (Shaltout and Omstedt 2012). Astraldi et al. (1999) calculated the annual average surface flow through the Sicily Channel to be 1.1 x 10^6 m^3/s. Bèranger et al. (2002) estimated that the average surface flow through the Channel was approximately 1.05 x 10^6 m^3/s. Molcard et al. (2002) suggested that the transport across the Sicily Channel increases linearly with the actual mean density difference between the basins from 0.3 to 0.8 x 10^6 m^3/s. Shaltout and Omstedt (2012) demonstrated that the surface flow through the channel displayed an annual value of 1.16 x 10^6 m^3/s.

The exchange through the Strait of Messina and Suez Canal can be neglected as they are smaller than the exchange through the Sicily Channel and Gibraltar Strait. Consequently in- and outflows are addressed by the exchange through the Gibraltar Strait and Sicily Channel. The Black Sea together with, in order of declining importance, the Nile, Po, Ceyhan, Adige, Drin, Vjose, Marista, Buyuk Menderes, and Shkumbini rivers are considered the dominant sources of fresh water to the EMB with a combined annual mean discharge of 11,209 m^3/s. The Rhone, Ebro, Tiber, Jucar, Cheliff, Moulouya, Mejerdah, and Tafna rivers are considered the dominant sources of fresh water to the WMB with an annual mean discharge of 2,811 m^3/s (Shaltout and Omstedt 2014).

2.2. BLACK SEA

2.2.1. Physical Geography

The Black Sea is a body of water and marginal sea of the Atlantic Ocean between Eastern Europe, the Caucasus, and Western Asia (Rekacewicz 2001). It is supplied by a number of major rivers, such as the Danube, Dnieper, Southern Bug, Dniester, Don, and the Rioni. Areas of many countries drain into the Black Sea, including Germany, Russia, Turkey and Ukraine (Figure 2.6). The Black Sea has an area of 436,400 km^2 (not including the Sea of Azov), a maximum depth of 2,212 m and a volume of 547,000 km^3 (Murray 1989). It is constrained by the Pontic Mountains to the south, Caucasus Mountains to the east, Crimean Mountains to the north, Strandzha to the southwest, Balkan Mountains to the west, Dobrogea Plateau to the northwest, and features a wide shelf to the northwest. The longest east–west extent is about 1,175 km (Cavendish 2010). The Black Sea is bordered by Ukraine, Romania, Bulgaria, Turkey, Georgia, and Russia. Important cities along the coast include Odessa, Sevastopol, Samsun, and Istanbul.

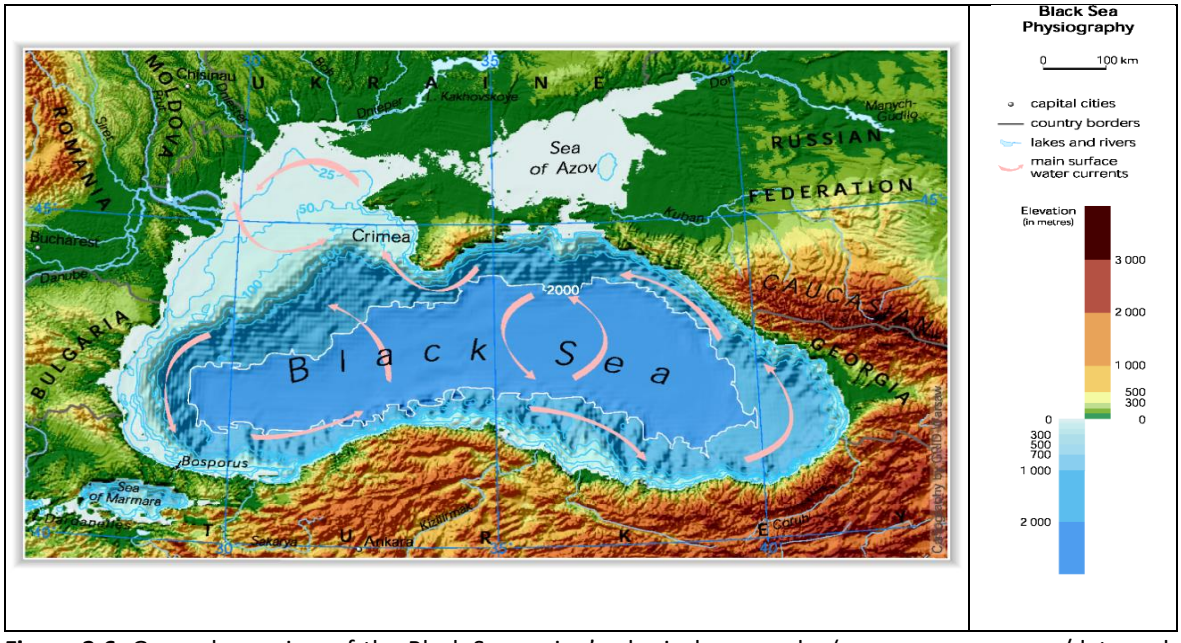

Figure 2.6. General overview of the Black Sea region's physical geography (www.eea.europa.eu/data-and-maps/figures/black-sea-physiography).

The geological origins of the basin can be traced back to two distinct relict back-arc basins, which were initiated by the splitting of an Albian volcanic arc and the subduction of both the Paleo- and Neo-Tethys Oceans, but the timings of these events remain controversial (McKenzie 1970, McClusky 2000). Since its initiation, compressional tectonic environments led to subsidence in the basin, interspersed with extensional phases

resulting in large-scale volcanism and numerous orogenies, causing the uplift of the Greater Caucasus, Pontides, Southern Crimean Peninsula and Balkanides mountain ranges (Shillington 2008). The ongoing collision between the Eurasian and African plates and westward escape of the Anatolian block along the North Anatolian Fault and East Anatolian Faults dictates the current tectonic regime, (Shillington 2008) which features enhanced subsidence in the Black Sea basin and significant volcanic activity in the Anatolian region (Nikishin 2003). In the long term, these geological mechanisms have caused the periodic isolations of the Black Sea from the rest of the global ocean system.

2.2.2. Hydrology

The Black Sea is a unique phenomenon. On the one hand, it was separated from the ocean for a long time and was almost a freshwater reservoir. On the other, it is connected with the ocean through the Mediterranean Sea through shallow straits, distinguishing the Black Sea from others by the presence of a thin layer (200–220 m) of oxygenated mobile water (the "zone of life") occurring on the world's largest hydrogen sulfide almost immovable mass. According to bathymetric data, the Black Sea basin is sub-divided into 3 parts: the shelf zone with depths of 100–200 m (~28% of the entire surface), the continental slope with a depth of 2,000 m (30%), and the clap hollow with depths of 2,000–2,150 m (42%). The origin of the Black Sea hollow is still under discussion. According to geophysical investigations it consists of two deep troughs (west and east) with a length >2,000 m. The earth's crust of 20-km thickness has two layers. But on the continental slope the third layer, "granites," appears and hence the crust thickness becomes 30–40 km. On the west, the basin is bounded by the Alps folded system of Balkan and Carpathian, on the north by the Ukrainian plate and Crimean folded carbonate rocks, on the northeast by the Alps folded system of Major and Minor Caucasus, and on the south by the orogenic system of West and East Ponte. The physical geography of the Black Sea region are given in Figure 2.6 (Zektser et al. 2007).

Black Sea has a positive water balance with a net water outflow of 300 km^3/year through the Bosporus and the Dardanelles into the Aegean Sea. There is a two-way hydrological exchange: the more saline and therefore denser, but warmer, Mediterranean water flows into the Black Sea under its less saline outflow. This creates a significant anoxic layer well below the surface waters. The Black Sea drains into the Mediterranean Sea, via the Aegean Sea and various straits, and is navigable to the Atlantic Ocean. The Bosporus Strait connects it to the Sea of Marmara, and the Strait of the Dardanelles connects that sea to the Aegean Sea region of the Mediterranean. The Black Sea is also connected, to the north, to the Sea of Azov by the Strait of Kerch.

The water level has varied significantly over geological time. Due to these variations in the water level in the basin, the surrounding shelf and associated aprons have sometimes

been dry land. At certain critical water levels, it is possible for connections with surrounding water bodies to become established. It is through the most active of these connective routes, the Turkish Straits, that the Black Sea joins the world ocean. During geological periods when this hydrological link was not present, the Black Sea was an endorheic basin, operating independently of the global ocean system (similar to the Caspian Sea nowadays). Currently, the Black Sea water level is relatively high; thus, water is being exchanged with the Mediterranean. The Turkish Straits connect the Black Sea with the Aegean Sea, and comprise the Bosporus, the Sea of Marmara and the Dardanelles. The Black Sea undersea river is a current of particularly saline water flowing through the Bosporus Strait and along the seabed of the Black Sea. The river, discovered in 2010, stems from salty water spilling through the Bosporus Strait from the Mediterranean Sea into the Black Sea, where the water has a lower salt content (Richard G. 2010).

2.2.3. General Circulation

The Black Sea is a marginal sea (Talley et al. 2011) and is the world's largest body of water with a meromictic (undergoing incomplete circulation at the fall overturn) basin. The deep waters do not mix with the upper layers of water that receive oxygen from the atmosphere. As a result, over 90% of the deeper Black Sea volume is anoxic water. The Black Sea's circulation patterns are primarily controlled by basin topography and fluvial inputs, which result in a strongly stratified vertical structure. Because of the extreme stratification, it is classified as a salt wedge estuary.

The Black Sea only experiences water transfer with the Mediterranean Sea, so all inflow and outflow occurs in the Bosporus and Dardanelles. Inflow from the Mediterranean has a higher salinity and density than the outflow, creating the classical estuarine circulation. This means that inflow of dense water from the Mediterranean occurs at the bottom of the basin while outflow of fresher Black Sea surface-water into the Marmara Sea occurs near the surface. Fresher surface water is the product of the fluvial inputs, and this makes the Black Sea a positive sea. The net input of freshwater creates an outflow volume about twice that of the inflow. Evaporation and precipitation are roughly equal at about 300 km^3/year (Talley et al. 2011).

Because of the narrowness and shallowness of the Bosporus and Dardanelles (their respective depths are only 33 and 70 meters), inflow and outflow current speeds are high and there is significant vertical shear. This allows for turbulent mixing of the two layers (Talley et al. 2011). Surface water leaves the Black Sea with a salinity of 17 psu and reaches the Mediterranean with a salinity of 34 psu. Likewise, inflow of the Mediterranean with salinity 38.5 psu experiences a decrease to about 34 psu (Talley et al. 2011).

Mean surface circulation is cyclonic and waters around the perimeter of the Black Sea circulate in a basin-wide shelf break gyre known as the Rim Current. The Rim Current

has a maximum velocity of about 50–100 cm/s. Within this feature, two smaller cyclonic gyres operate, occupying the eastern and western sectors of the basin (Talley et al. 2011). The Eastern and Western Gyres are well-organized systems in the winter but dissipate into a series of interconnected eddies in the summer and autumn. Mesoscale activity in the peripheral flow becomes more pronounced during these warmer seasons and is subject to inter-annual variability. Outside of the Rim Current, numerous quasi-permanent coastal eddies are formed as a result of upwelling around the coastal apron and "wind curl" mechanisms. The intra-annual strength of these features is controlled by seasonal atmospheric and fluvial variations. During the spring, the Batumi eddy forms in the southeastern corner of the sea (Korotaev 2003).

Beneath the surface waters (from about 50–100 meters), there exists a halocline that stops at the Cold Intermediate Layer (CIL). This layer is composed of cool, salty surface waters, which are the result of localized atmospheric cooling and decreased fluvial input during the winter months. It is the remnant of the winter surface mixed layer (Talley et al. 2011). The base of the CIL is marked by a major pycnocline at about 100–200 meters and this density disparity is the major mechanism for isolation of the deep water. Below the pycnocline is the Deep Water mass, where salinity increases to 22.3 psu and temperatures rise to around 8.9 °C (Talley et al. 2011). The hydrochemical environment shifts from oxygenated to anoxic, as bacterial decomposition of sunken biomass utilizes all of the free oxygen. Weak geothermal heating and long residence time create a very thick convective bottom layer (Korotaev 2003).

2.2.4. Climatology

Short-term climatic variation in the Black Sea region is significantly influenced by the operation of the North Atlantic Oscillation, the climatic mechanisms resulting from the interaction between the north Atlantic and mid-latitude air masses (Hurrell 1995). While the exact mechanisms causing the North Atlantic Oscillation remain unclear (Lamy et al. 2006), it is thought the climate conditions established in western Europe mediate the heat and precipitation fluxes reaching Central Europe and Eurasia, regulating the formation of winter cyclones, which are largely responsible for regional precipitation inputs (Türkeş 1996) and influence Mediterranean Sea Surface Temperatures (SST's) (Cullen and Kaplan 2002). The relative strength of these systems also limits the amount of cold air arriving from northern regions during winter (Ozsoy and Unluata 1997). Other influencing factors include the regional topography, as depressions and storms systems arriving from the Mediterranean are funneled through the low land around the Bosporus, Pontic and Caucasus mountain ranges acting as wave guides, limiting the speed and paths of cyclones passing through the region (Brody and Nestor 2010).

2.3. MBS MARINE REGIONS

The MBS comprises 4 major basins named as Western Mediterranean (WMED), Central Mediterranean (CMED), Eastern Mediterranean (EMED) and Black Sea (BLS). These primary marine regions have been further divided by the scientific community (e.g., Cruzado 1985; UNEP/MAP/MEDPOL 2005; Ludwig et al. 2009; Ludwig et al. 2010; UNEP 2012) into a number of domains (secondary regions) (Figure 2.7), for the requirements of regional physiographic, oceanographic and environmental investigations. For the aforementioned division, the sea limits provided by the IHO (1953 and its revised edition in 2002) have been adopted. The only sea limit not being introduced by IHO is the between the two sub-regions, central and Levantine, for which the geological/morphological boundary provided by Carter et al (1972) has been adopted. Thus, the WMED includes the Alboran (ALB), WestMED (WEST) and Tyrrhenian (TYR) seas, the CMED consists of the Adriatic (ADR), Ionian (ION) and CentralMED (CEN) seas, the EMED comprises the Levantine (LEV), Aegean (AEG) and Marmara (MAR) seas and, finally, the BLS additionally to the major basin area of Black Sea (BLA) incorporates the Azov Sea (AZOV). Furthermore, the marine regions WEST, LEV and BLA may be divided further into WEST_N/WEST_S, LEV_N/LEV_S, and BLA_W/BLA_E sub-regions (Figure 2.8).

Figure 2.7. The Mediterranean and Black Sea System and its division in sub-basins.

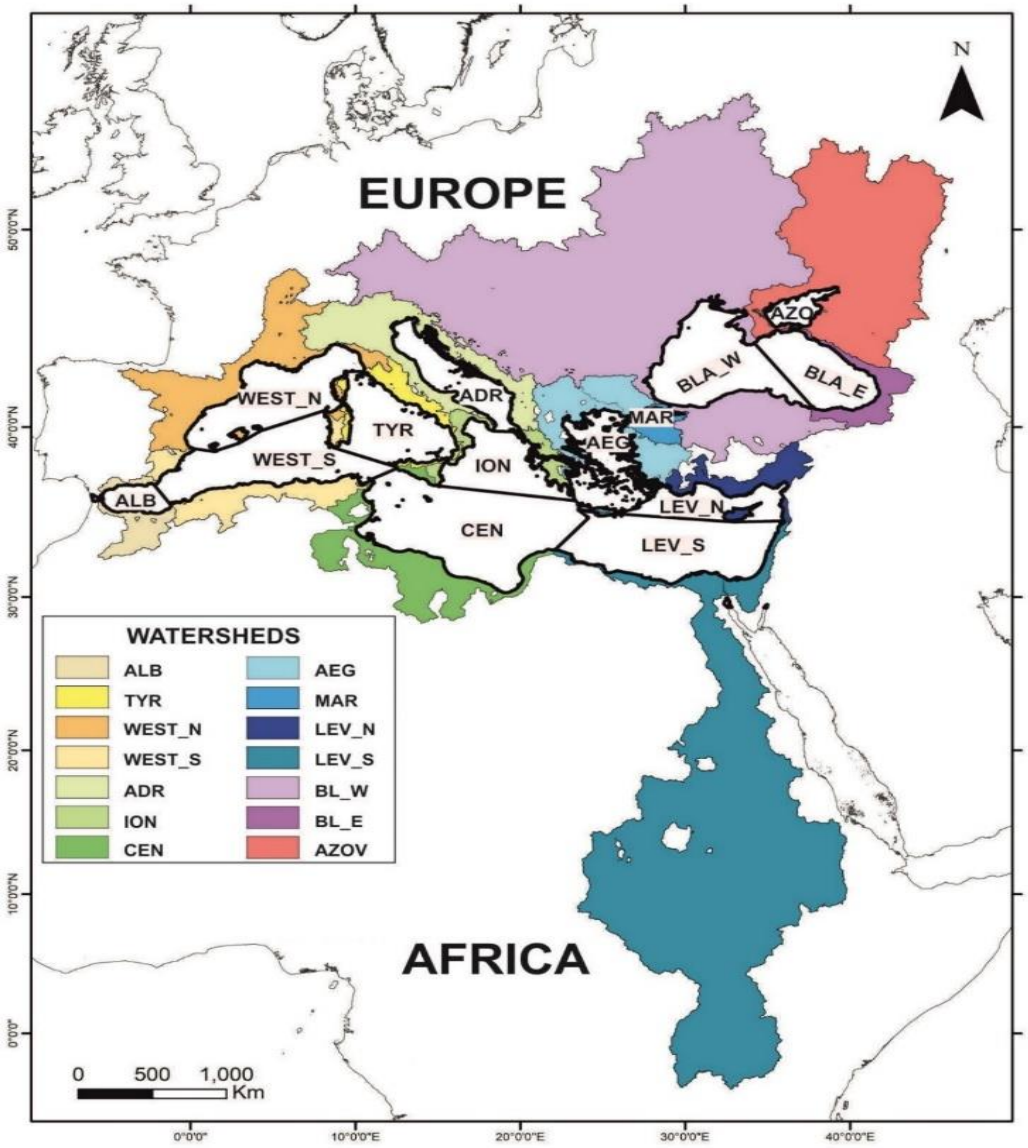

Figure 2.8. Mediterranean and Black Sea primary marine regions and their watersheds according to IH0 (2002) [WMED: West Mediterranean; CMED: Central Mediterranean; EMED: East Mediterranean and BLS: Black Sea system] (Poulos 2019).

2.4. CURRENT AND FUTURE TRENDS OF MBS's WATER BUDGET

An important concern about the Mediterranean water budget is the future evolution of its different components in a context of global warming. The Mediterranean is located at the frontier between the arid climate of North Africa and the continental European climate. Therefore, small perturbations of the conditions either in Europe or in Africa may induce significant changes in the Mediterranean Sea basin. The Mediterranean is not isolated from the global climate system, so in order to properly simulate the evolution of this region it is important to simulate the evolution of the whole globe. In this sense, the global climate models (GCMs) are the first required step. However, the Mediterranean has several characteristics (i.e. large spectrum of mesoscale processes, water mass formation

and strait dynamics) that require a relatively high spatial resolution in the models in order to produce a realistic behavior. Therefore, regional climate models (RCMs) are necessary to properly model the Mediterranean and to produce regional projections (Jorda et al. 2017).

The Mediterranean Sea region is strongly affected by global climate change and is considered as a 'hot spot' for climate change (Giorgi 2006, Lionello and Scarascia 2017). Both climate monitoring and modelling studies revealed a general trend toward drier and warmer conditions, which already started in the last century, and which is supposed to worsen even further in the future (Gibelin and Deque 2003; Milly et al. 2005; Norrant and Douguedroit 2005; Christensen et al. 2007; Giorgi and Lionello 2008). Strong repercussions to the total Water Budget of the MBS can be expected (Ludwig et al. 2009).

20th century simulations indicate that the 'transition' toward drier conditions has already started to occur and has accelerated around the turn of the century towards the larger rates projected for the 21st century. These tendencies are supported by observational evidence of century-long negative trends in regionally averaged precipitation and discharge from numerous rivers; and are consistent with reported increases in Mediterranean Sea water salinity because of increased evaporation. Simulations show how individual hydro-climatic changes will concur to determine even greater alterations of 21st century Mediterranean water cycle characteristics. By 2070–2099, the average of the models predicts a 20% decrease in land surface water availability and a 24% increase in the loss of fresh water over the Mediterranean Sea due to precipitation reduction and warming-enhanced evaporation. The projected decrease in river runoff from the surrounding land will further exacerbate the increase in Mediterranean Sea water budget deficit (Mariotti et al. 2008).

Projected changes of the different components of the freshwater budget obtained by different authors (Mariotti et al. 2015, Adloff et al. 2015, Sanchez-Gomez et al. 2009, Mariotti et al. 2008), predict a decrease in Precipitation over the basin with a reduction between -5 and -15%, although some projections reach up to a -28 % reduction. In addition, the Evaporation tends to increase a similar amount with some models projecting up to 18 % more evaporation. Riverine Discharge and Black Sea water net inflow both decrease respectively up to -87 % and -102 %. It is interesting to notice that the latter means that some studies even predict that the Black Sea would become an evaporative basin and, thus, the net water flow through the Dardanelles Strait would change its direction (from the Mediterranean to the Black Sea). Finally, net water inflow through Gibraltar could increase up to 60 %, as the result of the increase in the freshwater deficit. Adloff et al. (2015) have also shown that the changes in the components of the water budget are strongly linked to the socio-economic scenario which suggests that for higher Greenhouse Gases emissions, the water flux response is larger.

Water resources in the Mediterranean are scarce and anthropogenic pressures on rivers are particularly important. River damming and water extractions for irrigation and

other purposes rapidly evolved since the 1950s (Margat and Treyer 2004) and profoundly altered the natural functioning of Mediterranean rivers. Moreover, anthropogenic interventions (i.e. dam construction, freshwater utilization, etc.) have altered the natural flows, causing an overall reduction of riverine discharge, which in the case of BLS accounts for about 10% of its water discharge (Jahosvilli 2002). An analogous and even higher reduction is expected also for the Mediterranean's watershed as 40% of its water flow area is trapped, although temporarily, in reservoirs, and subsequently utilized for irrigation and watering purposes. In the future, a further reduction is expected due to climate change, which is associated with a reducing trend of precipitation levels (Giorgi and Lionello 2008), which is going to be more pronounced at the southern MED (Xoplaki et al. 2006). In addition, the variability of the freshwater discharge has significant impact on the habitats of the receiving waters, as they have to adjust their lives in different eutrophic status and sedimentological changes (e.g. channel abandonment, new depositional lobes) associated with morphological changes (Poulos 2019).

Projected changes in the heat fluxes through the surface and the Strait of Gibraltar obtained by different authors (Adloff et al. 2015, Dubois et al. 2012, Gualdi et al. 2013, Somot et al. 2008, Somot et al. 2006), showed that the surface heat loss of the Mediterranean is decreasing in all available climate projections. This positive surface heat change ranges from +25% to +118%, which means that some model predict that the Mediterranean could even gain heat through the surface in the future. As for the water fluxes component, the changes in surface heat fluxes are tightly related with the GHG concentrations in the scenarios. It is worth noting that results from the CIRCE project compiled in both Dubois et al. (2012) and Gualdi et al. (2013) refer to changes over the 2021–2050 period. Much larger changes are expected for the period 2061–2099, if the CIRCE simulations would have been performed up to 2099. Concerning the net heat exchange through Gibraltar, the ensemble of the CIRCE simulations displays a range between -11% and +3% (2021–2050 vs. 1961–1990), while the simulations carried up to the end of the 21st century predict an increase from 0% to +40% (2070–2099 vs. 1961–1990). The increase in the heat flux is linked to a combination of (i) an enhanced water flux required to compensate the increase in the water losses through the surface inside the Mediterranean and (ii) the increase in the temperature of the Atlantic waters flowing into the Mediterranean.

Most of the studies on the future climate of the Mediterranean Sea (Adloff et al. 2015, Macias et al. 2015, Carillo et al. 2012, Somot et al. 2006) have projected a significant warming and salinization at the end of the 21st century. This is consistent with the above mentioned results on the surface fluxes. An increase of the global temperature would also lead to a reduction of the heat loss through the sea surface and to an increase of the temperatures of the incoming Atlantic waters through the Strait of Gibraltar. This altogether would lead to an increase of the Mediterranean heat content. Also, an increase of the water loss through the sea surface would lead to a salinization of the basin, since

more salty water will enter the basin to compensate the fresh water deficit. However, the expected salinity of the Atlantic waters is not a straightforward issue. On one hand, some global models project an increase in the northeast Atlantic salinity due to increase evaporation in that region. On the other hand, other models suggest that the ice melting in the Arctic would imply a water freshening that could be advected towards the northeast Atlantic. In the latter case, the waters entering the Mediterranean through the Strait of Gibraltar may be fresher and could compensate, at least partially, the effects of enhanced evaporation.

Although most models agree on the general picture, the projected amount of change is quite diverse among the different studies. Somot et al. (2006) have projected an increase in the basin-averaged temperature of 1.5°C and of 0.23 psu in the salinity in 2099 with respect to the values in year 2000. Carillo et al. (2012) performed two simulations for the period 1950-2050. The difference between the two simulations was on the Atlantic boundary conditions, especially on the salinity. The simulated changes for the period 2001-2050 with respect to the period 1950-2000 was +0.38°C and +0.42°C and +0.03 and -0.08 psu, for the two simulations respectively. Adloff et al. (2015) performed an ensemble of six projections under different scenarios and with varying Atlantic, riverine and atmospheric conditions. Their results projected an averaged change for the period 2070–2099 with respect to 1961–1990 of +0.93°C to +1.35°C for the temperature and +0.28 and +0.52 psu for salinity. Finally, Macías et al. (2015) have projected an increase for the period 2096–2099 with respect to 2014–2017 of +1.30 and +2.50 °C for the temperature and +0.6 and 0.9 psu for the salinity. Part of the discrepancies among these studies are linked to the model characteristics and the way they simulate basic features of the basin.

The sea level in the Mediterranean will be affected by changes in the thermal content of the basin through the thermal expansion. Changes in the salt content are expected to have a minor effect (Jordà and Gomis 2013). Concerning the thermal expansion, Carillo et al. (2012) computed that thermosteric sea level would reach 5cm and 7cm by 2050, although one should keep in mind that the largest part of the oceanic response to climate change appears in the second half of the 21st century. The simulations of Adloff et al. (2015) projected a thermal expansion from 45 cm to 61 cm by the end of the 21st century. However, it has to be kept in mind that the Mediterranean Sea level is strongly affected by the changes in the nearby Atlantic (Tsimplis et al. 2013). This link with the Atlantic has clear consequences for the future evolution of the Mediterranean. First, the changes in the Mediterranean Sea level will be modulated by the Atlantic: if the Mediterranean sea level rose much more than the nearby Atlantic the increase in the along-strait pressure in Gibraltar will translate into a reduction of the net flow in the basin and thus a reduction of sea level. Second, in a similar way sea level changes in the Atlantic will be transferred to the Mediterranean. In that sense, recent projections for the nearby Atlantic (Bouttes et al. 2013) show that sea level in that region will be ~10 cm higher than the global sea level rise. This, in turn, it is projected to be between 50 and 150 cm by 2100

due to the combination of thermal expansion and water addition from land based ice melting. Therefore, it should be expected that the Mediterranean Sea level will rise much more than what is projected considering only the basin thermal expansion (e.g. Jordà et al. 2012).

Observed global climate change has a huge impact on the Mediterranean Sea region (Sarigu and Montaldo 2017, Adloff et al. 2015, Bethoux and Gentili 1999, Krahmann and Schott 1998), which truly is a vulnerable region to climate change impacts and considered as a 'hot spot' for present and future climate changes (Giorgi 2006, Lionello and Scarascia 2017). Recognizing and calculating the changes of the Mediterranean water budget is a key issue for the welfare, survival and evolution of the basin. The dynamics of the water budget does not only affect the mentioned physical parameters of the Mediterranean Sea, but more importantly, control the balances of ground and fresh water supply for the basins's nature and environment. This work provided a robust proof of the changing water budget of the Mediterranean and Black Sea system, with an increase of Evaporation, meaning the basin is becoming drier. Future projections are showing further increases in Evaporation, rising salt, temperature and sea level trends plus Precipitation and Riverine Discharge reductions (Borghini et al. 2014, Adloff et al. 2015, Schroeder et al. 2010, Gualdi et al. 2013). Future studies could provide more detailed future scenarios for the various regions of the Mediterranean and Black Sea system, in order to supply organizations and governments the right mechanisms for moderating present and future climate changes.

CHAPTER 3 : DATA COLLECTION AND METHODOLOGY

3.1. DATABASE INFO & FORMAT

3.1.1. European Centre for Medium-Range Weather Forecasts (ECMWF)

ECMWF is the European Centre for Medium-Range Weather Forecasts, based at Shinfield Park, in Reading, United Kingdom. It is both a research institute and a 24/7 operational service, producing and disseminating global numerical weather predictions and other data for the Member and Co-operating States and the broader community.

The Centre operates one of the largest supercomputer facilities and meteorological data archives in Europe, being the world's largest archive of numerical weather prediction data. Other strategic activities include delivering advanced training and assisting the WMO in implementing its programs.

The ECMWF is an independent intergovernmental organisation supported by most of the nations of Europe. ECMWF was established in 1975, in recognition of the need to pool the scientific and technical resources of Europe's meteorological services and institutions for the production of weather forecasts for medium-range timescales (up to approximately 2 weeks) and of the economic and social benefits expected from it.

It operates 2 services from the EU's Copernicus Earth observation program, the Copernicus Atmosphere Monitoring Service (CAMS) and the Copernicus Climate Change Service (C3S). It also contributes to the Copernicus Emergency Management Service (CEMS).All data is fully available to the national meteorological services in the Member States. The Centre also offers a catalogue of forecast data that can be purchased by businesses worldwide and other commercial customers. The supercomputer facility (and associated data archive) at ECMWF is one of the largest of its type in Europe and Member States can use 25% of its capacity for their own purposes.

ECMWF's core mission is the production of numerical weather forecasts and the monitoring of Earth's system. ECMWF additional goals are to carry out scientific and technical research to improve forecast skill and to maintain an archive of meteorological data. ECMWF is one of the 6 members of the Co-ordinated Organisations, which also include the North Atlantic Treaty Organisation (NATO), the Council of Europe (CoE), the European Space Agency (ESA), the Organisation for Economic Co-operation and Development (OECD), and the European Organisation for the Exploitation of Meteorological Satellites (EUMETSAT). The organisation up until now employs around 360 staff from more than 30 countries. It comprises 22 European countries, including Greece.

3.1.2. Reanalysis Method

ECMWF is at the forefront of research in numerical weather prediction. It uses the scientific advances made in areas such as data assimilation, Earth system modelling, predictability and reanalysis to improve its forecasts. Scientists across the world work collaboratively on all aspects of prediction systems as well as the many areas that support forecast production.

ECMWF makes significant contributions to support research on climate variability, pioneering an approach known as reanalysis. This involves feeding weather observations collected over decades into a NWP system to recreate past atmospheric, sea-surface and land-surface conditions over specific time periods to obtain a clearer picture of how the climate has changed. Reanalysis provides a 4-dimensional picture of the atmosphere and effectively allows monitoring of the variability and change of global climate, thereby contributing also to the understanding and attribution of climate change.

A climate reanalysis gives a numerical description of the recent climate, produced by combining models with observations. It contains estimates of atmospheric parameters such as air temperature, pressure and wind at different altitudes, and surface parameters such as rainfall, soil moisture content, and sea-surface temperature. The estimates are produced for all locations on earth, and they span a long time period that can extend back by decades or more. Climate reanalyses generate large datasets that can take up several petabytes of space.

Reanalysis is a scientific method for developing a comprehensive record of how weather and climate are changing over time. In it, observations and a numerical model that simulates one or more aspects of the Earth system are combined objectively to generate a synthesized estimate of the state of the system. Climate reanalyses combine past observations with models to generate consistent time series of multiple climate variables. Reanalyses are among the most-used datasets in the geophysical sciences. They provide a comprehensive description of the observed climate as it has evolved during recent decades, on 3D grids at sub-daily intervals.

ECMWF periodically uses its forecast models and data assimilation systems to 'reanalyse' archived observations, creating global data sets describing the recent history of the atmosphere, land surface, and oceans. Reanalysis data are used for monitoring climate change, for research and education, and for commercial applications.

Current research in reanalysis at ECMWF focuses on the development of consistent reanalyses of the coupled climate system, including atmosphere, land surface, ocean, sea ice, and the carbon cycle, extending back as far as a century or more. The work involves collection, preparation and assessment of climate observations, ranging from early in-situ surface observations made by meteorological observers to modern high-resolution satellite data sets. Special developments in data assimilation are needed to ensure the best possible

temporal consistency of the reanalyses, which can be adversely affected by biases in models and observations, and by the ever-changing observing system.

Reanalysis of past weather data presents a clear picture of past weather, independent of the many varieties of instruments used to take measurements over the years. Through a variety of methods, observations from various instruments are added together onto a regularly spaced grid of data. Placing all instrument observations onto a regularly spaced grid makes comparing the actual observations with other gridded datasets easier. In addition to putting observations onto a grid, reanalysis also holds the gridding model constant -it doesn't change the programming- keeping the historical record uninfluenced by artificial factors. Reanalysis helps ensure a level playing field for all instruments throughout the historical record.

Reanalysis is a relatively young field, with origins in the exploitation of meteorological data collected for the FGGE in 1979. Those data were reanalysed several times, mainly in order to learn how to make better use of observations to initialise numerical weather forecasts. However, it was soon realised that the datasets generated by such a reanalysis can be of great value for atmospheric research. Reanalysis data provide a multivariate, spatially complete, and coherent record of the global atmospheric circulation. Unlike archived weather analyses from operational forecasting systems, a reanalysis is produced with a single version of a data assimilation system -including the forecast model used- and is therefore not affected by changes in method (Dee et al. 2011).

Successive generations of atmospheric reanalyses produced at various institutes have improved in quality as a result of better models, better input data, and better assimilation methods. These include the global reanalyses from NCEP (Kalnay et al. 2006; Saha et al. 2010), from JMA (Onogi et al. 2007), and NASA (Schubert et al. 1993; Rienecker et al. 2011), in addition to those from ECMWF (Gibson et al. 1997; Uppala et al. 2005). The reanalyses have generated a growing variety of useful data products, spanning longer time periods at increasing spatial and temporal resolutions. A global reanalysis extending back to the late 19th century was recently produced by NOAA in collaboration with CIRES, using only surface pressure observations and prior estimates of SST and sea-ice distributions (Compo et al. 2011).

3.1.3. ECMWF Re-Analysis 5 (ERA5) Data

To date, and with support from Europe's National Meteorological Services and the European Commission, ECMWF has conducted several major reanalyses of the global atmosphere: the first ECMWF Re-Analysis (ERA-15) project generated reanalyses from December 1978 to February 1994; the ERA-40 project generated reanalyses from September 1957 to August 2002. The ERA-Interim reanalysis covered the period from 1979 onwards. A reanalysis product (ERA5) with higher spatial resolution (31 km) was released

by ECMWF in 2019 as part of the Copernicus Climate Change Service to replace previous ones.

ERA5 is the 5th generation ECMWF climate reanalysis dataset for the global climate and weather. Currently data is available from 1979 to present. When complete by mid 2020, ERA5 will contain a detailed record from 1950 to present. ERA5 replaces the ERA-Interim reanalysis, which stopped being produced on 31 August 2019. ERA5 is being developed through the EU-funded Copernicus Climate Change Service (C3S). ERA5 provides hourly estimates for a large number of atmospheric, ocean-wave and land-surface quantities. The name ERA refers to 'ECMWF ReAnalysis'. Reanalysis continues to be extended forward in time, with monthly updates of the ERA5 dataset being published within 3 months from real-time.

ERA5 data, produced by ECMWF using ECMWFS' Earth System model IFS (cycle 41r2), are available in the Climate Data Store on regular latitude-longitude grids (Gaussian-Tl639) at 0.25° x 0.25° resolution, with atmospheric parameters on 37 pressure levels from 1,000 hPa (surface) to 1 hPa (around the top of the stratosphere). ERA5 provides hourly data estimates of a large number of atmospheric, land and oceanic climate variables. The data cover the Earth on a 31km grid and resolve the atmosphere using 137 levels from the surface up to a height of around 80km (1 Pa). This spans the troposphere, stratosphere and mesosphere. There are both analysis fields and short forecast fields that link the assimilation windows used in 4D-Var. To facilitate many climate applications, monthly-mean averages have been pre-calculated as well (Hersbach and Dee 2016).

ERA5 data is open access and free to download for all uses, including commercial and public use through the C3S Climate Data Store. ERA5 data are currently available for the period 1979 to present at full resolution with flexible options for regional selection and gridding. Global fields are available at full or reduced resolution, both vertically and horizontally. A detailed description can be found in the online ERA5 documentation.

The Copernicus Climate Change Service (C3S) supports society by providing authoritative information about the past, present and future climate in Europe and the rest of the World. The C3S mission is to support adaptation and mitigation policies of the European Union by providing consistent and authoritative information about climate change. C3S is implemented by the ECMW on behalf of the European Commission. Climate data and information is provided on impacts on a range of topics and sectoral areas through the Climate Data Store (CDS). The CDS is designed to enable users to tailor services to more specific public or commercial needs. C3S offers free and open access to climate data and tools based on the best available science, so as to listen to its users and endeavor to help them meet their goals in dealing with the impacts of climate change.

3.1.4. NetCDF (Network Common Data Form) Data

Network Common Data Form (NetCDF) is a set of interfaces for array-oriented data access and a freely distributed collection of data access libraries for C, Fortran, C++, Java, and other languages, including MATLAB. The NetCDF libraries support a machine-independent format for representing scientific data. Together, the interfaces, libraries, and format support the creation, access, and sharing of scientific data. NetCDF, as a set of software libraries and self-describing, machine-independent data formats support the creation, access, and sharing of array-oriented scientific data.

NetCDF is commonly used in climatology, meteorology and oceanography applications (e.g., weather forecasting, climate change) and GIS applications. It is an input/output format for many GIS applications, and for general scientific data exchange.

A wide range of application software has been written which makes use of netCDF files. These range from command line utilities to graphical visualization packages. Also, a commonly used set of Unix command line utilities for netCDF files is the NetCDF Operators (NCO), which provide a range of commands for manipulation and analysis of netCDF files including basic record concatenating, array slicing and averaging. NCO is a suite of Earth sciences software programs operating in Linux and Microsoft Windows designed to facilitate manipulation and analysis of self-describing data stored in the netCDF format.

Moreover, ArcGIS (versions after 9.2) supports netCDF files that follow the Climate and Forecast Metadata Conventions and contain rectilinear grids with equally spaced coordinates. The Multidimensional Tools toolbox can be used to create raster layers, feature layers, and table views from netCDF data in ArcMap, or convert feature, raster, and table data to netCDF.

3.2. USED DATA OVERVIEW

ERA5 data in NetCDF format, was downloaded for research use from the Climate Data Store (CDS), at (https://cds.climate.copernicus.eu/cdsapp#!/dataset/reanalysis-era5-single-levels-monthly-means?tab=overview), provided by the Copernicus Climate Change Service (C3S) at ECMWF. A Python web API was used to download a subset of evaporation and precipitation datasets for a limited region and selected time period. ERA5 data is accessible to registered users in ECMWF Member States and Co-operating States and the required registration was free of charge.

For the surface (single level) parameters, our evaporation and total precipitation data are available as monthly means in form of monthly means of daily means for the month as a whole (in the CDS, referred to as "monthly averaged"). Monthly means of daily means are produced by averaging all daily data (summing the average of the 4 main

synoptic monthly means at 00, 06, 12, and 18 UTC). These averages represent means for the entire month. Therefore, monthly means of daily means for E and P accumulations are created from contiguous data with periods spanning from 00 UTC on the first day of the month to 00 UTC on the first day of the following month.

Table 3.1. Info details of ERA5 Evaporation and Precipitation datasets.

ECMWF ERA5 Reanalysis Datasets monthly averaged data on single levels from 1979 to 2018	
DATA DESCRIPTION	
Horizontal coverage	Global
Area	Europe: Mediterranean & Black Sea Custom: 50° N, -10° W, 29° N, 45° E
Spatial resolution	Reanalysis: 0.25° x 0.25°
Temporal coverage	Jan 1979 to Dec 2018
Temporal resolution	Monthly
File format	NetCDF-3
Data type	Grid

MAIN VARIABLES	**Units**
Evaporation (e)	m of water equivalent
total Precipitation (tp)	m of water equivalent

3.2.1. Evaporation (E)

Evaporation is the accumulated amount of water that has evaporated from the Earth's surface, including a simplified representation of transpiration (from vegetation), into vapor in the air above. Evaporation is accumulated over a particular time period, which depends on the data extracted. Evaporation is normally negative due to the convention for fluxes. The meteorological convention for all vertical fluxes is that downwards is positive. Positive evaporation represents condensation. The ECMWF Integrated Forecasting System convention is that downward fluxes are positive. Therefore, negative values indicate evaporation and positive values indicate condensation.

3.2.2. Total Precipitation (P)

Total precipitation is the accumulated liquid and frozen water, including rain and snow that falls to the Earth's surface. It is the sum of large-scale precipitation (that precipitation which is generated by large-scale weather patterns, such as troughs and cold fronts) and convective precipitation (generated by convection, which occurs when air at lower levels in the atmosphere is warmer and less dense than the air above, so it rises). Precipitation parameters do not include fog, dew or the precipitation that evaporates in the atmosphere before it lands at the Earth's surface. This parameter is the total amount of water accumulated over a particular time period, which depends on the data extracted. The units of precipitation are depth in meters. It is the depth the water would have if it was spread evenly over the grid box.

3.2.3. Riverine Discharge (RD)

Rivers play a key role in sustaining the coastal environment transferring water and sediment to the sea, with the former being associated with nutrient and/or pollutants concentrations in coastal waters, while the latter having implications for shelf sedimentation, coastline evolution, benthic ecosystem and the potential of burial of pollutants (e.g. Ludwig et al. 2003; Syvitski et al. 2005; Hill et al. 2007; Poulos, 2019).

The rivers of the MED and BLS watersheds have not been studied to the same extend. Small Mediterranean rivers (<1,000 km^2) that usually represent non-perennial rivers and streams (i.e. cease to flow for some time of the year) with remarkable hydro-geo-morphological diversity have rarely been monitored (Skoulikidis et al. 2017), while long-term hydrological observations are available for the majority of rivers with watersheds >104 km^2. Usually, data sets refer to freshwater discharges. Besides, bed load is the least measured hydrological element, due to the complex nature of its formation and the difficulties involved in measuring it (Jaoshvilli 2002). Overall, more data are available for the rivers debouching into the Black Sea than those debouch into the Mediterranean Sea.

3.2.4. Submarine Groundwater Discharge (SGD)

Submarine groundwater discharge (SGD) includes any and all flow of water on continental margins from the seabed to the coastal ocean, with scale lengths of meters to kilometers, regardless of fluid composition or driving force (Burnett et al. 2003) (Figure 3.1). Where sediments are saturated, as expected in submerged materials, groundwater is synonymous with pore water; thus, advective pore water exchange falls under this definition of SGD. The definition of SGD does not include such processes as deep-sea

hydrothermal circulation, deep fluid expulsion at convergent margins, and density-driven cold seeps on continental slopes (Moore 2009).

SGD provides a major pathway for solute and particulate transport across the groundwater/seawater interface. Nutrients and contaminants carried by discharging groundwater have considerable potential to cause deterioration of the overall ecological status of coastal marine environments. Related detrimental impacts include contamination and eutrophication of the coastal sea, contamination of seafood, disturbance of coastal marine ecosystems as well as harmful algal blooms (Schubert et al. 2017).

SGD has an influence on the coastal environment despite being long overlooked and considered as a “local phenomenon”. Associated with SGD is the release of nutrients, xenobiotics, as well as trace gases. Furthermore, SGD affects hydrological budgets as well as landside studies on groundwater renewal. Recent data compilations revealed the worldwide occurrence of SGD in coastal areas, especially near karst areas.

Most of the coastal aquifers discharge at least a part of their resource directly into the sea. Many researchers study submarine groundwater discharge (SGD), because this is a contribution to aquatic biodiversity (Spiteri et al. 2008) as well as an unknown part of the groundwater balance. However, most works consider only diffuse SGD from porous or fissure aquifers because this is the most common SGD along the world’s coasts. A global assessment (Fleury et al. 2007) showed that concentrated SGD’s occur along coastal volcanic and karst aquifers. Among them, karst submarine springs (KSMS) are the most common and are known everywhere offshore carbonate rock formations. However, according to Bakalowicz 2018, more than 90% of them occur along the Mediterranean coasts where the most spectacular ones are described. They are related to carbonate formations which outcrop all around the Mediterranean, up to 500,000 km^2 of the Mediterranean watershed (Margat 2008).

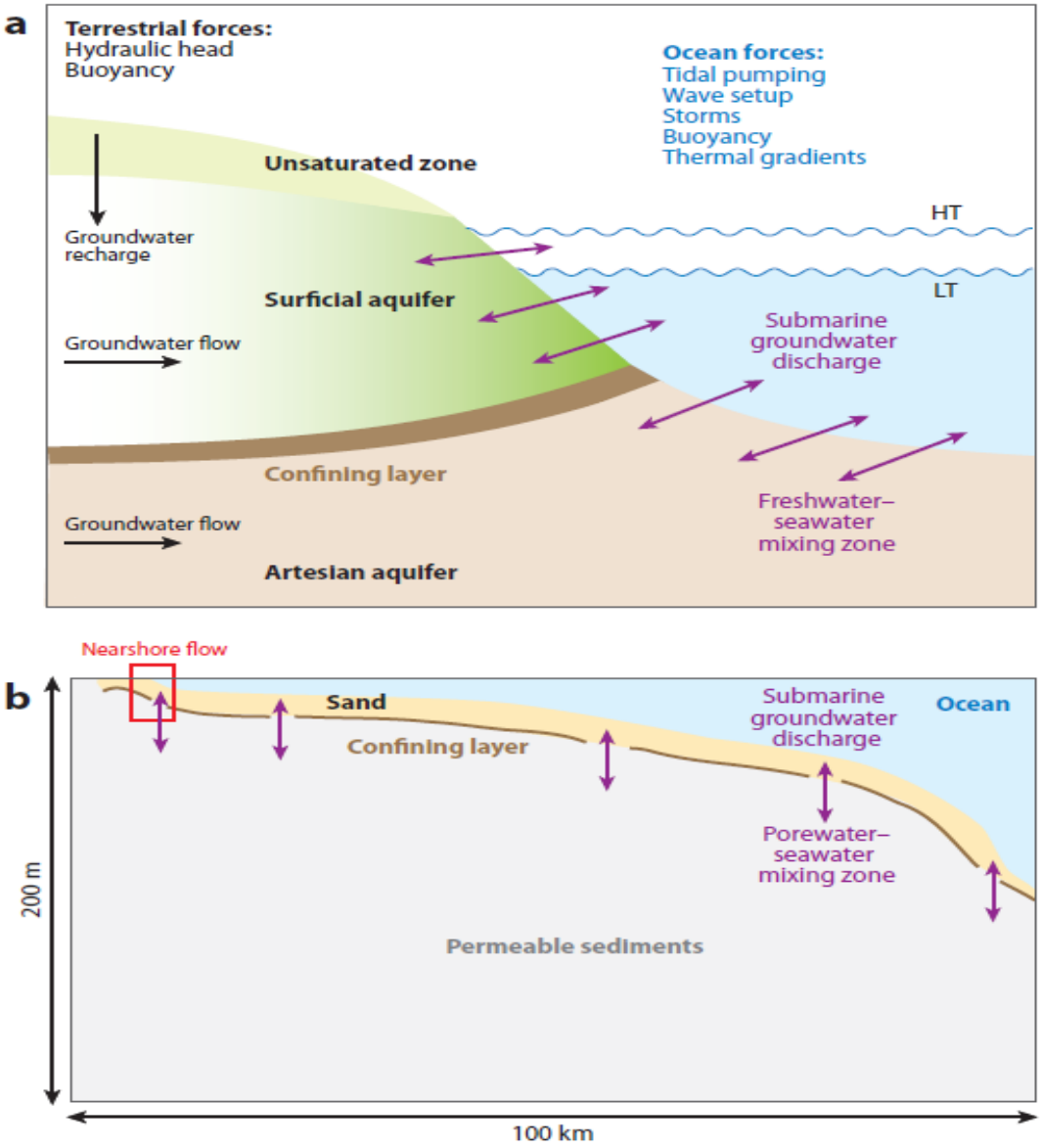

Figure 3.1. (a) Near the shoreline SGD is driven by a combination of terrestrial and ocean physical forces operating in a complex geological environment. The coastline may consist of fractured rocks, limestone, or clastic deposits. Sediments may be deposited in layers that have high hydraulic conductivity, such as coarse gravel and karstic limestone, or low hydraulic conductivity, such as mudstones. The latter are called confining layers. The interplay of the physical forces with the geology produces zones of mixing of terrestrial and sea water. These mixing zones are temporally and spatially variable due to the variety of forces, with each having different time and space scales. (b) Submarine groundwater discharge extends from the red box (labeled "Nearshore flow" and representing Figure 3.1a) throughout the continental shelf. Here flow is driven by interactions of ocean forces with geothermal heating and over pressurized zones beneath discontinuous confining layers (Moore 2009).

3.3. METHODOLOGY

3.3.1. Water Budget Equation in a Closed Basin

The water budget, under steady-state conditions and after applying the conservation of mass to a box of volume V filled with sea water, is:

Conservation of Volume (input = output):

Total Water Budget (TWB) = Vi - Vo = P – E + (RD + SGD),

where **Vi** is inflow, **Vo** is outflow, **P** is Precipitation (input), **E** is Evaporation (output), **RD** is Riverine Discharge (input) and **SGD** is Submarine Groundwater Discharge (input) (Figure 3.2). All of them are volume flux rates measured in units of km^3 / year.

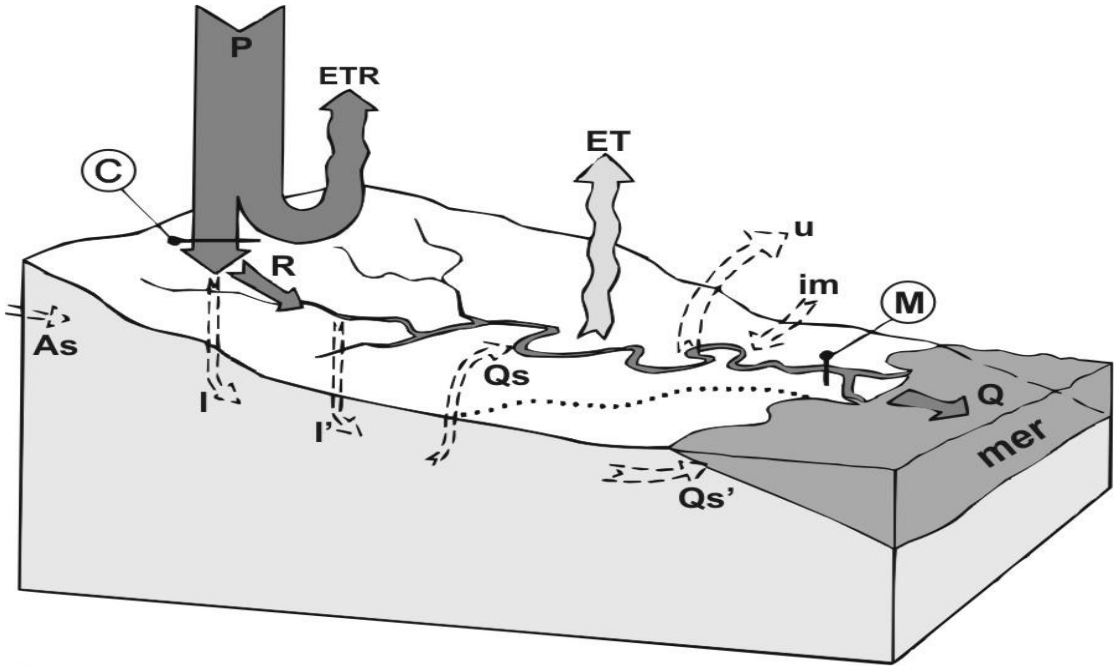

Figure 3.2. Scheme of water cycle in a sea basin. (**P**: Precipitation, **ETR**: Evapotranspiration, **R**: Runoff, **I**: infiltration, **As**: underground flow entering, **im**: importations, **I'**: surface water losses by infiltration, **Qs**: subterranean flow collected by streams, **ET**: loss of flow by evapotranspiration, **u**: anthropogenic consumptions, **Q**: outgoing surface flow, **Qs'**: subterranean flow (sea or other basin), **C**: calculation of natural interior inputs (P-ETR), **M**: actual outflow measurement Q) (Margat 2008).

3.3.2. Water Budget Equation in Mediterranean & Black Sea (MBS) System

On an annual mean basis, the equation for long-term mean of the Mediterranean and Black Sea system Total Water Budget is:

MBS's TWB = P – E + (RD + SGD) + G + B

where G and B are the total water inputs at the Gibraltar Strait and from the Black Sea, respectively (Mariotti et al. 2002). The Mediterranean Sea Water Budget (MWB) is approximately equal to:

$$MWB = Vi - Vo = P - E + (RD + SGD)$$

The main components of the Mediterranean Sea hydrological cycle are shown in the schematic two-box diagram of Figure 3.3.

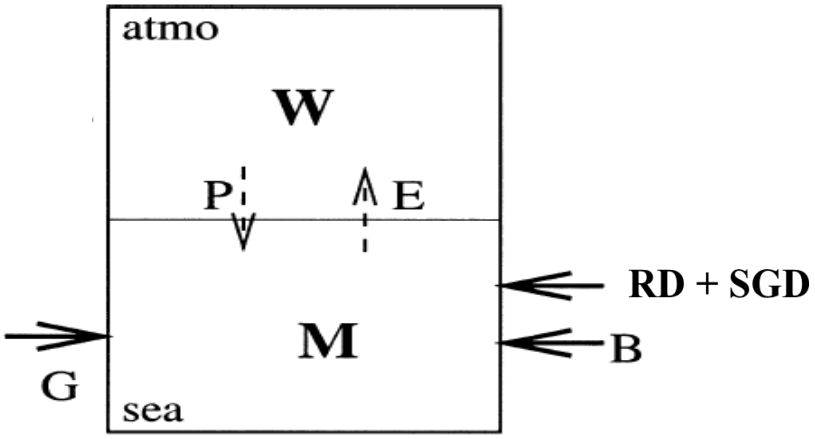

Figure 3.3. A schematic two-box diagram illustrating the main components of the Mediterranean and Black Sea system's hydrological cycle. W and M are the total Mediterranean atmospheric and oceanic water content, respectively. P is Precipitation, E is Evaporation, RD is Riverine Discharge, B and G are the total water fluxes from the Black Sea and the Strait of Gibraltar, respectively (Mariotti et al. 2002).

3.3.3. Calculation of Water Budget Equation Components

Monthly means of total Precipitation and Evaporation data for these 40 years, from 1979 to 2018, archived by the ERA5 reanalysis datasets, the Riverine Discharge yearly data and the Submarine Groundwater Discharge were all necessary to calculate the total water budget for Mediterranean and Black Sea System plus each of their 11 sub-basins.

For the calculation of average precipitation and evaporation per year in each sub-basin, the ECMWF datasets were used with a spatial resolution of 0.25° x 0.25° (about 27.5 km^2), which use a latitude/ longitude geographic coordinate system (the datum is WGS'84). The datasets include monthly average values of evaporation and precipitation for the years 1979–2018. The yearly averages of evaporation and precipitation for these 40 years were calculated by using a netCDF Operator (NCO) in Linux Operating System. Then, the average precipitation and evaporation was calculated for each sub-basin of Mediterranean and Black Sea system with the use of Geographical Information System (G.I.S.) techniques. For the purpose of this study, MATLAB was also used for displaying the average evaporation and average total precipitation, their sum along with their averages for each month from 1979 to 2018 (Figures in Chapters 4.1.1 and 4.1.2). Average volume flow rates of

evaporation and total precipitation in each sub-basin was calculated by multiplying the yearly average precipitation and evaporation with the Sea Surface Area (SSA) that is assigned to each sub-basin.

Annual estimates of Riverine Discharge (RD) in km^3 were provided for the watersheds of the 4 primary (WMED, CMED, EMED, BLS) and 11 secondary sub-basins of the Mediterranean and the Black Sea (Poulos 2019). Riverine Discharge was estimated based on a compilation of published data (from 1974 to 2018) that referred to field measurements (prior to 2000) regarding mean annual riverine fluxes (excluding bed load) of 207 rivers with drainage basins >250 km^2, discharging along the coast of the Mediterranean (150) and the Black Sea (57) (Table A1 in Appendix) covering >60% of the catchment area in most of the marine regions. Then, estimates of freshwater were calculated for the measured part of the watersheds. Subsequently, these values were used to provide a gross estimate of this part of the watershed not covered by in-situ measurements (often in the case of rivers with watersheds < 1000 km^2), assuming a rather uniform spatial behaviour of the runoff and weathering processes. Thus, the total potential riverine (natural) flux for each marine region was provided by the sum of the measured and estimated fluxes. It is mentioned that in the case of the CEN, the Libyan sector was excluded from the calculations, as it was deprived of surface water flows.

Several studies have estimated the fresh groundwater discharge to the Mediterranean Sea, using hydrologic approaches (Zektser et al. 2007, PNUE/PAM/PLAN BLEU, 2004). With these in mind, Submarine Groundwater Discharge (SGD) was calculated from multiplying each country's coastline (in Km) and its average groundwater flux (in $L/s.km^2$) along with an inland factor (in km) depending on its geomorphology. The final SGD volume flow rate for each sub-basin was calculated in km^3 per year.

All annual volume flow rates of Evaporation (E), Precipitation (P), Riverine Discharge (RD), Submarine Groundwater Discharge (SGD) and the Total Water Budget (TWB) for each sub-basin of Mediterranean and Black Sea System (MBS) are presented in Chapter 4 (Table 4.7).

CHAPTER 4 : RESULTS

4.1. COMPONENTS OF THE WATER BUDGET

4.1.1. Evaporation (E)

The Annual Evaporation of the 40 years (Figure 4.1) gives over the maritime regions a maximum of 1,700 mm/year and a minimum of about 400 mm/year for the MBS.

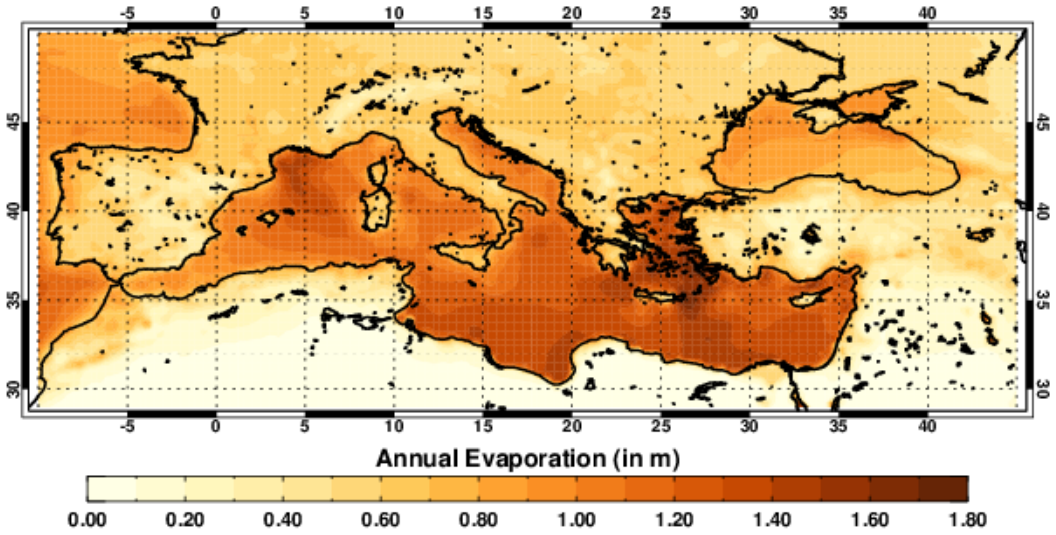

Figure 4.1. Annual Evaporation of MBS in meters (m) for the 40-year period.

The monthly Evaporation per each month for the Mediterranean Sea (Figure 4.2), has a broad maximum with higher values from October to January and smaller ones from April to June.

Mediterranean Evaporation is most intense during climatological winter (December–February) (Figure 4.2), primarily because of the stronger winds and drier air above. Rates of 180 mm/year and more are found in the North of the WEST sub-basin and in the southeastern part of the sea basin, especially in the sub-basins of LEV, AEG, and the South of the CEN. Lower rates are found at other sea sub-basins, particularly in the Black Sea. Summer (June–August) Evaporation in the Mediterranean (Figure 4.2) is much lower than in winter, with rates of 120 mm/year or less over most of the basin. Black Sea has a yearly minimum (less than 50 mm/year) in April and May and a yearly maximum (about 150 mm/year and more) in August and September.

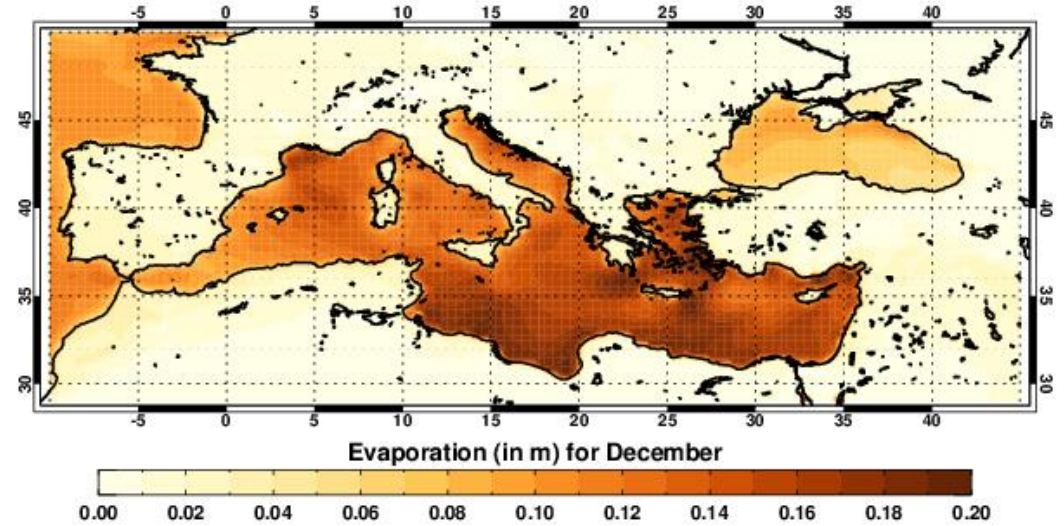
-5 0 5 10 15 20 25 30 35 40
45 40 35 30
Evaporation (in m) for December
0.00 0.02 0.04 0.06 0.08 0.10 0.12 0.14 0.16 0.18 0.20

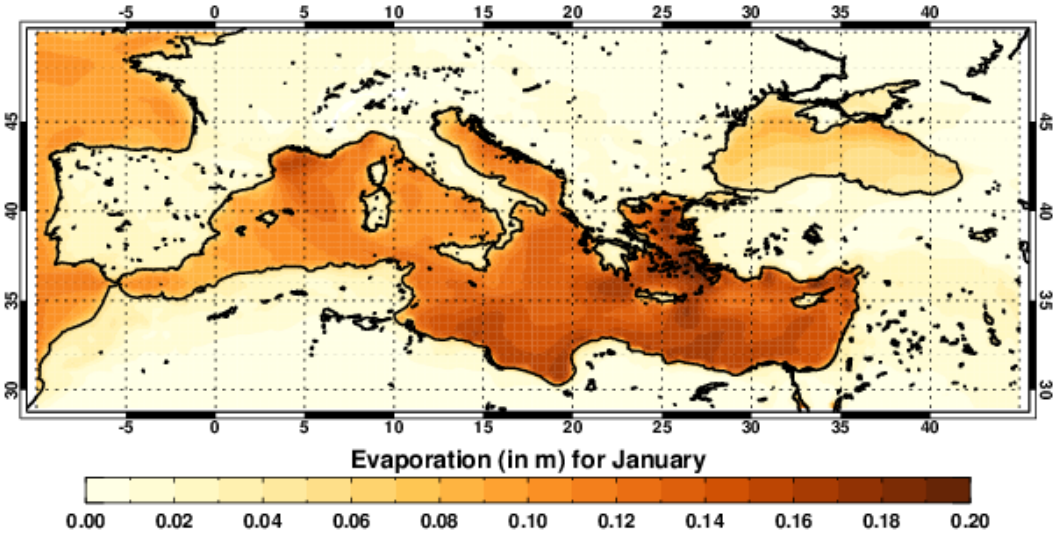
-5 0 5 10 15 20 25 30 35 40
45 40 35 30
Evaporation (in m) for January
0.00 0.02 0.04 0.06 0.08 0.10 0.12 0.14 0.16 0.18 0.20

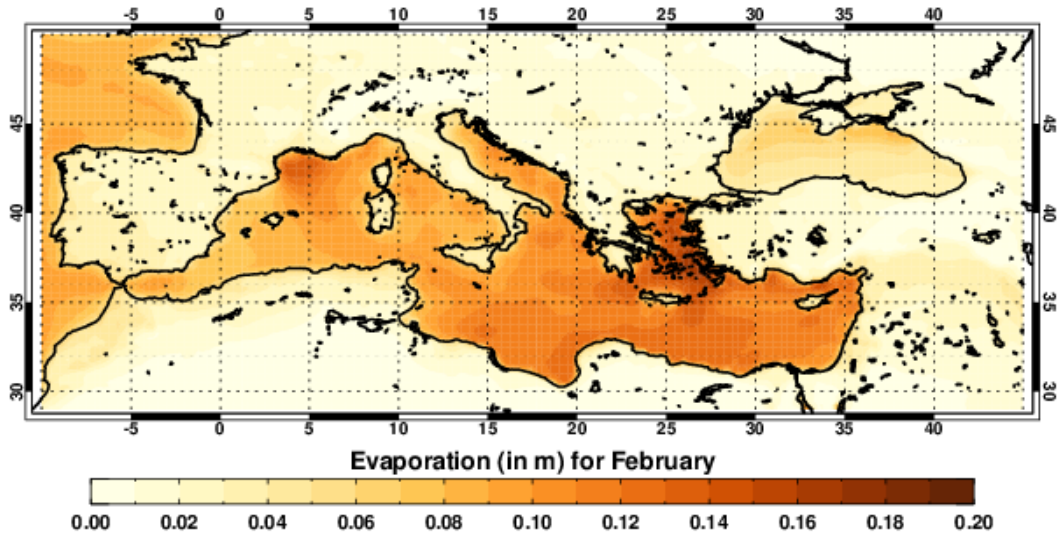
-5 0 5 10 15 20 25 30 35 40
45 40 35 30
Evaporation (in m) for February
0.00 0.02 0.04 0.06 0.08 0.10 0.12 0.14 0.16 0.18 0.20

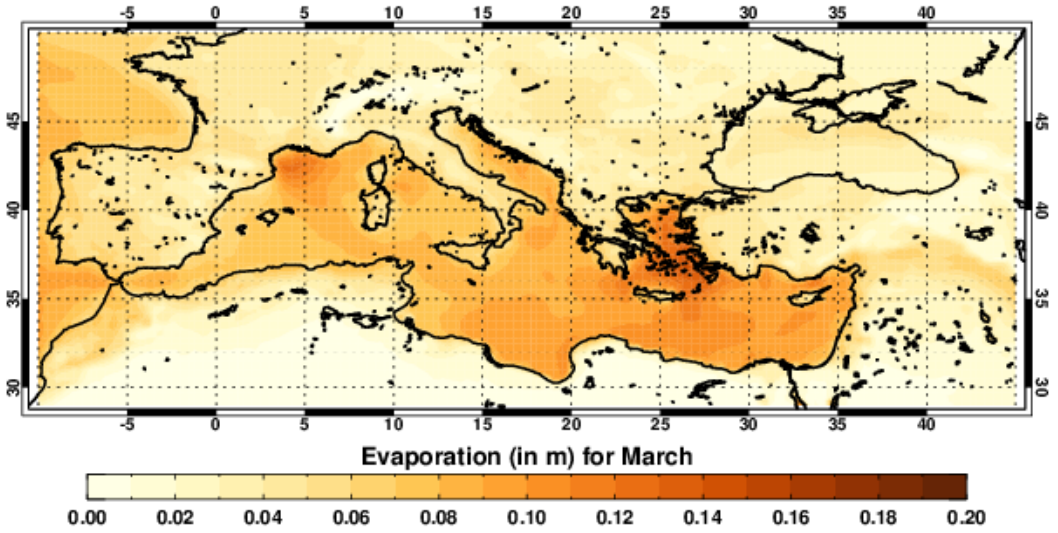
-5 0 5 10 15 20 25 30 35 40
45 40 35 30
Evaporation (in m) for March
0.00 0.02 0.04 0.06 0.08 0.10 0.12 0.14 0.16 0.18 0.20

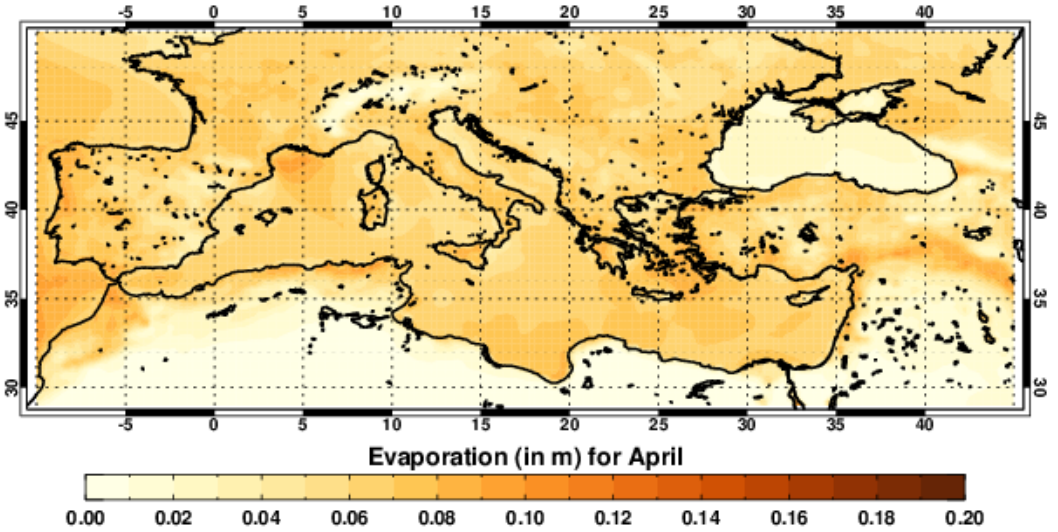
-5 0 5 10 15 20 25 30 35 40
45 40 35 30
Evaporation (in m) for April
0.00 0.02 0.04 0.06 0.08 0.10 0.12 0.14 0.16 0.18 0.20

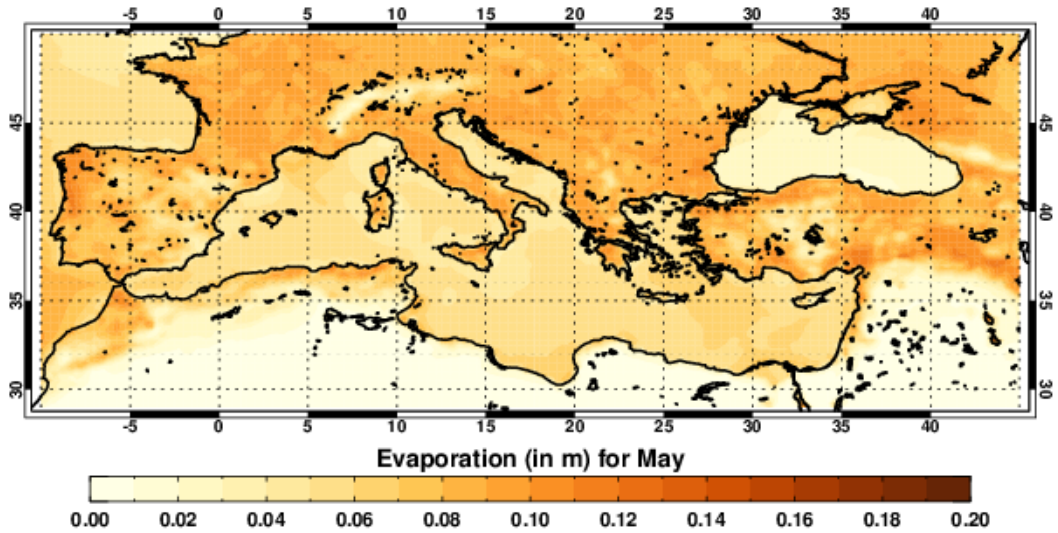
-5 0 5 10 15 20 25 30 35 40
45 40 35 30
Evaporation (in m) for May
0.00 0.02 0.04 0.06 0.08 0.10 0.12 0.14 0.16 0.18 0.20

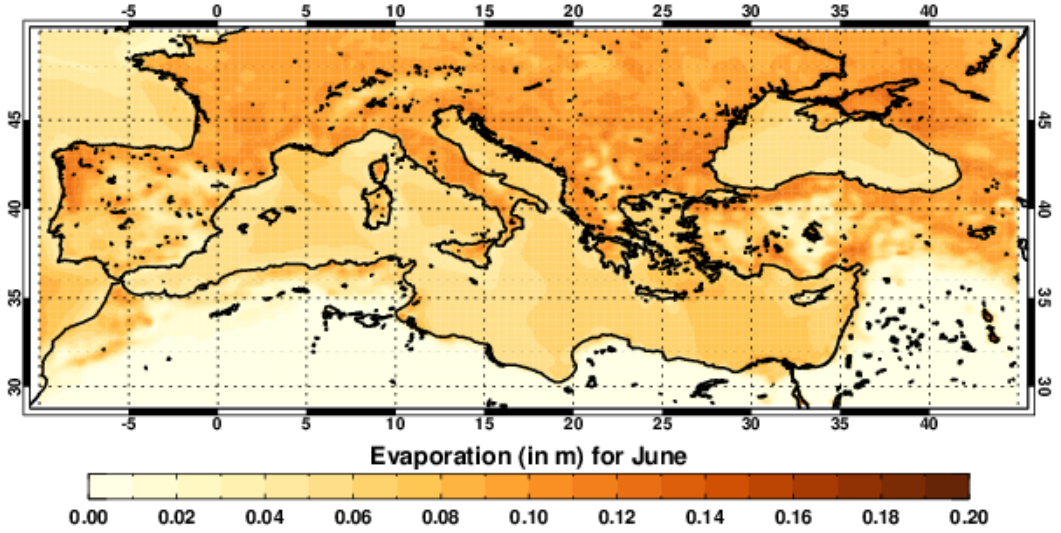
-5 0 5 10 15 20 25 30 35 40
45 40 35 30
Evaporation (in m) for June
0.00 0.02 0.04 0.06 0.08 0.10 0.12 0.14 0.16 0.18 0.20

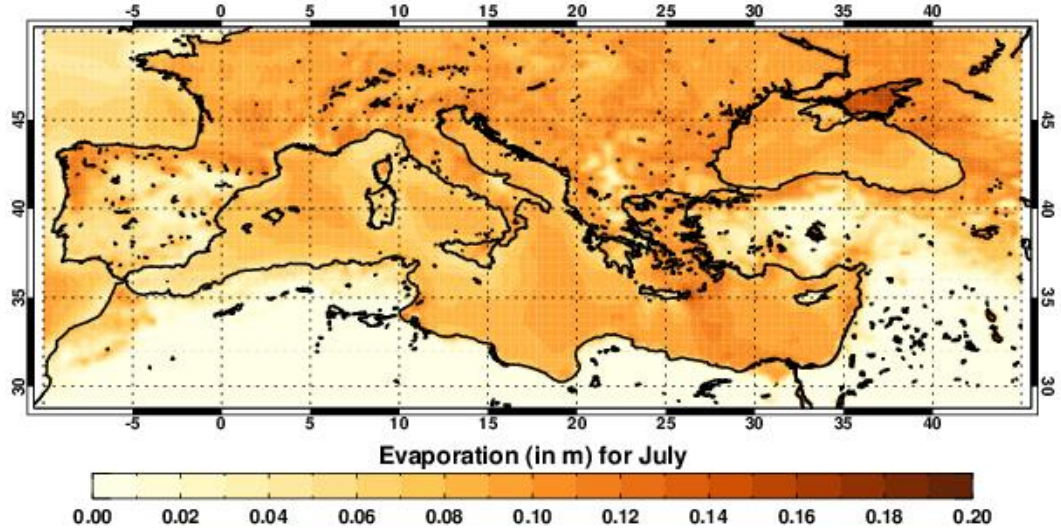
-5 0 5 10 15 20 25 30 35 40
45 40 35 30
Evaporation (in m) for July
0.00 0.02 0.04 0.06 0.08 0.10 0.12 0.14 0.16 0.18 0.20

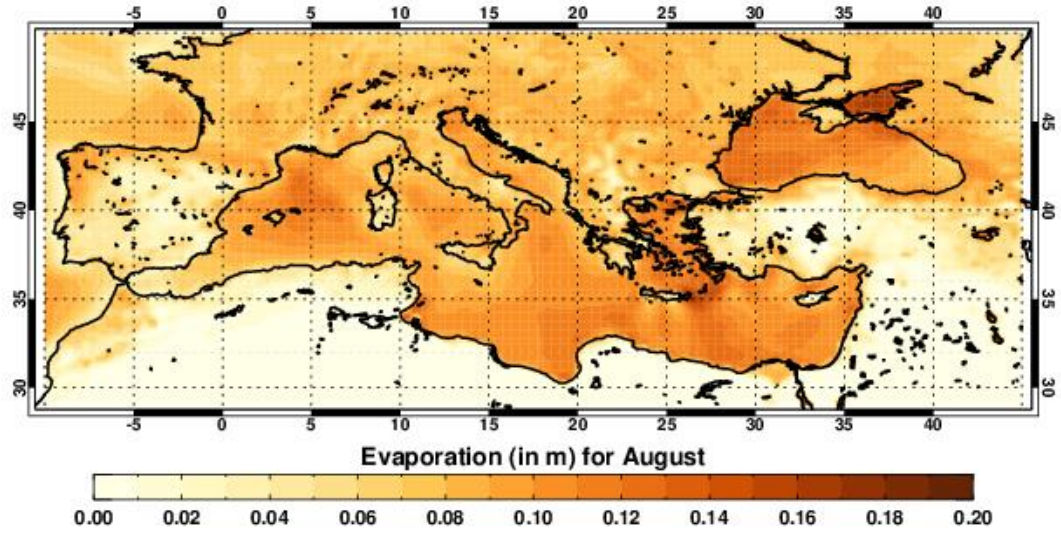
-5 0 5 10 15 20 25 30 35 40
45 40 35 30
Evaporation (in m) for August
0.00 0.02 0.04 0.06 0.08 0.10 0.12 0.14 0.16 0.18 0.20

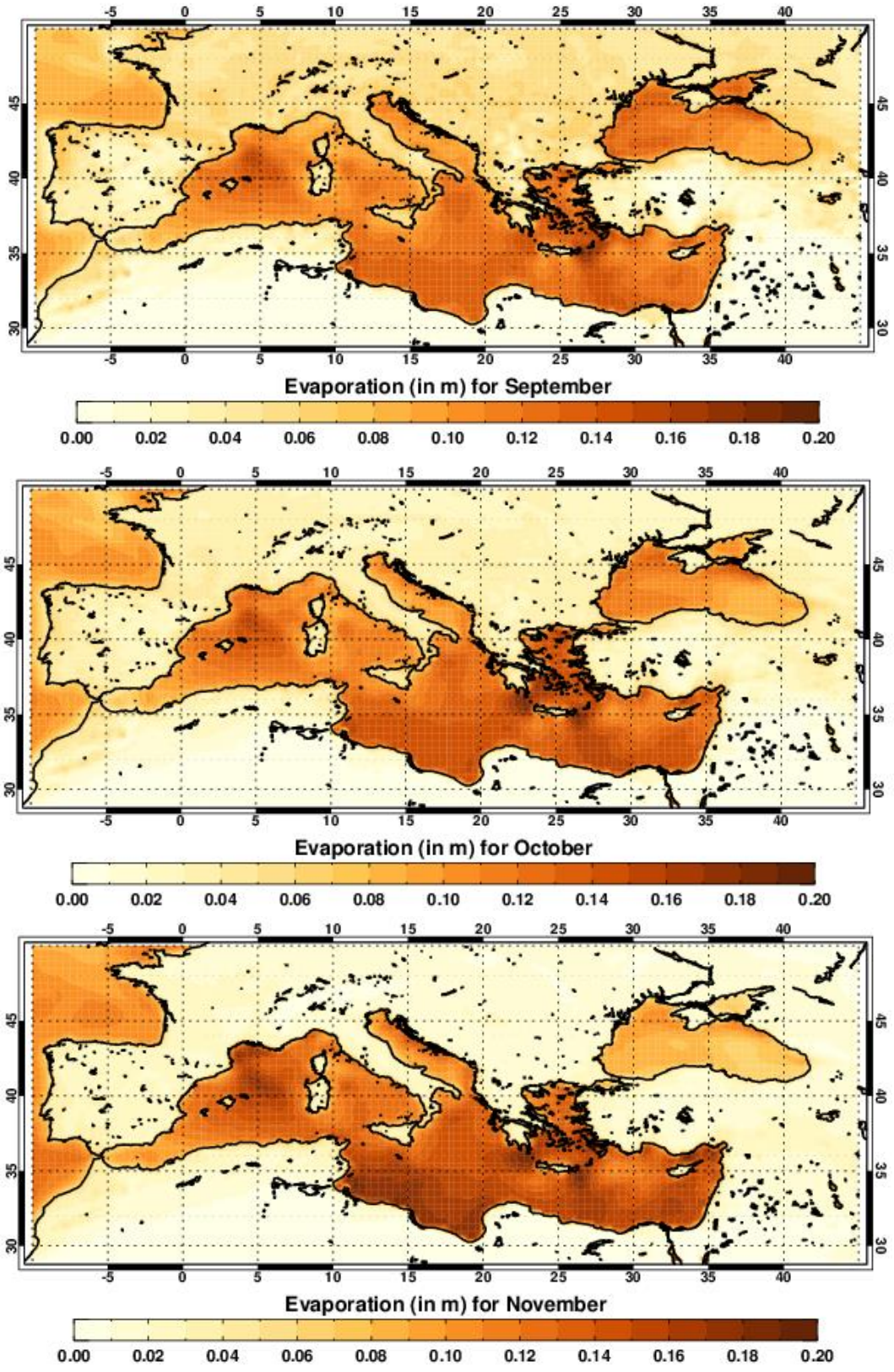

Figure 4.2. Monthly Evaporation of MBS in meters (m) per each month from 1979 to 2018.

4.1.2. Precipitation (P)

The annual total Precipitation of the 40 years (Figure 4.3) gives over the maritime regions a maximum of about 1000 mm/year and a minimum of less than 200 mm/year for the MBS.

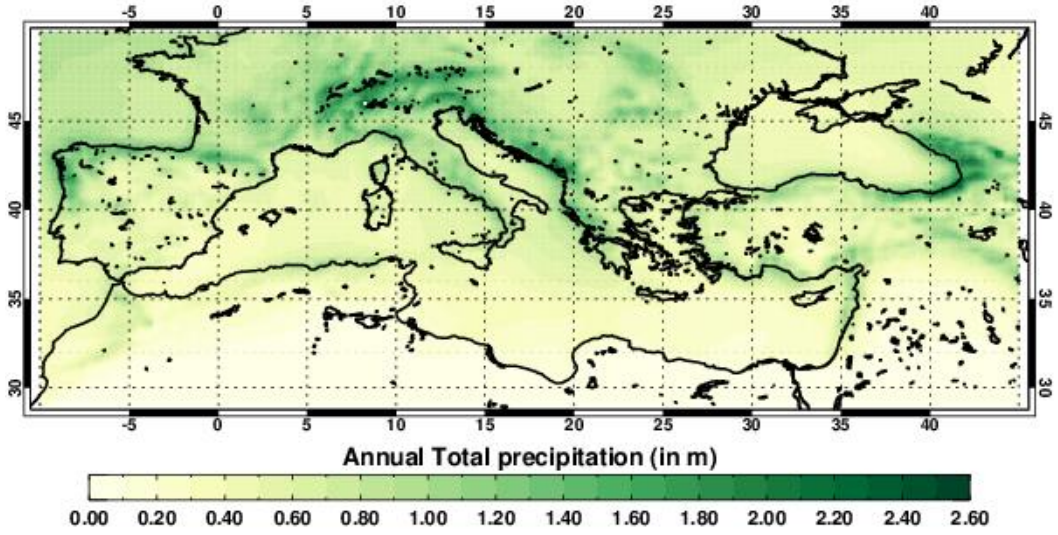

Figure 4.3. Annual Total Precipitation of MBS in meters (m) for the 40-year period.

The monthly total Precipitation per each month for the Mediterranean Sea (Figure 4.4), has a broad maximum which suggests that the rainy season extends beyond the conventional winter season well into autumn. Larger amounts occur from October to January while smaller ones occur from May to August.

Total Precipitation of Mediterranean Sea is most intense during climatological winter (December–February) (Figure 4.4). Along the African coast, total Precipitation is about 100 mm/year. Rates of 220 mm/year and more are found across the whole west coastline of the Balkan peninsula, along the eastern rim of the basin (Peninsula of Lesser Asia) and across the coastline of the Middle-East. The dataset indicates that on area average the western Mediterranean basin tends to be drier than its eastern counterpart.

During summer (June–August), the whole Mediterranean Sea south of 40^{o} N is very dry, receiving less than 20 mm/year (Figure 4.4). Between 40^{o} N and 45^{o} N, total Precipitation increases to approximately 40 mm/year. Only slightly more rates are found at the Black Sea (about 50 mm/year). In all seasons, the latitudinal gradient is the predominant feature of precipitation in the Mediterranean region with drier areas along the African coast and wetter ones north of it.

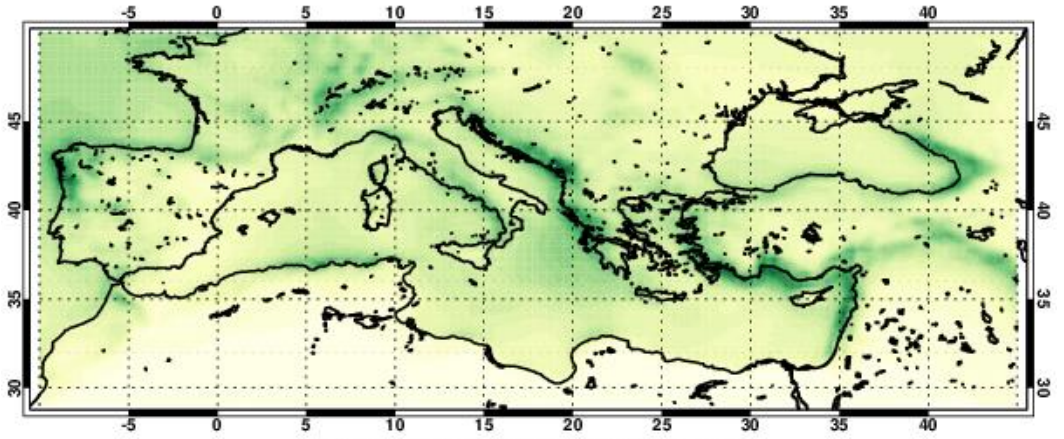

Total precipitation (in m) for December

0.00 0.02 0.04 0.06 0.08 0.10 0.12 0.14 0.16 0.18 0.20 0.22 0.24 0.26 0.28

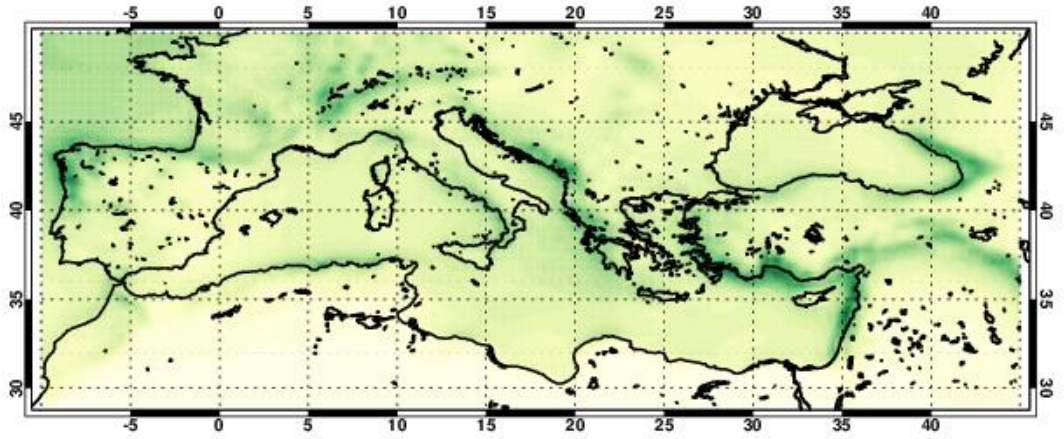

Total precipitation (in m) for January

0.00 0.02 0.04 0.06 0.08 0.10 0.12 0.14 0.16 0.18 0.20 0.22 0.24 0.26 0.28

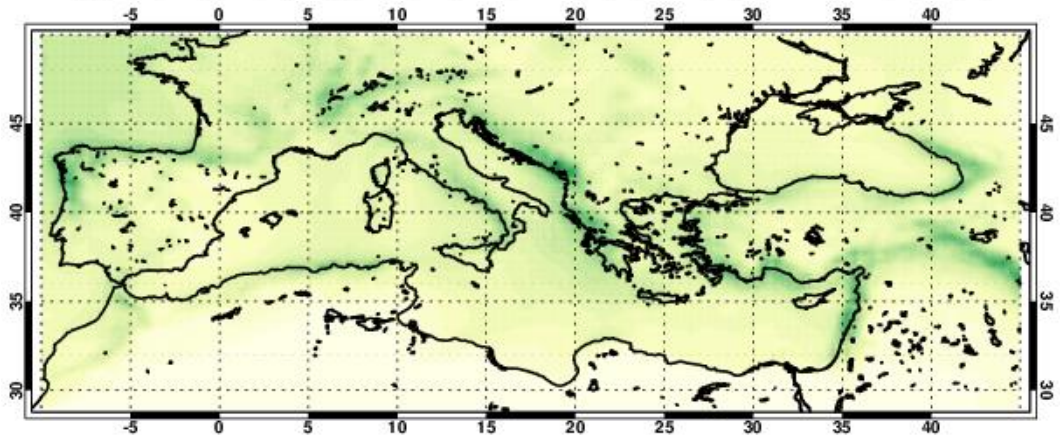

Total precipitation (in m) for February

0.00 0.02 0.04 0.06 0.08 0.10 0.12 0.14 0.16 0.18 0.20 0.22 0.24 0.26 0.28

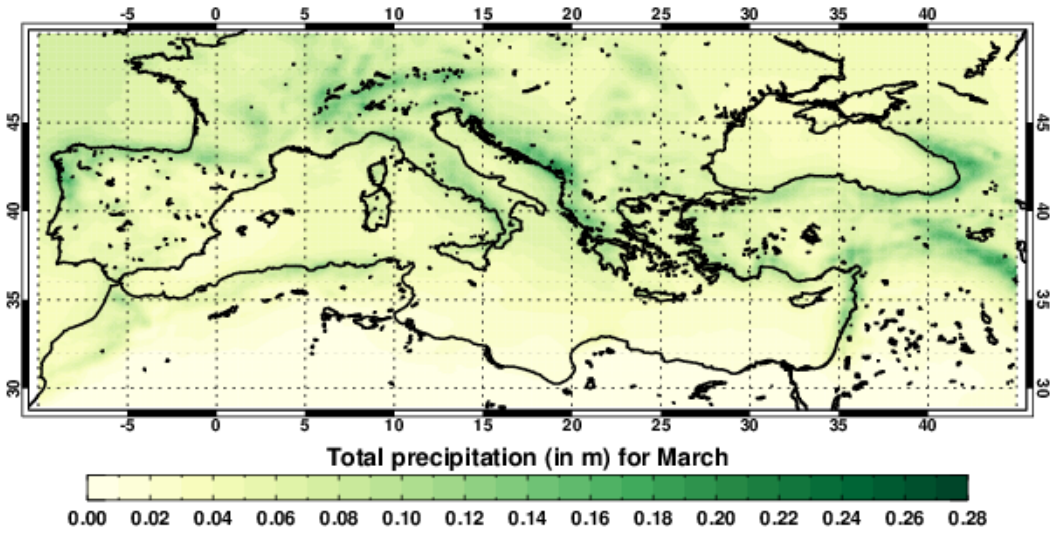

Total precipitation (in m) for March

0.00 0.02 0.04 0.06 0.08 0.10 0.12 0.14 0.16 0.18 0.20 0.22 0.24 0.26 0.28

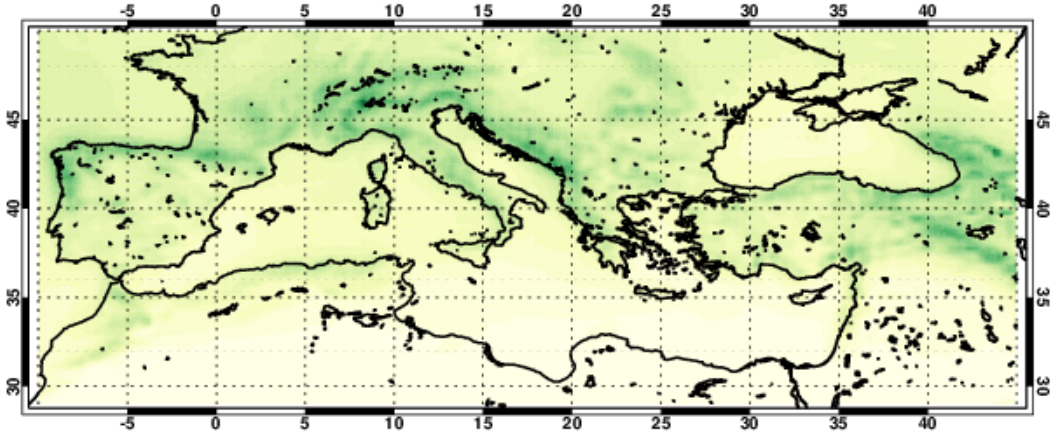

Total precipitation (in m) for April

0.00 0.02 0.04 0.06 0.08 0.10 0.12 0.14 0.16 0.18 0.20 0.22 0.24 0.26 0.28

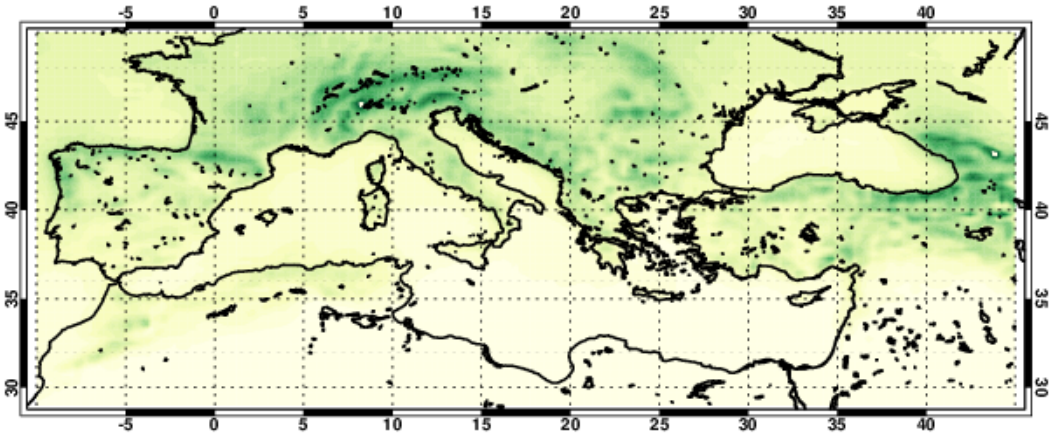

Total precipitation (in m) for May

0.00 0.02 0.04 0.06 0.08 0.10 0.12 0.14 0.16 0.18 0.20 0.22 0.24 0.26 0.28

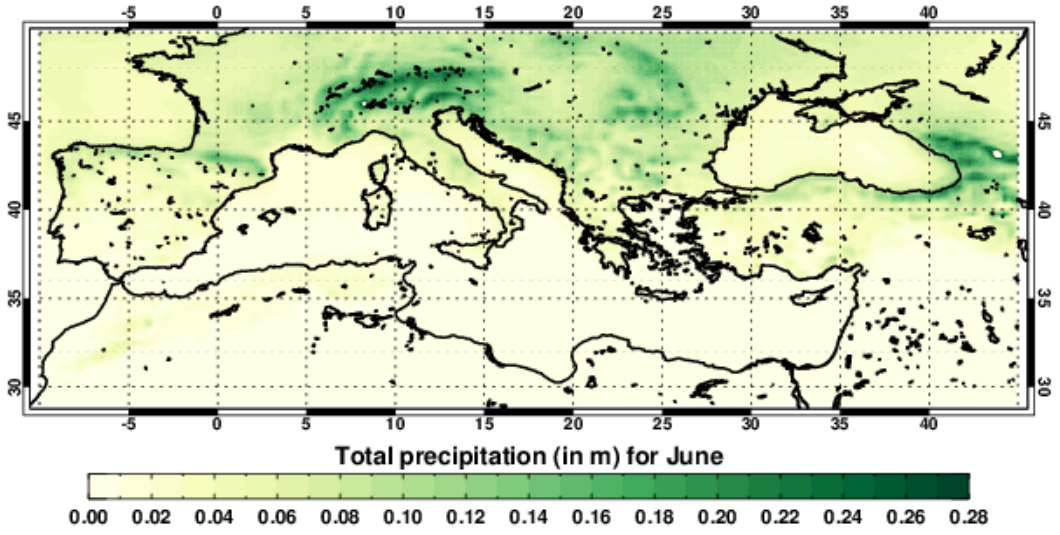
-5 0 5 10 15 20 25 30 35 40
45 40 35 30
Total precipitation (in m) for June
0.00 0.02 0.04 0.06 0.08 0.10 0.12 0.14 0.16 0.18 0.20 0.22 0.24 0.26 0.28

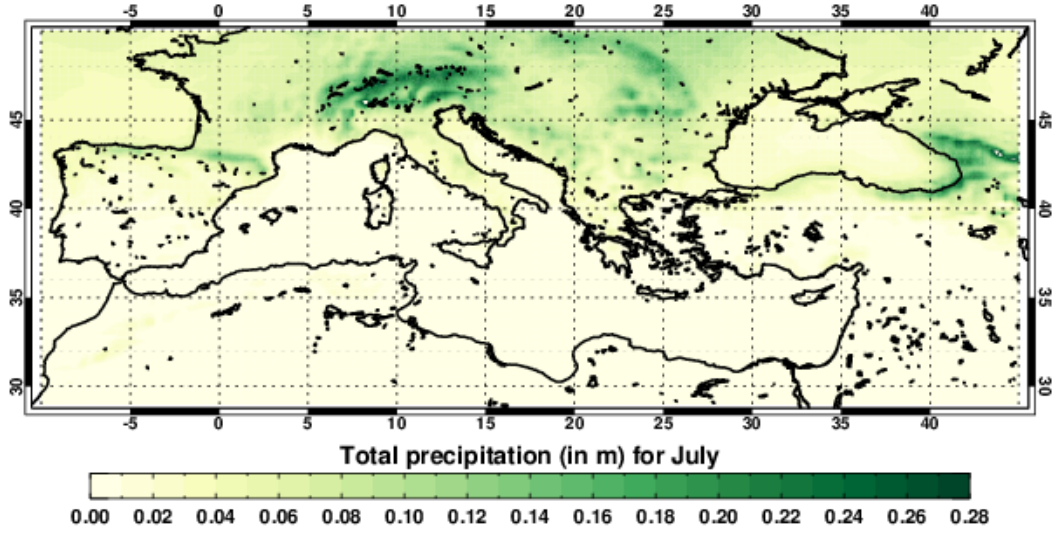
-5 0 5 10 15 20 25 30 35 40
45 40 35 30
Total precipitation (in m) for July
0.00 0.02 0.04 0.06 0.08 0.10 0.12 0.14 0.16 0.18 0.20 0.22 0.24 0.26 0.28

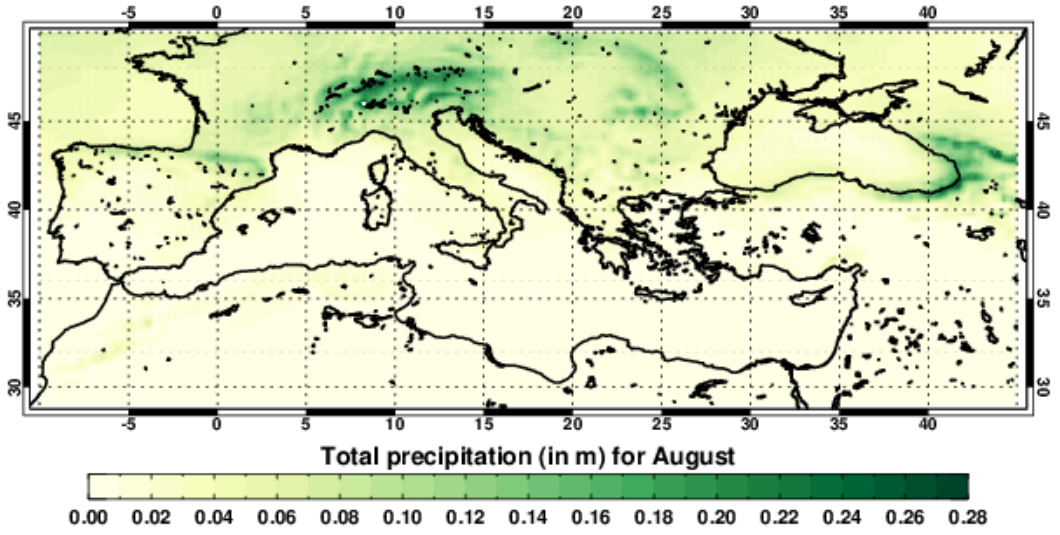
-5 0 5 10 15 20 25 30 35 40
45 40 35 30
Total precipitation (in m) for August
0.00 0.02 0.04 0.06 0.08 0.10 0.12 0.14 0.16 0.18 0.20 0.22 0.24 0.26 0.28

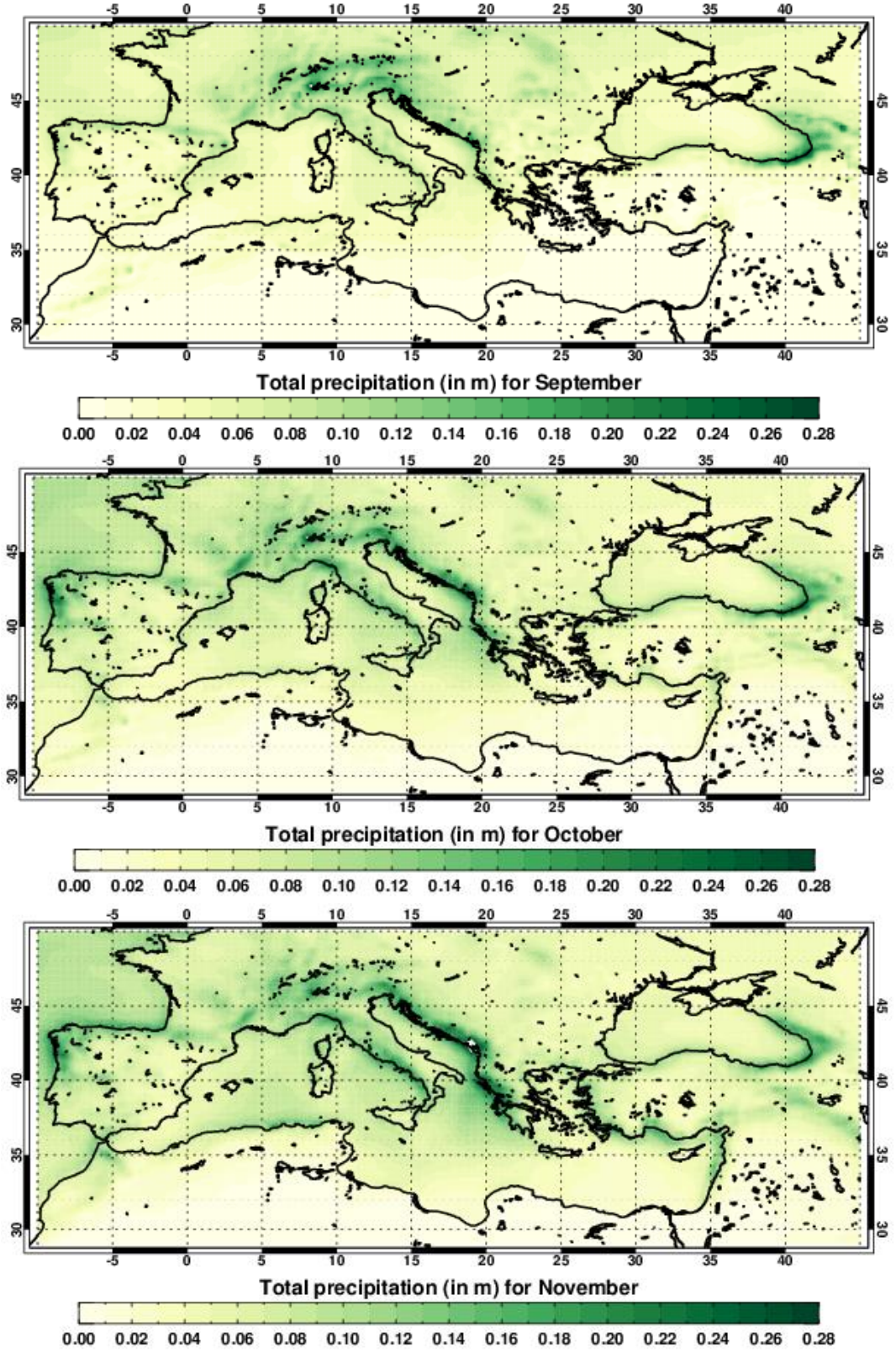

Figure 4.4. Monthly total Precipitation of MBS in meters (m) per each month from 1979 to 2018.

4.1.3. Time series and trends of Evaporation (E) & Precipitation (P)

The time series of Evaporation and Precipitation volume flow rates for all sub-basins of the Mediterranean and Black Sea system for the period 1979 – 2018 are shown in Figures 4.5 to 4.15. Annual Evaporation is colored with orange and total Precipitation with blue, along with their respective trendlines. The Mediterranean Sea is well known for its intense Evaporation (Mariotti et al. 2002, Tanhua et al. 2013), which is largely exceeding Precipitation and Riverine Discharge. This pattern seems to get reinforced due to strong positive Evaporation trends in the entire Mediterranean and Black Sea system apart from ADR and MAR sub-basins, combined with statistically not significant changes for Precipitation apart from a positive trend in the sub-basin of ION (Table 4.1). The analysis of our ERA5 data sets in this study confirms previous findings.

Specifically, in the time series of Evaporation data for the period 1979–2018, results indicate a long-term Evaporation increase in all sub-basins, except for ADR (Figure 4.9) and MAR (Figure 4.13) sub-basins. The statistically significant (at confidence level 95%) increase of Evaporation for these sub-basins is possibly driven by the rapid warming of the Mediterranean surface during the last decades implying an increase of latent heat loss (Skliris et al. 2012) from the late 1960s to mid-1990s mainly attributed to an increasingly positive phase of the North Atlantic Oscillation (Mariotti et al. 2002). In the time series of Precipitation data for the period 1979-2018, results don't indicate a statistically significant change for Precipitation except for an increase in the sub-basin of ION (Figure 4.10).

Table 4.1. Trends of Evaporation (E) and total Precipitation (P) for all sub-basins of the Mediterranean and Black Sea system along with their Sea Surface Area (SSA in km^2). All trends were calculated in km^3/year for the 40-year period. Statistically significant (at confidence level 95%) values are denoted in bold font style.

BASINS	SSA	E	P
ALB	54,520.22	**0.079**	0.049
WEST	571,094.73	**1.541**	0.742
TYR	217,366.20	**0.559**	0.454
CEN	599,787.98	**2.062**	-0.162
ADR	137,551.79	0.030	0.308
ION	168,894.27	**0.573**	**0.450**
LEV	568,522.03	**2.424**	-0.359
AEG	186,945.31	**0.450**	0.229
MAR	11,022.78	0.010	0.010
BLA	420,565.50	**1.591**	-0.306
AZO	36,761.05	**0.159**	-0.078

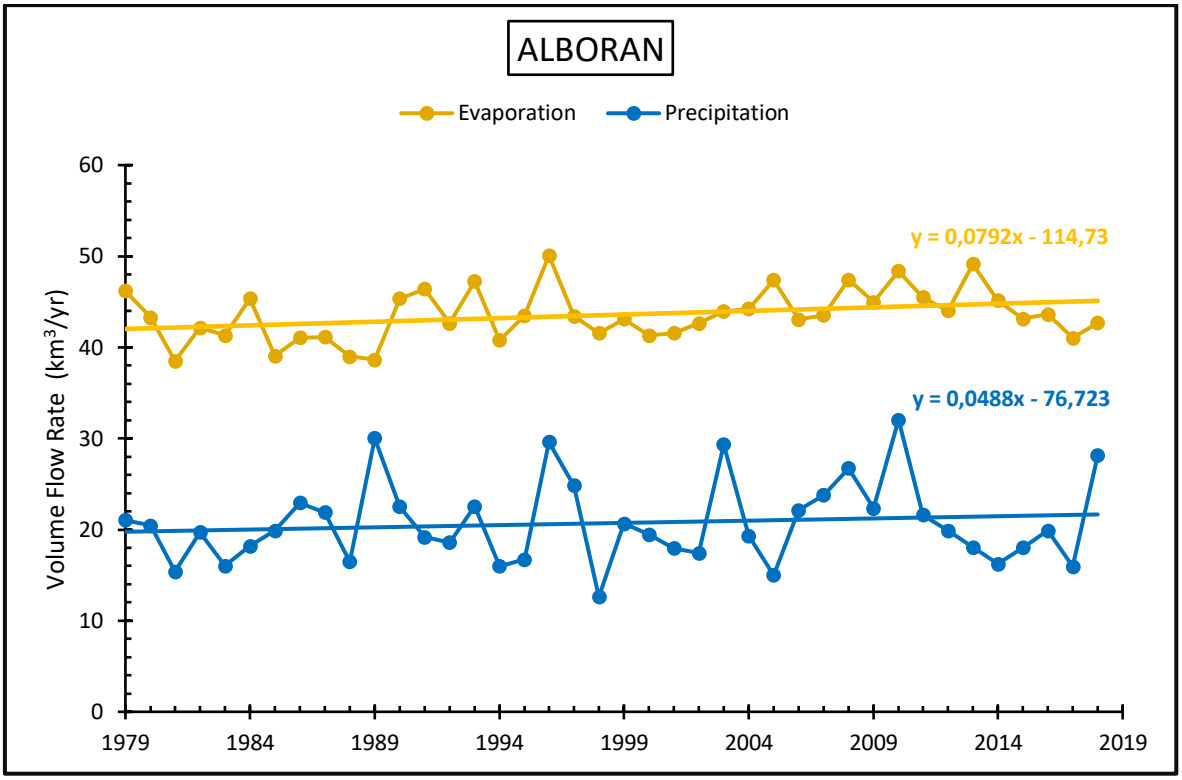

Figure 4.5. Annual time series of Evaporation and Precipitation volume flow rates for Alboran sub-basin of Mediterranean and Black Sea system for the period 1979 – 2018.

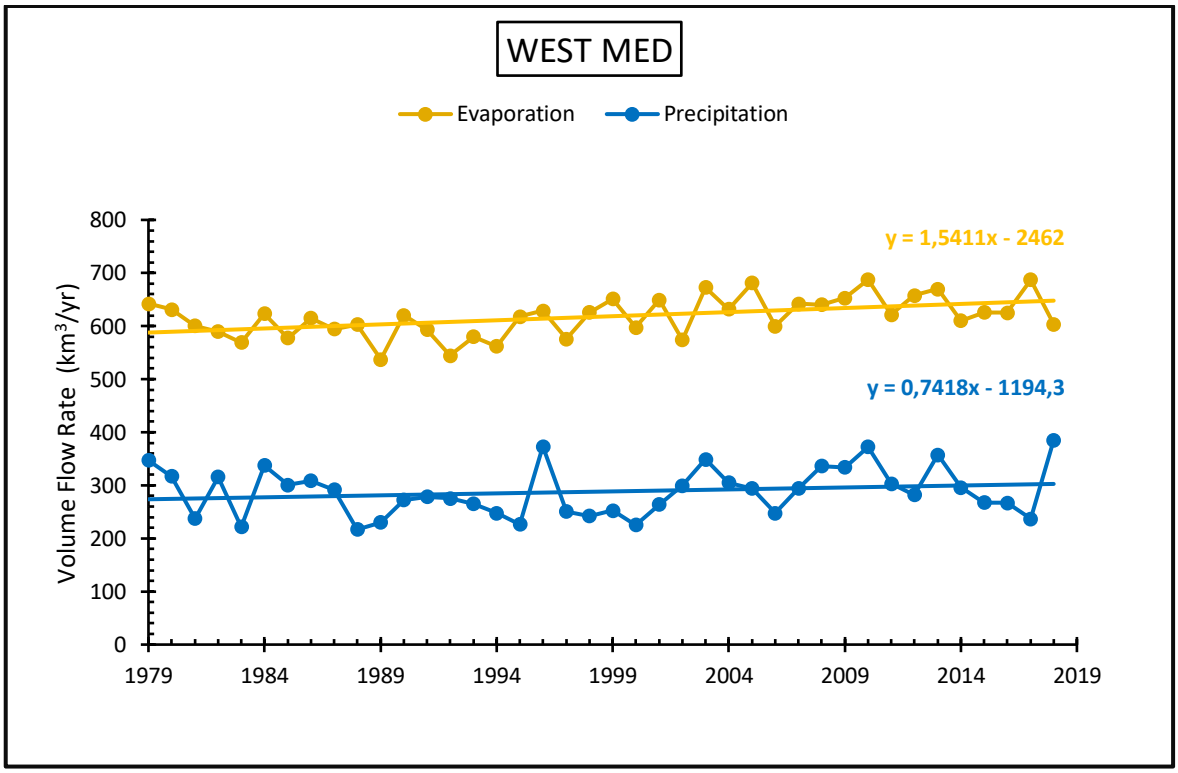

Figure 4.6. Annual time series of Evaporation and Precipitation volume flow rates for West Med sub-basin of Mediterranean and Black Sea system for the period 1979 – 2018.

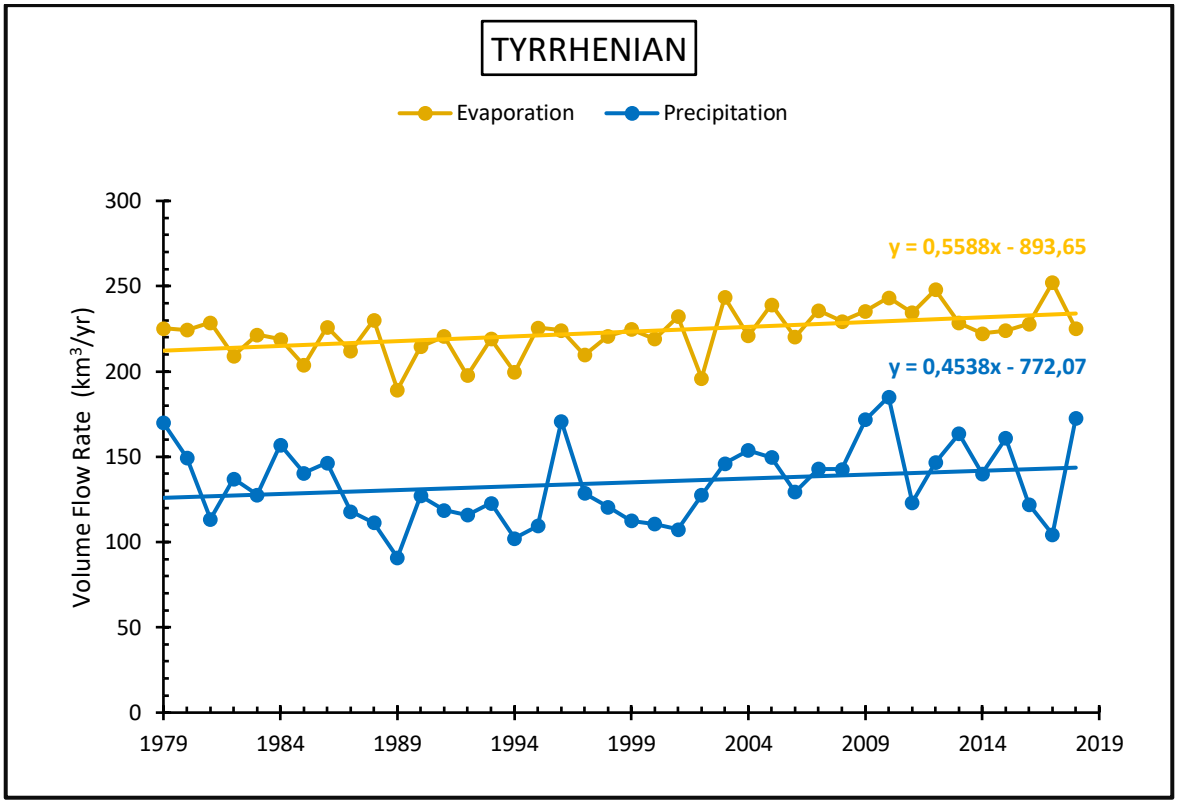

Figure 4.7. Annual time series of Evaporation and Precipitation volume flow rates for Tyrrhenian sub-basin of Mediterranean and Black Sea system for the period 1979 – 2018.

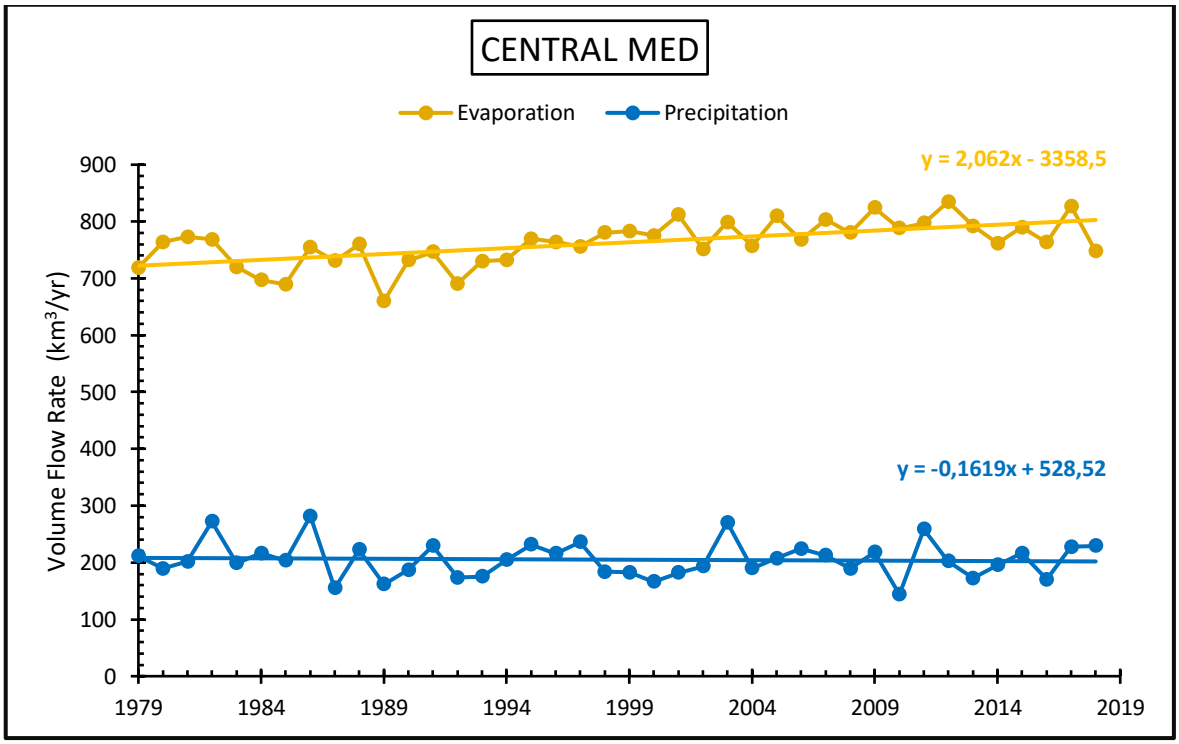

Figure 4.8. Annual time series of Evaporation and Precipitation volume flow rates for Central Med sub-basin of Mediterranean and Black Sea system for the period 1979 – 2018.

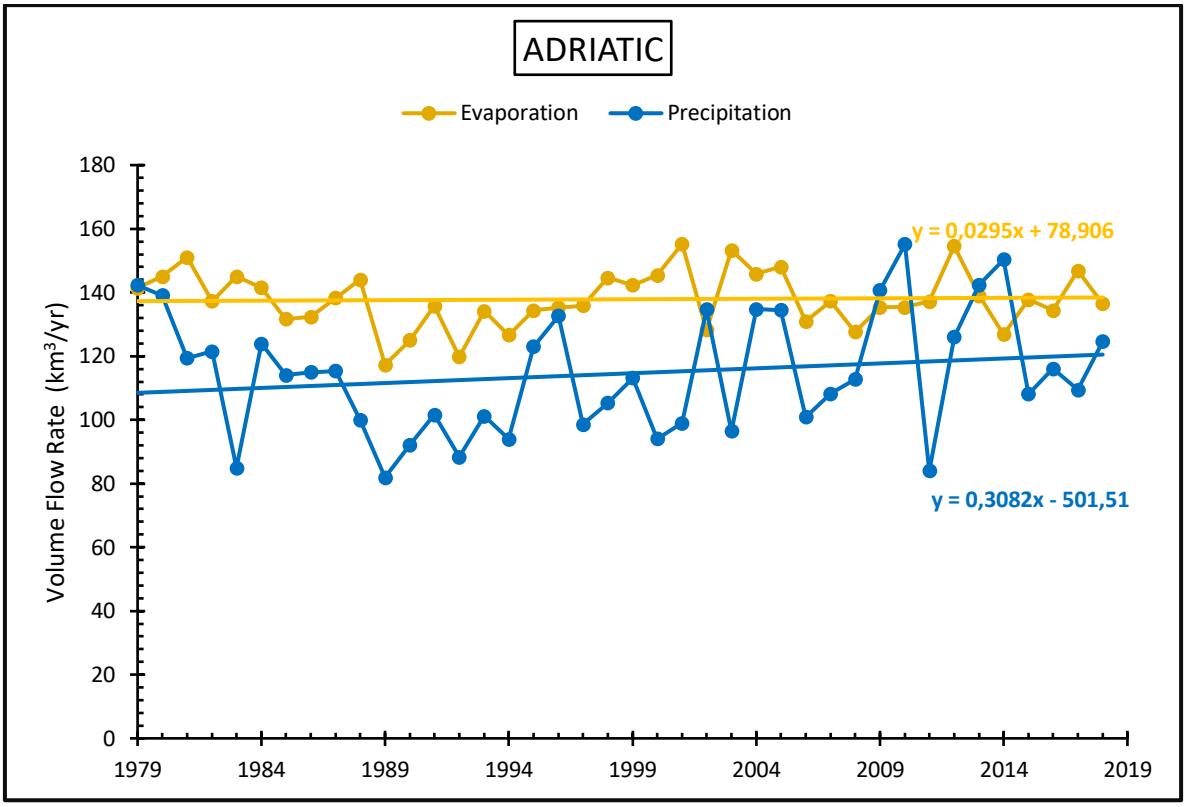

Figure 4.9. Annual time series of Evaporation and Precipitation volume flow rates for Adriatic sub-basin of Mediterranean and Black Sea system for the period 1979 – 2018.

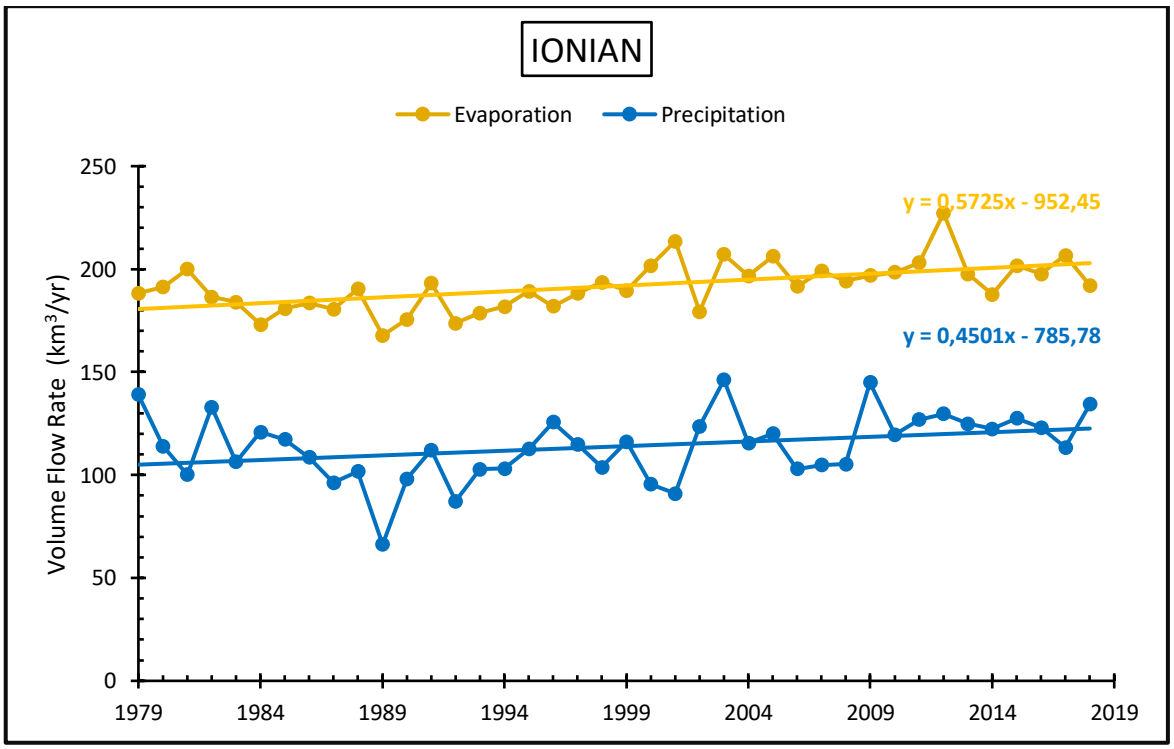

Figure 4.10. Annual time series of Evaporation and Precipitation volume flow rates for Ionian sub-basin of Mediterranean and Black Sea system for the period 1979 – 2018.

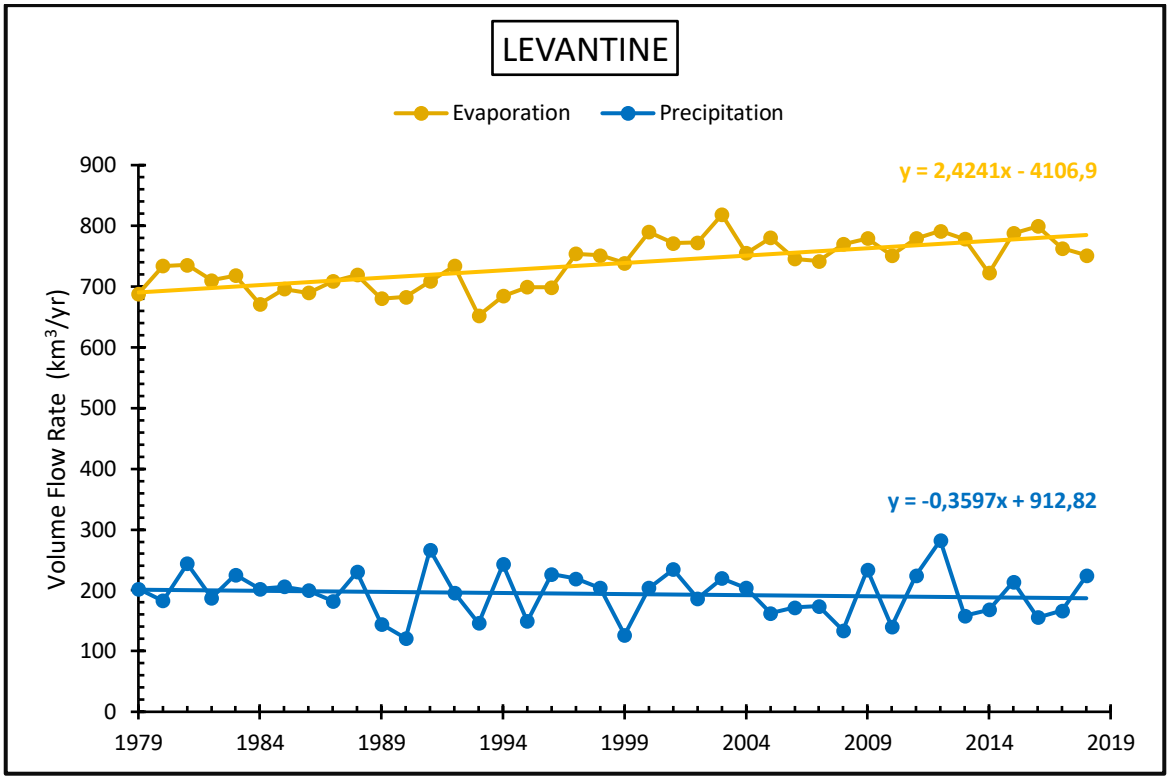

Figure 4.11. Annual time series of Evaporation and Precipitation volume flow rates for Levantine sub-basin of Mediterranean and Black Sea system for the period 1979 – 2018.

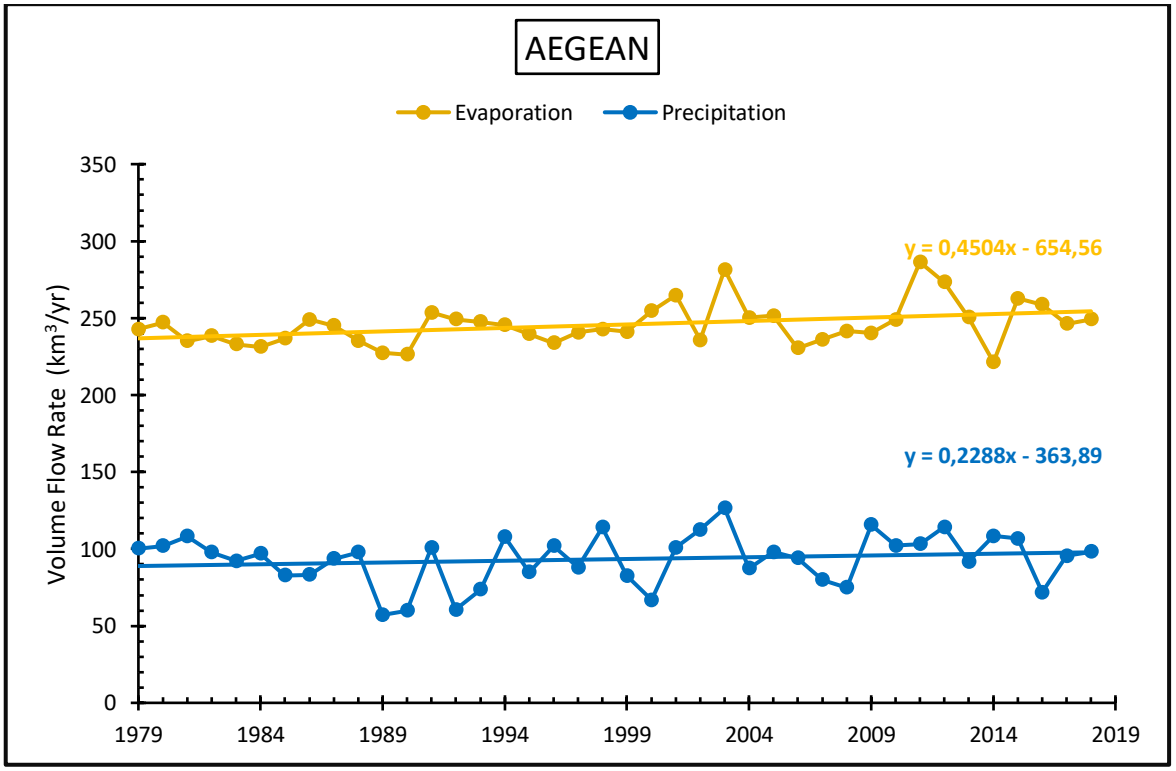

Figure 4.12. Annual time series of Evaporation and Precipitation volume flow rates for Aegean sub-basin of Mediterranean and Black Sea system for the period 1979 – 2018.

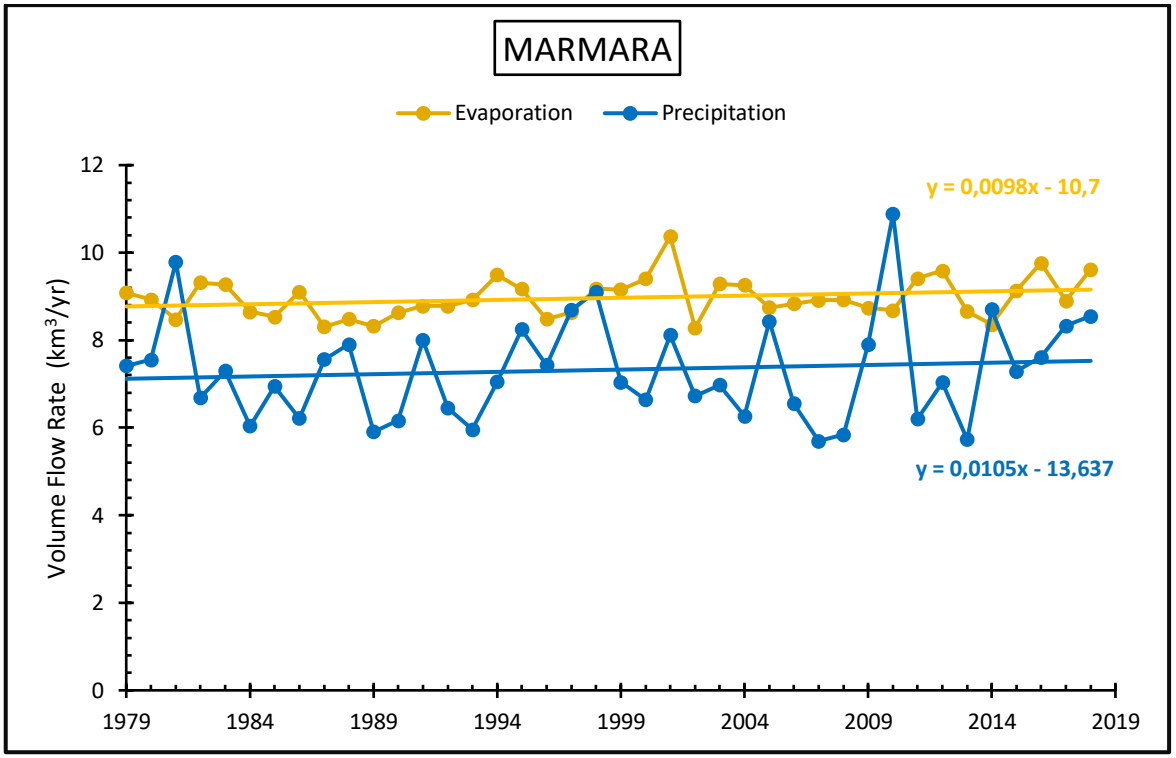

Figure 4.13. Annual time series of Evaporation and Precipitation volume flow rates for Marmara sub-basin of Mediterranean and Black Sea system for the period 1979 – 2018.

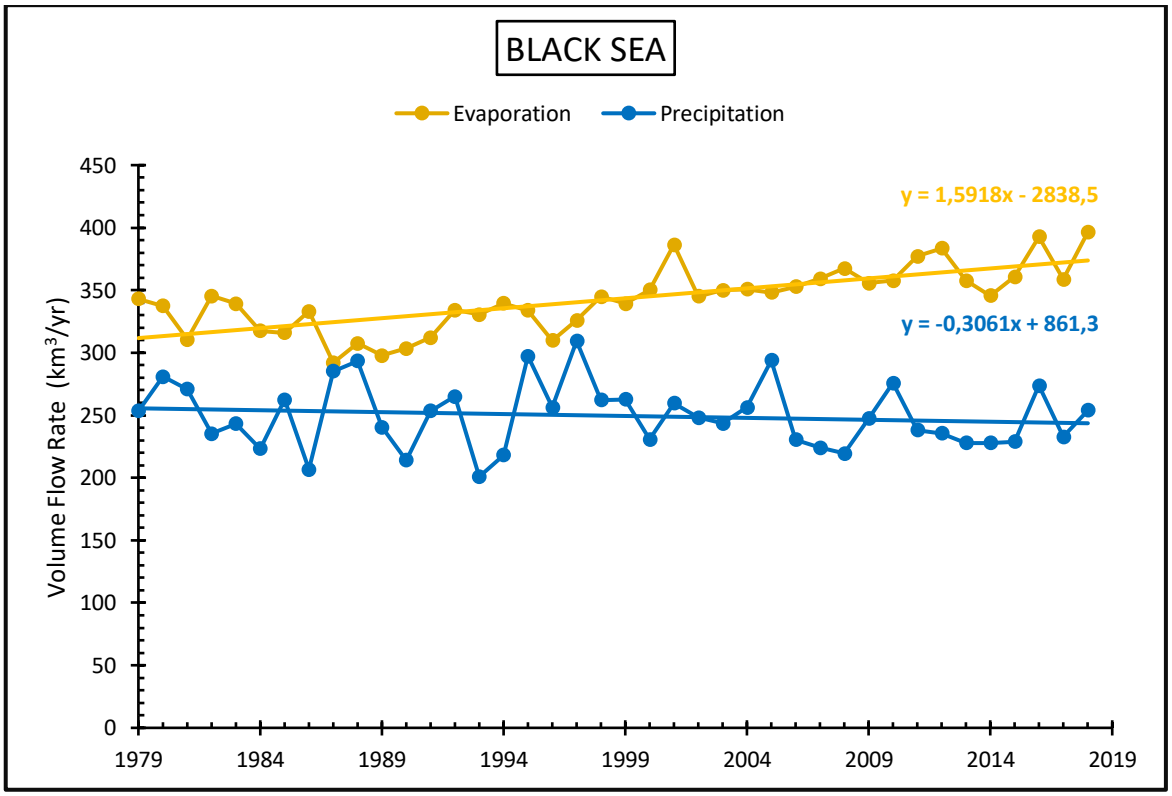

Figure 4.14. Annual time series of Evaporation and Precipitation volume flow rates for Black Sea basin of Mediterranean and Black Sea system for the period 1979 – 2018.

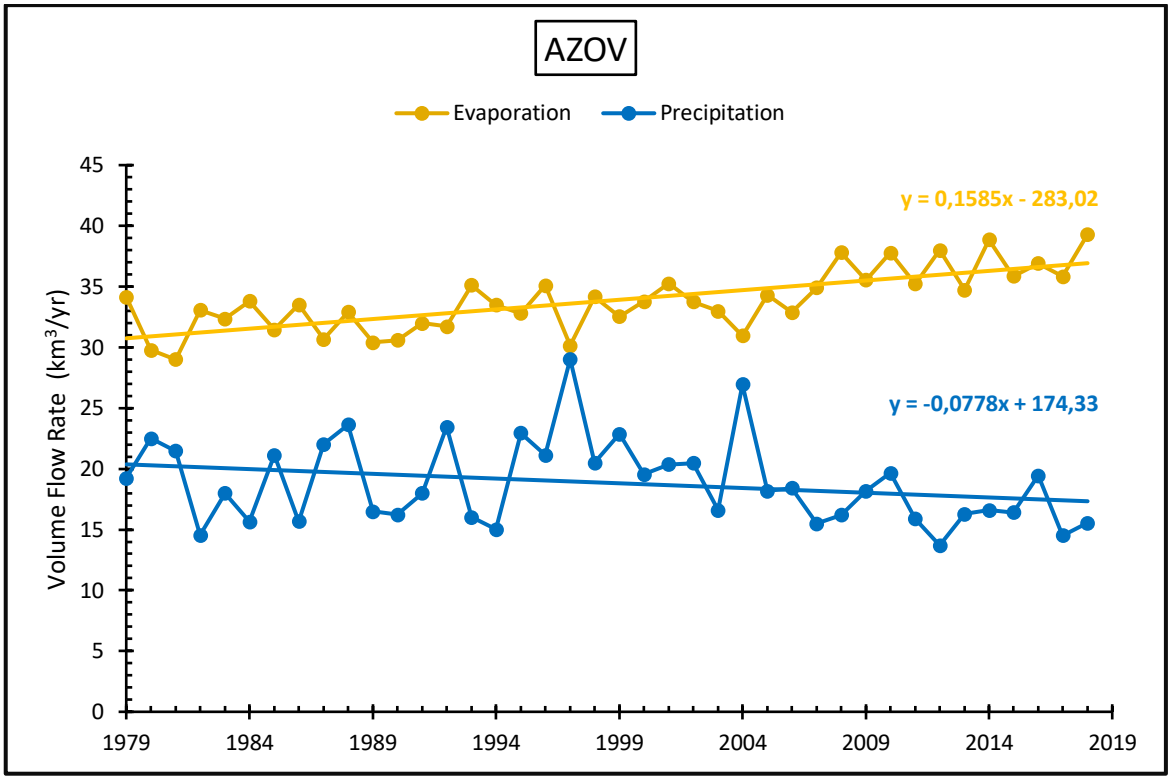

Figure 4.15. Annual time series of Evaporation and Precipitation volume flow rates for Azov sub-basin of Mediterranean and Black Sea system for the period 1979 – 2018.

4.1.4. Riverine Discharge (RD)

A quantitative assessment of the annual Riverine Discharge volume flux rate was provided for the watersheds of the 4 primary (Western Mediterranean-WMED, Central Mediterranean-CMED, Eastern Mediterranean-EMED and Black Sea-BLS) and 11 secondary marine regions of the Mediterranean and Black Sea Earth System (MBES). On the basis of measured values that cover spatially >65% and >84% of Mediterranean and Black Sea watersheds, respectively, water discharge of the MBES reached annually almost the 1 million km^3, with Mediterranean Sea (including the Marmara Sea) to provide 576 km^3 and the Black Sea (included the Azov Sea) 418 km^3. Among the watersheds of Mediterranean primary marine regions, the total water load was distributed as follows: WMED = 180 km^3; CMED = 209 km^3; and EMED = 187 km^3. The large river systems (watershed >10^4 km^2) provided >85% of the water load of both Mediterranean and Black Sea Systems.

Riverine freshwater load of the MBS reaches almost 1 million km^3/year (Table 4.2), from which on an annual basis, 418.4 km^3 are provided by the Black Sea (included the Azov) and 575.9 km^3 by the Mediterranean: the latter is allocated among the catchment of Mediterranean primary marine regions as follows: WMED= 180.1 km^3; CMED= 208.9 km^3; and EMED= 186.9 km^3 (Poulos 2019). Between the secondary marine regions, the largest amount is provided by the BLA (370.8 km^3) and the smallest by the MAR (8.1 km^3) and ALB (3.6 km^3) due to their small watersheds. Interestingly, LEV presents a relatively low value of 134.5 km^3 despite its huge catchment area due to Nile's drainage basin (2,880,000 km^2) (Table 4.2).

During the past decades, water have been modified following the regulation of river flows through dam construction for hydroelectric power and irrigation purposes. CIESM (2006) has referred that about 50% of Mediterranean catchment is dammed, causing an analogous reduction, primarily in sediment fluxes and secondarily to water discharge. For the Mediterranean catchment, Ludwig et al. (2003) have reported a continuous decrease in water discharge because of both climate change and anthropogenic water use, which in the case of the Black Sea was estimated to be about 10% (CIESM 2006).

The large rivers (>10,000 km^2) in the case of Mediterranean provide about 60% of its freshwater loads although they represent the 79% of the total catchment area, while in the case of BLS, the large river systems provide about 83%, corresponding to the 91% of BLS's catchment area. The smaller riverine freshwater potential of the Mediterranean (126 m^3/km^2) (compared to 174 m^3/km^2 of the BLS), is explained by the fact that the African part of Mediterranean's watershed (Libya and Egypt) is deprived form surface flows due to very low precipitation levels (<100 mm; Jaoshvilli 2002). Even the huge size of the Nile River used to provide about 80 km^3 that corresponds to a water yield of only 27.8 m^3/km^2. The large freshwater influx in the case of the Black Sea basin has many environmental implications, among which the most important could be considered the strong stratification of its water column with brackish waters (salinities <25 psu) at the upper layer

and the anoxic conditions developed in its lower water mass (Konovalov et al. 2005). Moreover, anthropogenic interventions (i.e. dam construction, freshwater utilization, etc.) have altered the natural flows, causing an overall reduction, which in the case of BLS accounts for about 10% of its water discharge (Jaoshvilli 2002). An analogous and even higher reduction is expected also for the Mediterranean's watershed as 40% of its water flows area is trapped, although temporarily, in reservoirs, and subsequently utilized for irrigation and watering purposes.

In the future, a further reduction is expected due to climate change, which is associated with a reducing trend of precipitation levels (Giorgi and Lionello 2008), which is going to be more pronounced at the southern Mediterranean (Xoplaki et al. 2004). Vörösmarty (1997) predicted that within the next few decades, more than 50% of the total global river flow would be dammed, having a series of environmental implications, such as the export of carbon to the atmosphere and ocean by fluvial systems and continental shelves receiving fewer nutrients that leads to reduced fish production. In addition, the variability of the freshwater discharge has significant impact on the habitats of the receiving waters, as they have to adjust their lives in different eutrophic status and sedimentological changes (e.g. channel abandonment, new depositional lobes) associated with morphological changes.

Table 4.2. Annual estimates of Riverine Discharge (RD) in km^3 and Catchment area (CA) in km^2 for the sub-basins of the Mediterranean and Black Sea System (from Poulos 2019).

SUB-BASINS	CA (in km^2)	RD (in km^3)
ALB	90,000	3.6
WEST	488,000	159.3
TYR	74,000	17.2
WMED	652,000	180.1
CEN(-Lib.)*	45,700	3.3
ION	70,400	51.1
ADR	229,000	154.5
CMED	605,400	208.9
AEG	240,000	44.3
MAR	40,000	8.1
LEV	3,159,000	134.5
EMED	3,439,600	186.9
MED	4,697,000	**575.9**
BLA	1,808,000	370.8
AZOV	590,000	47.6
BLS	2,398,000	**418.4**
MBS	7,095,000	**994.3**

**CEN (total)= 306,000 km^2*

4.1.5. Submarine Groundwater Discharge (SGD)

SGD volume flux rate of about 16 km^3/year was used for the complete Black Sea basin locally equaling values in order 3.9% of the respective river water runoff (with a total flux of about 418.4 km^3/year for the Black Sea basin) (Wang et al. 2019). It was assumed that SGD is mainly occurring on the Crimean Peninsula and the Georgian coast (Schubert et al. 2017). After dividing the shelf into 3 principal types, a SGD value of 16.4 km^3/year was evaluated, though roughly (Zektser et al. 2007). According to (Zektser et al. 2007), the following types for the entire Black Sea basin were determined (Table 4.3):

I. Plane part of coastal zone, so-called stable zone (or intensive sinking area) with wide shelf. The main aquifer is represented by Lower Quaternary alluvial deposits. In the whole module is 4–5 times less than previous, but even in some cases it is only 2–3 times less.
II. Carbonate rocks (karsts intensive processes) with module and resources equal to 30 Lt/s.km^2 and 50 m^3/s, respectively. The type of discharge is concentrated (springs, Gagra, Ganthiadi) and dissipated (Leselidze).
III. Volcanogenic rocks of folded systems with fissured circulation. The module equals 1.5–2.0 times less than described above.

Table 4.3. Summary of SDG in the Black Sea Basin (Zektser et al. 2007).

No.	Shelf Type	Shelf Surface 10^3 (km^2)	SGD (km^3/year)
I	Wide Shelf (stable area)	115.5	8.9
II	Shelf of carbonate rock (karstic systems)	3.3	4.5
III	Shelf of Volcanogenic rock (folded systems)	2.8	3.0
TOTAL		**121.6**	**16.4**

Submarine groundwater discharge to the Mediterranean Sea is formed within coastal zones of 3 continents, mostly from Europe's coasts. A major part of the groundwater discharge to the Mediterranean Sea is formed within the European continent. This is connected with favorable climate, orographic, and geologic-hydrogeological conditions. Maximum precipitation falls in winter, favoring more active recharge of groundwater. Mountainous relief of the coasts exerts a screening effect on atmospheric circulation and causes a higher wetting. A basic factor causing intensive groundwater discharge is widely developed karst. Karst hollows absorb precipitation and surface waters and often conduct them into the sea (Zektser et al. 2007). It has been reported that the submarine or coastal karst comprises 60% of the shoreline of the Mediterranean Sea

(UNESCO 2004), and most of them are in Europe (Fleury 2005; Gilli 2015). UNESCO (2004) mentioned that karstic systems account for around 75% of the freshwater input into the Mediterranean Sea with most of the flux being SGD (Figure 4.17).

Several studies have estimated the fresh groundwater discharge to the Mediterranean Sea using hydrologic approaches (Zektser et al. 2007, PNUE/PAM/PLAN BLEU 2004)**.** Zektser and Everett (2004) and Zektser et al. (2007) estimated SGD freshwater flows into the Mediterranean Sea of 52 and 68 km^3/year, respectively. Margat and Treyer (PNUE/PAM/PLAN BLEU 2004) obtained from national water statistics a total flux of 43 km^3/year with Italy, Turkey and Croatia reporting the largest contributions (Figure 4.16). Rodellas et al. (2015) reported a value in the range of 300 – 4,800 km^3/year of submarine groundwater exchanges, of which 1–25% is fresh groundwater.

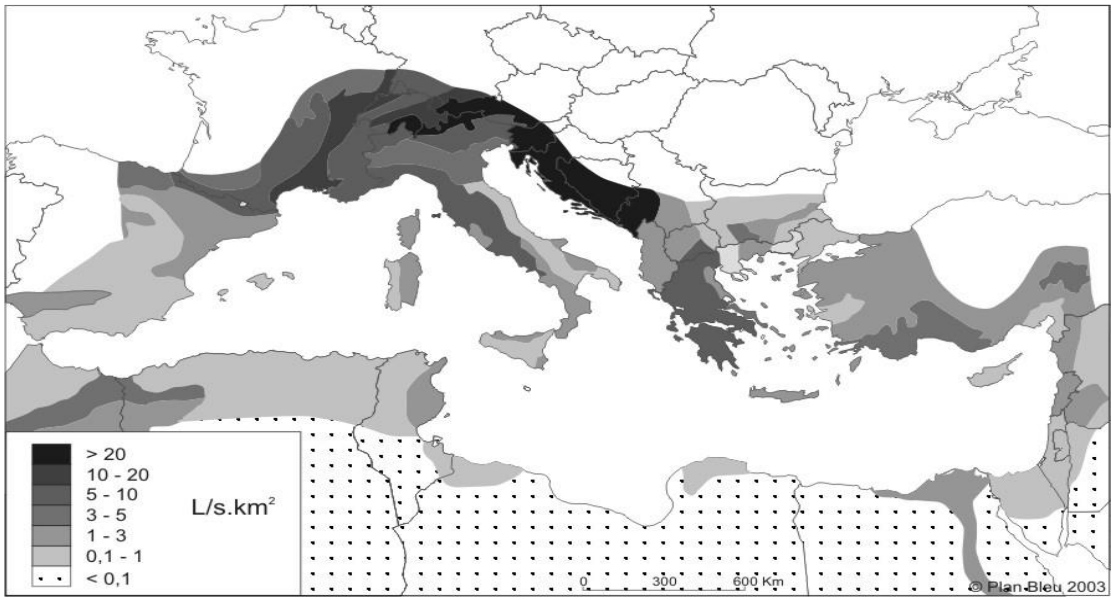

Figure 4.16. Distribution by order of specific groundwater discharge values in the Mediterranean Basin, in Lt/s km^2 (Zektser et al. 1989, 1993).

Taking into account the total Mediterranean shore length (47,227 km), our calculation results in a total SGD volume flow rate of 56.14 km^3/year (Table 4.4) which is equal to 9.75% of the respective river runoff. This figure is distributed among the continents as: discharge from the territory of Europe is 37.63 km^3/year [Italy (11.62 km^3) and Croatia (13.84 km^3)], Asia 12.46 km^3/year [Turkey (11.47 km^3)], Africa 0.59 km^3/year and the largest islands 5.46 km^3/year. This SGD estimate is in good agreement with local studies conducted along the Mediterranean Sea (Zektser et al. 2007, PNUE/PAM/PLAN BLEU 2004), reinforcing the consistency of our estimates.

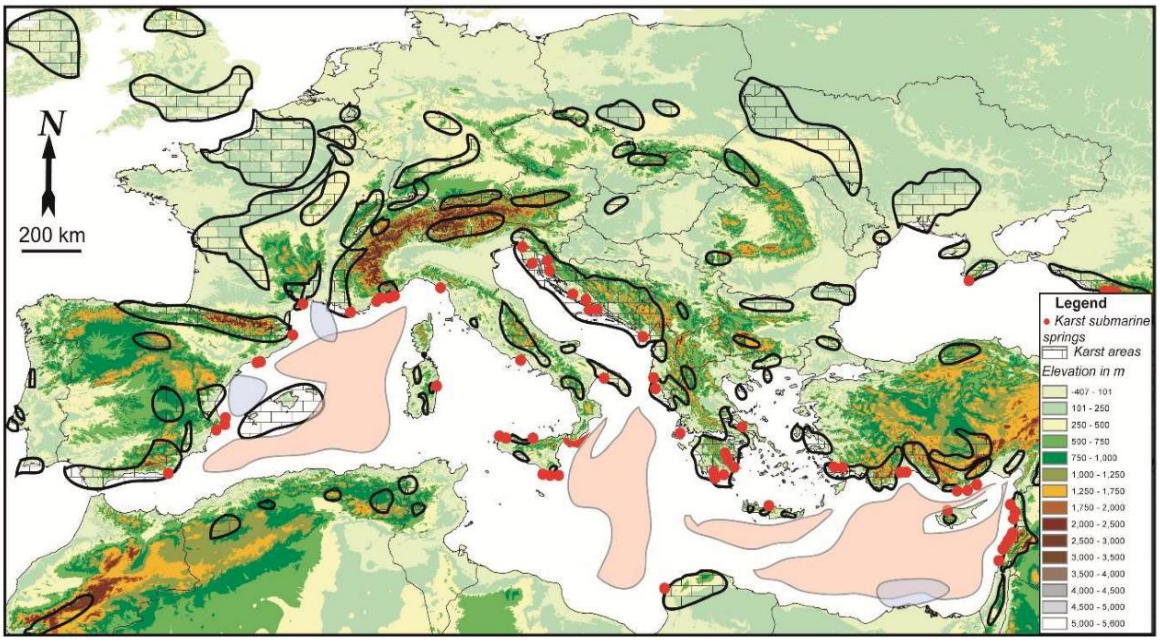

Figure 4.17. Schematic map of karst areas around the Mediterranean with the location of the main known karst submarine springs. The 3 main remaining hypersaline basins at the Messinian low stage are shown in pink with the main post-Messinian fluvial fans in grey (Bakalowicz 2018).

Table 4.4. Annual average volume flux rates of Submarine Groundwater Discharge (SGD) measured in km^3/year for all sub-basins of the Mediterranean Sea, calculated from multiplying each country's coastline (in Km), its average groundwater flux ($Lt/s.km^2$) along with an inland factor (in km) depending on its geomorphology.

Sub-basins		Country/Area	Coastline (Km)		Flux	Inland (Km)	Discharge per Year			Sum
			Total	Part	$Lt/s.km^2$		Liters	m^3	km^3	km^3
1	ADR	Albania	350	350	3	25	827,820,000,000	827,820,000	0.82782	
	ADR	Bosnia - Er	20	20	20	5	63,072,000,000	63,072,000	0.06307	
	ADR	Croatia	5,850	5,850	15	5	13,836,420,000,000	13,836,420,000	13.83642	
	ADR	Italy	1,940	390	4	20	983,923,200,000	983,923,200	0.98392	
	ADR	Italy	1,940	1,104	0.5	20	348,157,440,000	348,157,440	0.34816	**18.61066**
	ADR	Italy	1,940	446	2	20	562,602,240,000	562,602,240	0.56260	
	ADR	Monten_Yug	200	200	20	10	1,261,440,000,000	1,261,440,000	1.26144	
	ADR	Slovenia	46	46	20	25	725,328,000,000	725,328,000	0.72533	
	ADR	Corfu_N	30	30	1	2	1,892,160,000	1,892,160	0.00189	
2	AEG	TUR+Island	2,805	1,245	3	25	2,944,674,000,000	2,944,674,000	2.94467	
	AEG	TUR+Island	2,805	1,070	1	25	843,588,000,000	843,588,000	0.84359	
	AEG	TUR+Island	2,805	490	5	25	1,931,580,000,000	1,931,580,000	1.93158	**6.11447**
	AEG	GRE	10,472	944	0.5	10	148,849,920,000	148,849,920	0.14885	
	AEG	GRE	10,472	691	1	10	217,913,760,000	217,913,760	0.21791	
	AEG	GRE-Island	10,472	8,837	0.5	0.2	27,868,363,200	27,868,363	0.02787	
3	ALB	Algeria	160	60	3	5	28,382,400,000	28,382,400	0.02838	
	ALB	Algeria	160	100	0.1	5	1,576,800,000	1,576,800	0.00158	
	ALB	Morocco	512	384	0.5	5	30,274,560,000	30,274,560	0.03027	**0.27105**
	ALB	Morocco	512	128	4	5	80,732,160,000	80,732,160	0.08073	
	ALB	Spain	330	330	0.5	25	130,086,000,000	130,086,000	0.13009	
4	CEN	Sicily _S	480	480	1	25	378,432,000,000	378,432,000	0.37843	
	CEN	Libya 1	1,340	384	0.5	5	30,274,560,000	30,274,560	0.03027	
	CEN	Libya 2	1,340	956	0.05	5	7,537,104,000	7,537,104	0.00754	

	CEN	Malta	180	180	0.5	15	42,573,600,000	42,573,600	0.04257	**0.70243**
	CEN	Tunisia 1	970	660	2	5	208,137,600,000	208,137,600	0.20814	
	CEN	Tunisia 2	970	310	0.5	5	24,440,400,000	24,440,400	0.02444	
	CEN	Crete W	70	70	1	5	11,037,600,000	11,037,600	0.01104	
5	ION	Albania_S	68	68	3	25	160,833,600,000	160,833,600	0.16083	**4.14128**
	ION	Sicily _E	363	260	1	25	204,984,000,000	204,984,000	0.20498	
	ION	Sicily _E	363	103	3	25	243,615,600,000	243,615,600	0.24362	
	ION	Italy_SE	867	527	2	20	664,778,880,000	664,778,880	0.66478	
	ION	Italy_SE	867	340	0.5	20	107,222,400,000	107,222,400	0.10722	
	ION	Greece_mainland	3,362	3,362	5	5	2,650,600,800,000	2,650,600,800	2.65060	
	ION	Ionian Island	752	752	3	1	71,145,216,000	71,145,216	0.07115	
	ION	Kithira	108	108	1	1	3,405,888,000	3,405,888	0.00341	
	ION	Laconikos	220	220	5	1	34,689,600,000	34,689,600	0.03469	
6	LEV	Cyprus	789	789	1	10	248,819,040,000	248,819,040	0.24882	**5.90501**
	LEV	Egypt	950	215	0.5	5	16,950,600,000	16,950,600	0.01695	
	LEV	Egypt	950	460	1	5	72,532,800,000	72,532,800	0.07253	
	LEV	Egypt	950	275	0.05	5	2,168,100,000	2,168,100	0.00217	
	LEV	Israel	273	273	0.1	10	8,609,328,000	8,609,328	0.00861	
	LEV	Lebanon	225	225	3	25	532,170,000,000	532,170,000	0.53217	
	LEV	Libya_part	430	200	0.5	5	15,768,000,000	15,768,000	0.01577	
	LEV	Libya_part	430	230	0.05	5	1,813,320,000	1,813,320	0.00181	
	LEV	Syria	183	183	3	25	432,831,600,000	432,831,600	0.43283	
	LEV	Turkey	1,578	884	5	25	3,484,728,000,000	3,484,728,000	3.48473	
	LEV	Turkey	1,578	282	3	25	666,986,400,000	666,986,400	0.66699	
	LEV	Turkey	1,578	412	1	25	324,820,800,000	324,820,800	0.32482	
	LEV	Crete S	392	392	1	5	61,810,560,000	61,810,560	0.06181	
	LEV	Crete_E	60	60	1	5	9,460,800,000	9,460,800	0.00946	

	LEV	Rhodes_E+Karpa+k	162	162	1	5	25,544,160,000	25,544,160	0.02554	
7	MAR	Turkey	927	440	1	10	138,758,400,000	138,758,400	0.13876	**1.29061**
	MAR	Turkey	927	487	3	25	1,151,852,400,000	1,151,852,400	1.15185	
8	TYR	Cicily _N	580	580	1	25	457,272,000,000	457,272,000	0.45727	**9.69669**
	TYR	Corsica _E	400	400	3	25	946,080,000,000	946,080,000	0.94608	
	TYR	Italy	1,527	870	10	20	5,487,264,000,000	5,487,264,000	5.48726	
	TYR	Italy	1,527	657	2	20	828,766,080,000	828,766,080	0.82877	
	TYR	Sardinia _E	836	836	3	25	1,977,307,200,000	1,977,307,200	1.97731	
9	WEST	Algeria	1,040	1,040	0.1	5	16,398,720,000	16,398,720	0.01640	**9.40924**
	WEST	France (Corsica-W)	1,303	516	10	20	3,254,515,200,000	3,254,515,200	3.25452	
	WEST	France (Corsica-W)	1,303	461	5	20	1,453,809,600,000	1,453,809,600	1.45381	
	WEST	France (Corsica-W)	1,303	326	1	20	205,614,720,000	205,614,720	0.20561	
	WEST	Italy	420	420	10	20	2,649,024,000,000	2,649,024,000	2.64902	
	WEST	Sardinia 1	940	115	3	25	271,998,000,000	271,998,000	0.27200	
	WEST	Sardinia 2	940	825	1	25	650,430,000,000	650,430,000	0.65043	
	WEST	Spain 1	1,490	680	1	25	536,112,000,000	536,112,000	0.53611	
	WEST	Spain 2	1,490	810	0.5	25	319,302,000,000	319,302,000	0.31930	
	WEST	Tunisia	330	220	0.5	5	17,344,800,000	17,344,800	0.01734	
	WEST	Tunisia	330	110	2	5	34,689,600,000	34,689,600	0.03469	
TOTAL									**56.14144**	**56.14144**

4.2. TOTAL WATER BUDGET

4.2.1. Total Water Budget of each marine region

After computing averages of Evaporation, Precipitation, Riverine Discharge and Submarine Groundwater Discharge for each sub-basin, changes in the water volume of each sub-basin can be obtained from applying the Water Budget Equation in each one of them. All volume flux rates of Evaporation (E), total Precipitation (P), Riverine Discharge (RD), Submarine Groundwater Discharge (SGD) and Total Water Budget (TWB) for all sub-basins of the Mediterranean and Black Sea system are shown below in Table 4.5.

Table 4.5. Annual averaged volume flux rates of Evaporation (E), total Precipitation (P), Riverine Discharge (RD), Submarine Groundwater Discharge (SGD) and Total Water Budget (TWB) for all sub-basins of the Mediterranean and Black Sea system along with their Sea Surface Area (SSA in km^2). All volume flux rates were calculated in km^3/year for the 40-year period.

BASINS	SSA	E	P	RD	SGD	TWB
ALB	54,520.22	43.56	20.71	3.60	0.27	-18.98
WEST	571,094.73	617.83	288.18	159.30	9.41	-160.95
TYR	217,366.20	223.08	134.77	17.20	9.70	-61.42
CEN	599,787.98	762.48	205.05	3.30	0.70	-553.43
ADR	137,551.79	137.87	114.49	154.50	18.61	149.74
ION	168,894.27	191.74	113.79	51.10	4.14	-22.72
LEV	568,522.03	737.65	193.99	134.50	5.91	-403.26
AEG	186,945.31	245.61	93.35	44.30	6.11	-101.85
MAR	11,022.78	8.96	7.32	8.10	1.29	7.75
BLA	420,565.50	342.71	249.56	370.80	16.00	293.64
AZO	36,761.05	33.83	18.85	47.60	0.40	33.01

Assuming steady-state conditions, Precipitation, River Discharge and Submarine Groundwater Discharge are considered as water inputs. Evaporation is considered as water output for the closed basin. In the sub-basins of ALB, CEN, WEST, TYR, LEV, AEG, ION, the results of Water Budget Equation indicate a water deficit. As for the ADR, MAR, BLA and AZO sub-basins of MBS, the results of Water Budget Equation indicate a water surplus (Figure. 4.2.3). So, the Total Water Budget of Black Sea System, Marmara and Adriatic sub-basins is positive and as for the remaining sub-basins, their Total Water Budget is negative.

These results indicate that the excessive water quantity from the Black Sea is heading towards the Mediterranean Sea basin, specifically through the Marmara sub-basin and finally pouring itself into the Aegean Sea. Also, the excessive water quantity from the Adriatic sub-basin is heading towards the Ionian Sea.

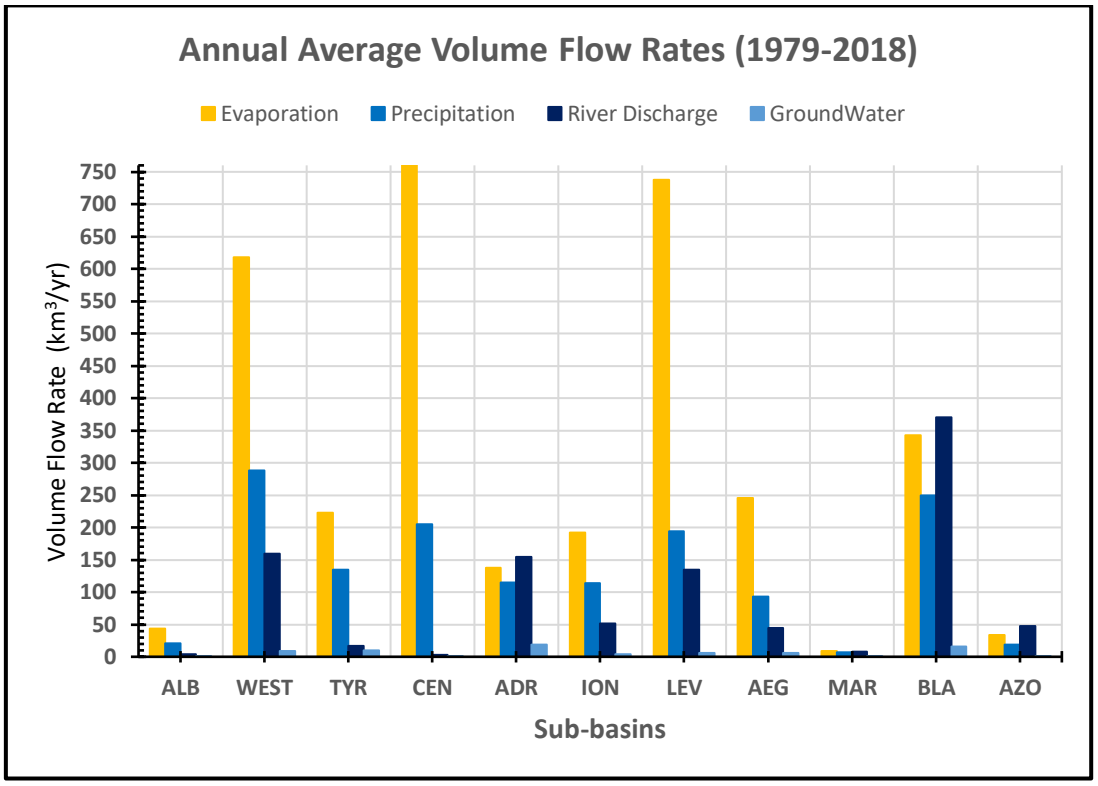

Figure 4.18. Annual average Volume Flow rates of each sub-basin for the 40-year period (1979-2018).

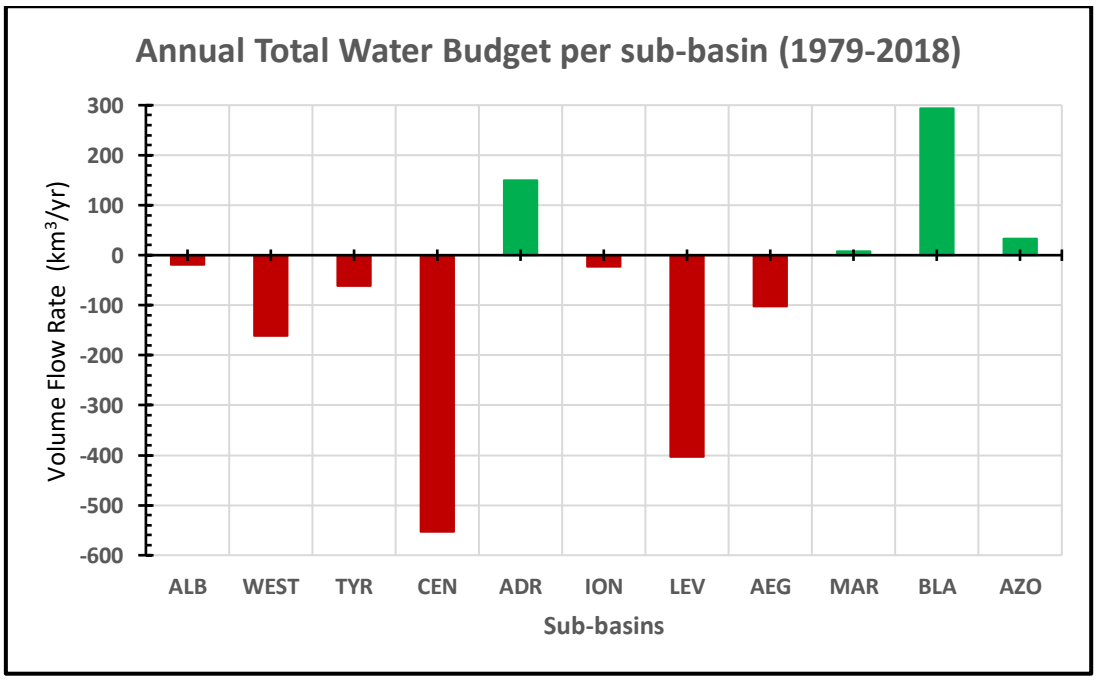

Figure 4.19. Annual average Total Water Budget of each sub-basin for the 40-year period (1979-2018).

4.2.2. Total Water Budget of Mediterranean & Black Sea (MBS) System

The Mediterranean Sea is well known for its intense Evaporation, which is largely exceeding Precipitation and Riverine Discharge. The analysis of our ERA5 data sets in this study confirms previous findings (Mariotti et al. 2002, Tanhua et al. 2013). This pattern seems to get reinforced due to strong positive Evaporation trends combined with statistically not-significant (at a=0.05 significance level) changes for Precipitation (Table 4.1). Specifically, for the period 1979–2018, the time series of Evaporation data indicate a statistically significant (at confidence level 95%) increase of Evaporation for all sub-basins apart from the sub-basins of ADR and MAR. The time series of Precipitation data don't indicate statistically significant changes for Precipitation except for an increase in the sub-basin of ION which is still lower than its Evaporation counterpart. Adding together the Riverine Discharge, the Submarine Groundwater Discharge, the total Precipitation and deducting the Evaporation from their sum, the Total Water Budget of the Black Sea system is positive and its Mediterranean Sea counter-part is negative. It is crystal clear that the water cycle has changed and continues to change rapidly, with the Black Sea gaining water quantities and the Mediterranean basin becoming on average a dryer region. Combined as one system, the Total Water Budget for MBS is negative (Tables 4.6 and 4.7), with the Black Sea not being able enough to counterbalance the excessive water loss of the Mediterranean Sea.

Table 4.6. Annual averaged volume flux rates of Evaporation (E), total Precipitation (P), Riverine Discharge (RD), Submarine Groundwater Discharge (SGD) and Total Water Budget (TWB) for the Mediterranean and Black Sea system (MBS) along with their Sea Surface Area (SSA in km^2). All volume flux rates were calculated in km^3/year for the 40-year period.

AREA	SSA	E	P	RD	SGD	TWB
WMED	842,981.16	884.48	443.65	180.10	19.38	-241.35
CMED	906,234.03	1,092.09	433.33	208.90	23.45	-426.41
EMED	766,490.11	992.23	294.66	186.90	13.31	-497.35
MED	2,515,705.31	2,968.80	1,171.64	575.90	56.14	-1,165.11
BLS	457,326.55	376.55	268.41	418.40	16.40	326.66
MBS	2,973,031.86	3,345.35	1,440.05	994.30	72.54	-838.45

On an annual mean basis, the Water Budget Equation for the Total Mediterranean Sea is:

$$TWB = P - E + (RD + SGD) + G + B,$$

where G and B are the total water inputs from the Gibraltar Strait and from the Black Sea, respectively. Using the Water Budget Equation and treating Mediterranean Sea as a 'box model', its TWB is negative, where E > (P + RD + SGD), meaning that the Mediterranean Sea is becoming more salty than the Atlantic Ocean, thus, water quantities flow into the Mediterranean Sea through the Strait of Gibraltar. The Gibraltar strait plays an important role in the Mediterranean Sea water circulation with the Atlantic water (AW) inflow, whose net value accounts roughly for 0.04 Sv per second (=1,260 km^3/year), counterbalancing the Mediterranean Water Budget deficit. Specifically, the inflow of Atlantic Water (AW) has been estimated to be 0.72 – 0.92 Sv and the outflow of Mediterranean Overflow Water (MOW) to be 0.68 – 0.88 Sv (Tsimplis and Bryden 2000; Baschek et al. 2001; García Lafuente et al. 2011, Tanhua et al. 2013). As for the Black Sea, its TWB is positive, where E < (P + RD + SGD), meaning that the Black Sea is becoming less salty than the Mediterranean Sea, therefore, water quantities of 327 km^3/year flow out of the Black Sea through Bosporus into the Mediterranean Sea (BSW inflow of 0.039 Sv and NAS outflow of 0.030 Sv, Tanhua 2013).

The Total Water Budget deficit is compatible with the observed changes in the various components of the water budget, mostly attributed to the increase of Evaporation, driven by surface warming over the last decades (Mariotti et al. 2002, Romanou et al. 2010) combined with a decrease in Precipitation observed from 1960s to 1990s and mainly associated with the North Atlantic Oscillation (NAO) (Krahmann and Schott 1998, Mariotti et al. 2002, Mariotti 2010, Tsimplis and Josey 2001) and a reduction of Riverine Discharge (RD) attributed to climate change and river damming of Mediterranean rivers (Rohling and Bryden 1992, 2004, Ludwig et al. 2009). Our results indicate that the sum of Precipitation, Riverine Discharge and Submarine Groundwater Discharge cannot exceed the extreme Evaporation in the whole Mediterranean Sea basin. The 'transition' toward drier conditions has already started to occur, therefore, the Mediterranean Sea is classified surely as an Evaporation (concentration) basin.

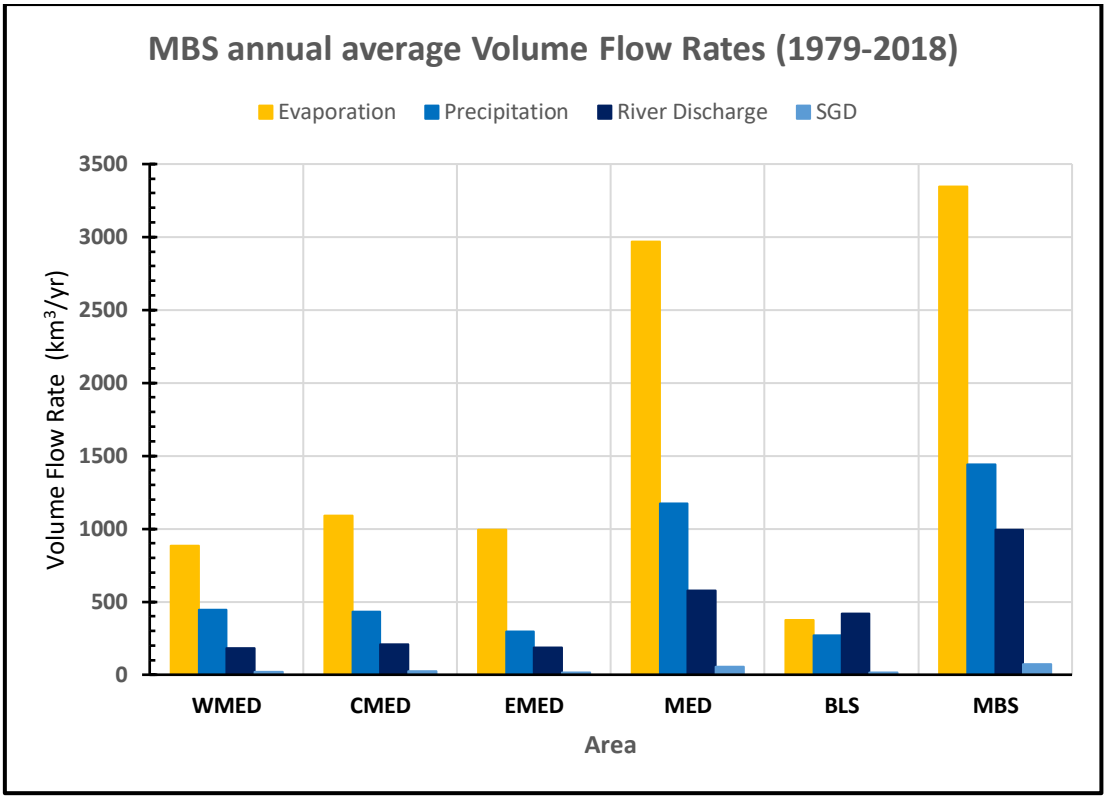

Figure 4.20. Annual average Volume Flow rates of MBS from 1979 to 2018.

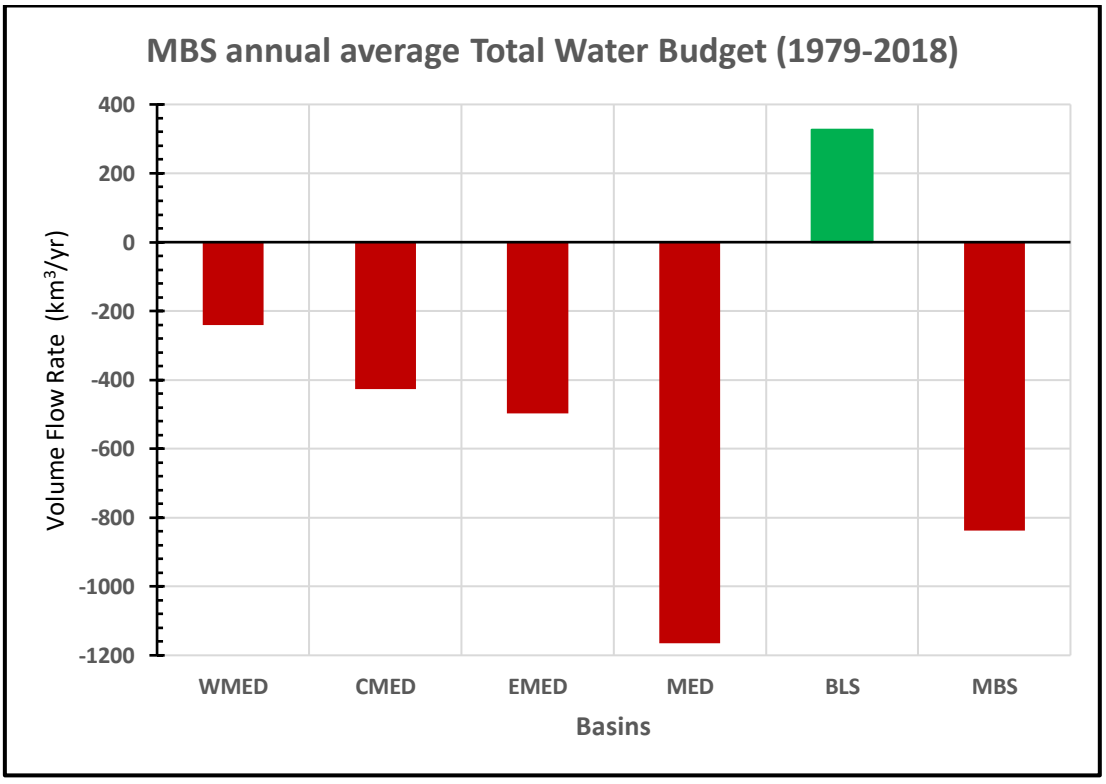

Figure 4.21. Annual average Total Water Budget of MBS from 1979 to 2018.

Table 4.7. Annual volume flux rates of Evaporation (E), total Precipitation (P), Riverine Discharge (RD), Submarine Groundwater Discharge (SGD) and Total Water Budget (TWB) for all sub-basins of the Mediterranean and Black Sea system along with their Sea Surface Area (SSA in km^2). All volume flux rates were calculated in km^3/year.

Sub-Basins			Sea Surface Area	Evaporation	Total Precipitation	Riverine Discharge	Groundwater Discharge	Total Water Budget
				E	P	RD	SGD	TWB
			SSA	OUTPUT	INPUT	INPUT	INPUT	+/-
			km^2	km^3/year	km^3/year	km^3/year	km^3/year	km^3/year
	Western Mediterranean	WMED	842,981.16	**884.48**	**443.65**	**180.10**	**19.38**	**-241.35**
1	WestMED	WEST	571,094.73	617.83	288.18	159.30	9.41	-160.95
2	Alboran	ALB	54,520.22	43.56	20.71	3.60	0.27	-18.98
3	Tyrrhenian	TYR	217,366.20	223.08	134.77	17.20	9.70	-61.42
	Central Mediterranean	CMED	906,234.03	**1,092.09**	**433.33**	**208.90**	**23.45**	**-426.41**
4	Adriatic	ADR	137,551.79	137.87	114.49	154.50	18.61	149.74
5	Ionian	ION	168,894.27	191.74	113.79	51.10	4.14	-22.72
6	CentralMED	CEN	599,787.98	762.48	205.05	3.30	0.70	-553.43
	Eastern Mediterranean	EMED	766,490.11	**992.23**	**294.66**	**186.90**	**13.31**	**-497.35**
7	Levantine	LEV	568,522.03	737.65	193.99	134.50	5.91	-403.26
8	Aegean	AEG	186,945.31	245.61	93.35	44.30	6.11	-101.85
9	Marmara	MAR	11,022.78	8.96	7.32	8.10	1.29	7.75
MEDITERRANEAN SEA		MED	2,515,705.31	**2,968.80**	**1,171.64**	**575.90**	**56.14**	**-1,165.11**
10	Black Sea	BLA	420,565.50	342.71	249.56	370.80	16.00	293.64
11	Azov Sea	AZOV	36,761.05	33.83	18.85	47.60	0.40	33.01
BLACK SEA (total)		BLS	457,326.55	**376.55**	**268.41**	**418.40**	**16.40**	**326.66**
Med & Black Sea System		**MBS**	2,973,031.86	**3,345.35**	**1,440.05**	**994.30**	**72.54**	**-838.45**

The relationship between E, P, RD and SGD with TWB could be further investigated through their percentage ratios (E/TWB, P/TWB, RD/TWB and SGD/TWB) which are demonstrated in Table 4.8) of each MBS sub-basin. The contribution of Evaporation present ratios ranging from 32% and up to 79%, which show its strongest role among all the components in determining each sub-basin's TWB. The contribution of Precipitation presents ratios between 18% and 35% in all sub-basins. The contribution of RD presents ratios between 4.5% and 47% in all sub-basins apart from the petty 0.3% in CEN. The contribution of SGD presents ratios from 5% and below in the entire MBS, which shows its weakest role among all the components in determining each sub-basin's TWB. The differences between the E/TWB, P/TWB, RD/TWB and SGD/TWB ratios within the MBS are related to different hydromorphological conditions, induced by climate and geomorphological variability.

Table 4.8. Annual averaged volume flux rates of Evaporation (E), total Precipitation (P), Riverine Discharge (RD), Submarine Groundwater Discharge (SGD) and Total Water Budget (TWB) for all sub-basins of the Mediterranean and Black Sea system along with their percentage of contribution in the TWB (% of TWB). All volume flux rates were calculated in km^3/year for the 40-year period.

BASINS	TWB (km^3)	E (km^3)	E/TWB (%)	P (km^3)	P/TWB (%)	RD (km^3)	RD/TWB (%)	SGD (km^3)	SGD/TWB (%)
ALB	-18.98	43.56	63.93	20.71	30.39	3.60	5.28	0.27	0.40
WEST	-160.95	617.83	57.49	288.18	26.81	159.30	14.82	9.41	0.88
TYR	-61.42	223.08	57.98	134.77	35.03	17.20	4.47	9.70	2.52
CEN	-553.43	762.48	78.48	205.05	21.11	3.30	0.34	0.70	0.07
ADR	149.74	137.87	32.40	114.49	26.91	154.50	36.31	18.61	4.37
ION	-22.72	191.74	53.15	113.79	31.54	51.10	14.16	4.14	1.15
LEV	-403.26	737.65	68.81	193.99	18.10	134.50	12.55	5.91	0.55
AEG	-101.85	245.61	63.08	93.35	23.97	44.30	11.38	6.11	1.57
MAR	7.75	8.96	34.90	7.32	28.52	8.10	31.55	1.29	5.03
MED	-1,165.12	2,968.78	62.21	1,171.65	24.55	575.9	12.07	56.14	1.18
BLA	293.64	342.71	35.00	249.56	25.49	370.80	37.87	16.00	1.63
AZO	33.01	33.83	33.60	18.85	18.72	47.60	47.28	0.40	0.40
BLS	326.65	376.54	34.87	268.41	24.86	418.4	38.75	16.4	1.52
MBS	-838.45	3,345.4	57.16	1,440.1	24.61	994.3	16.99	72.54	1.24

The Mediterranean Sea also receives significant amounts of freshwater from Riverine Discharge. Significant temporal changes and variations in the RD to the Mediterranean is evident. During the past decades, the construction of river dams for irrigation and watering purposes have had a great impact, especially in RD, as most of water is trapped in reservoirs. In the case of the Mediterranean Sea basin, more than 40% of its watershed (excluding the Nile) is dammed; this becomes 80% when the Nile's watershed is included in the analysis (Poulos and Collins 2002). Similarly, on the basis of measured flows, an equal reduction has been reposted for the BLS watershed by Jahosvilli (2002).

In addition to the RD to the Mediterranean Sea, an often overlooked source of freshwater is provided by SGD. Although the importance of SGD to the Mediterranean Sea is currently poorly constrained, its magnitude is likely similar to the RD (Tanhua et al. 2013). SGD is likely an important source of freshwater, nutrients, trace metals, alkalinity etc. to the Mediterranean System (Moore 2006a,b), particularly since the Mediterranean Sea is landlocked.

In terms of water mass exchanges, the inflow of Atlantic Water (AW) has been estimated to be 0.72 – 0.92 Sv and the outflow of Mediterranean Overflow Water (MOW) to be 0.68 – 0.88 Sv (Tsimplis and Bryden 2000; Baschek et al. 2001; García Lafuente et al. 2011, Tanhua et al. 2013). Thus, AW inflow is 25,859.52 km^3/year ±12.5% and the MOW is 24,598.08 ± 12.8%, which accounts to a net influx of 1,261.44 km^3/year ± 25.3%.

Moreover, the exchange between the Mediterranean (Aegean) and the Black Sea through the Marmara Sea, based on estimates at the Dardanelles strait, have been estimated a Black Sea Water (BSW) outflow of 0.039 Sv to the Aegean and an inflow from the Aegean of 0.030 Sv (Tanhua 2013); this exchange of 283.8 km^3/year is in the form of two layers with the top (outflowing) to reach a depth of ~25 m. The latter value of Black Sea outflow is comparable with the estimated surplus of the Black Sea that equals to 326.7 km^3/year.

The Evaporation is the second largest term in the total water budget. However, in terms of freshwater content, Precipitation is the dominating source, followed by Riverine Discharge and SGD input. Combined as one system, the Total Water Budget for MBS has a deficit of 838.5 km^3/year. When considering the net influx at Gibraltar Straits, 1,261.5 +/- 319.1 km^3/year, then the aforementioned deficit of freshwater (838.5 km^3) for the entire MBS is close to the lower value of the range of the net AW influx, i.e., from 942.4 to 1,580.6 km^3/year. Moreover, while Evaporation and Precipitation datasets are both state-of-the-art (ERA5) and SGD's contribution in adjusting the TWB is pretty weak (<5% of TWB), the water surplus of >100 km^3/year could be explained by the uncertainties regarding the quantitative assessment of the RD, as it may be much lower due to several factors (e.g. damming, water use, data quality). Also, the available quantitative assessment of the water exchange in the strait of Gibraltar could not be that accurate as it has been based on mathematical simulations and/or short periods of field data and not to a long interannual period of flow measurements.

CHAPTER 5 : SYNOPSIS AND CONCLUSIONS

Mediterranean-averaged annual total Precipitation for the period 1979–2018 ranges among datasets from 200 to 1000 mm per year, with a seasonal cycle of maximum from September to January and minimum from May to August. Evaporation has an annual mean in the range of 400 to 1700 mm per year with a mean seasonal cycle of maximum from November to February and minimum from May to July. Annual Riverine Discharge of the MBS reached almost 1 million km^3/year, from which on an annual basis, 418.4 km^3 are provided by the Black Sea (included the Azov) and 575.9 km^3 by the Mediterranean Sea; the latter is allocated among the catchment of MED primary marine regions as follows: WMED = 180.1 km^3, CMED = 208.9 km^3, and EMED = 186.9 km^3. Submarine Groundwater Discharge (SGD) rates of 16.4 km^3/year and 56.14 km^3/year were used for the total Black Sea basin and the total Mediterranean Sea basin, respectively.

The analysis of the Water Budget Equation components, derived from various data sets, showed that in total the Evaporation exceeds the sum of Precipitation, Riverine Discharge and Submarine Groundwater Discharge in the Mediterranean and Black Sea system (MBS). The contribution of Evaporation present ratios ranging from 32% and up to 79%, which show its strongest role among all the components in determining each sub-basin's TWB. The contribution of Precipitation presents ratios between 18% and 35% in all sub-basins. The contribution of Riverine Discharge (RD) presents ratios between 4.5% and 47% in all sub-basins apart from the petty 0.3% in CEN. The contribution of Submarine Groundwater Discharge (SGD) presents ratios from 5% and below in the entire MBS, which shows its weakest role among all the components in determining each sub-basin's TWB.

The Mediterranean Sea exhibits an annual water budget deficit of 1,165.1 km^3, while the Black Sea a surplus of 326.7 km^3, over the period from 1979 to 2018. Therefore, the MBS is characterized as an Evaporation (concentration) basin, which has important implications for the circulation and the biogeochemistry of the sea, when the Black Sea as a dilution basin. Combined as one system, the Total Water Budget for MBS has a deficit of 838.5 km^3/year.

The water exchange between the Mediterranean (Aegean) and the Black Sea through the Marmara Sea, estimated at the Dardanelles strait to be in the order of 0.009 Sv (=238.8 Km^3/year) (Black Sea Water outflow = 0.039 Sv and the influx from the Aegean to Black Sea = 0.030 Sv; after Tanhua 2013) is comparable with the estimated surplus of the Black Sea that equals to 326.6 km^3/year. In addition, the exchange through the Strait of Gibraltar estimated on average 1,261.5 +/- 319.1 km^3/year (Atlantic Water inflow = 0.72-0.92 Sv and Mediterranean Overflow Water (MOW) = 0.68-0.88 Sv after Tsimplis and Bryden 2000, Baschek et al. 2001, García Lafuente et al. 2011, Tanhua et al. 2013) is also comparable to the estimated value of freshwater deficit (838.5

km^3) for the entire MBS; the latter value is close to the lower value of the range of the net water exchange that ranges from 942.3 to 1,580.6 km^3/year. While Evaporation and Precipitation datasets are both state-of-the-art (ERA5) and SGD's contribution in adjusting the TWB is pretty weak (<5% of TWB), the water surplus of >100 km^3/year could be explained by the uncertainties regarding the quantitative assessment of the RD, as it may be much lower due to several factors (e.g. damming, water use, data quality). Also, the available quantitative assessment of the water exchange in the strait of Gibraltar could not be that accurate as it has been based on mathematical simulations and/or short periods of field data and not to a long interannual period of flow measurements.

REFERENCES

Adloff, F., Somot, S., Sevault, F., Jorda, G., Aznar, R., Déqué, M., Herrmann, M., Marcos, M., Dubois, C., Padorno, E., Alvarez-Fanjul, E., Gomis, D., 2015. Mediterranean Sea response to climate change in an ensemble of twenty first century scenarios. *Climate Dynamics,* 45**,** 2775-2802.

Alpert, P., Baldi, M., Ilani, R., Krichak, S., Price, C., Rodó, X., et al., 2006a. Chapter 2. Relations between climate variability in the Mediterranean region and the tropics: ENSO, south Asian and African monsoons, hurricanes and Saharan dust. Dev. Earth Environ. Sci. 4 (C), 149–177.

Alpert, P., Ilani, R., da-Silva, A., Rudack, A., Mandel, M., 2006b. Seasonal prediction for Israel winter precipitation based on northern Hemispheric EOF, MERCHAVIM special issue in honour of Prof. Arie Bitan, 397–412.

Angelucci, M. G., N. Pinardi, and S. Castellari, 1998. Air–sea fluxes from operational analyses fields: Intercomparison between ECMWF and NCEP analyses over the Mediterranean area. *Phys. Chem. Earth,* 23, 569–574.

Arpe, K., and E. Roeckner, 1999. Simulation of the hydrologic cycle over Europe: Model validation and impacts of increasing greenhouse gases. *Adv. Water Res.,* 23, 105–119.

Artale V., Calmanti S., Malanotte-Rizzoli P., Pisacane G., Rupolo V., Tsimplis M., 2006. Developments in Earth and Environmental Sciences, Volume 4, Pages 283-323.

Astraldi, M., Balopoulos, S., Candela, J., Font, J., Gacic, M., Gas-parini, G.P., Manca, B., Theocharis, A., Tintoré, J., 1999. The role of straits and channels in understanding the characteristics of Mediterranean circulation. Prog. Oceanogr. 44, 65—108.

Bakalowicz M., 2018. Coastal Karst Groundwater in the Mediterranean: A Resource to Be Preferably Exploited Onshore, Not from Karst Submarine Springs.

Bakalowicz, M., 2015. Karst and karst groundwater resources in the Mediterranean. *Environmental Earth Sciences* 74, 5–14.

Bèranger, K., Mortier, L., Crèpon, M., 2002. Seasonal transport variability through Gibraltar, Sicily and Corsica Straits. In: The 2nd Meeting on the Physical Oceanography of Sea Straits, Ville-franche, France, April 2002, 77—81.

Bethoux, J.P., Durieu de Madron, X., Nyffeler, F., Tailliez, D., 2002. Deep water in the western Mediterranean: peculiar 1999 and 2000 characteristics, shelf formation hypothesis, variability since 1970 and geochemical inferences. J. Mar. Syst. 33 (34), 117—131.

Bethoux, J. & Gentili, B., 1999. Functioning of the Mediterranean Sea: past and present changes related to freshwater input and climate changes. *Jour. of Marine Systems,* 20**,** 33-47.

Bethoux, Gentili, and D. Taillez, 1998. Warming and freshwater budget change in the Mediterranean since the 1940s, their possible relation to greenhouse effect. *Geophys. Res. Lett.,* 25, 1023–1026.

Bethoux, J. P., 1979. Budgets of the Mediterranean Sea: Their dependence on the local climate and on the characteristics of the Atlantic waters. *Oceanol. Acta,* 2, 157–163.

Borghini, M., Bryden, H., Schroeder, K., Sparnocchia, S. & Vetrano, A. 2014. The Mediterranean is becoming saltier. *Ocean Science,* 10**,** 693-700.

Bormans, M., Garrett, C., 1989a. The effects of rotation on the surface inflow through the strait of Gibraltar. J. Phys. Oceanogr. 19, 1535—1542.

Bormans, M., Garrett, C., 1989b. The effects of non rectangular cross section, friction, and barotropic fluctuations on the exchange through the Strait of Gibraltar. J. Phys. Oceanogr. 19, 1543—1557.

Bosc, E., Bricaud, A. and Antoine, D., 2004. Seasonal and interannual variability in algal biomass and primary production in the Mediterranean Sea, as derived from 4 years of SeaWiFS observations. *Global Biogeochemical Cycles* 18, GB1005.

Boukthir, M., and B. Barnier, 2000. Seasonal and inter-annual variations in the surface freshwater flux in the Mediterranean Sea from the ECMWF re-analysis project. *J. Mar. Syst.,* 24, 343–354.

Bouraoui, F., Grizzetti, B. & Aloe, A., 2010. Estimation of water fluxes into the Mediterranean Sea. *Journal of Geophysical Research* 115.

Bouttes, N., Gregory, J.M., Kuhlbrodt, T., Smith, R.S., 2013. The drivers of projected North Atlantic sea level change. Clim. Dyn.

Brody, L. R., Nestor, M.J.R., 1980. Regional Forecasting Aids for the Mediterranean Basin. Handbook for Forecasters in the Mediterranean, Naval Research Laboratory. Part 2

Bryden, H. L. , Candela, J., and Kinder, T. H., 1994. Exchange through the Strait of Gibraltar. *Progress in Oceanography* 33: 201–48.

Bryden, H. L. and Kinder, T. H., 1991. Steady two-layer exchange through the Strait of Gibraltar. *Deep-Sea Research* 38: S445–S463.

Bryden, H. L., and T. H. Kinder, 1991a. Recent progress in strait dynamics. *Rev. Geophys.* (Suppl.), 617–631.

Burnett, W. C., Bokuniewicz, H., Huettel, M., Moore,W. S. and Taniguchi, M., 2003. Groundwater and pore water inputs to the coastal zone. *Biogeochemistry* 66, 3–33.

Carillo, A., Sannino, G., Artale, V., Ruti, P.M., Calmanti, S., Dell'Aquila, A., 2012. Steric sea level rise over the Mediterranean Sea: present climate and scenario simulations. Clim. Dyn. 39 (9–10), 2167–2184.

Carter, G.T., Flanagan, J.P., Jones, C.R., Marchant, F.L., Murhinson, R.R., et al., 1972. A new bathymetric chart and physiography of the Mediterranean Sea, p. 1-23, In: The Mediterranean Sea: a Natural Sedimentation Laboratory. Stanley, D.J. Stroudsburg, Pennsylvania: Dowden, Hutchinson & Ross.

Castellari, S., N. Pinardi, and K. Leaman, 1998. A model study of air–sea interactions in the Mediterranean Sea. *J. Mar. Syst.,* 18, 89–114.

Cavendish M., 2010. World and Its Peoples.

Chahine, M. T., 1992. The hydrological cycle and its influence on climate. *Nature,*359,373–380.

Christensen, J.H., Hewitson, B., Busuioc, A., Chen, A., Gao, X., Held, I., Jones, R., Kolli, R.K., Kwon, W.T., Laprise, R., Magaρa Rueda, V., Mearns, L., Menιndez, C.G., Risnen, J., Rinke, A., Sarr, A., Whetton, P., 2007. Regional climate projections. Climate Change 2007: The Physical Science Basis. In: Solomon, S., Qin, D., Manning, M., Chen, Z., Marquis, M., Averyt, K.B., Tignor, M., Miller, H.L. (Eds.), Contribution of Working Group I to the Fourth Assessment Report of the Intergovernmental Panel on Climate Change. Cambridge University Press, Cambridge, United Kingdom.

Compo GP, Whitaker JS, Sardeshmukh PD, Matsui N, Allan RJ, Yin X, Gleason Jr BE, Vose RS, Rutledge G, Bessemoulin P, Br¨onnimann S, Brunet M, Crouthamel RI, Grant AN, Groisman PY, Jones PD, Kruk MC, Kruger AC, Marshall GJ, Maugeri M, Mok HY, Nordli Ø, Ross TF, Trigo RM, Wang XL, Woodruff SD, Worley SJ, 2011. The 20th Century Reanalysis Project. *Q. J. R. Meteorol. Soc.* 137: 1–28.

Cruzado, A., 1985. Chemistry of Mediterranean Waters. Editor: Pergamon Press.

Cullen, H. M.; A. Kaplan; et al., 2002. Impact of the North Atlantic Oscillation on Middle Eastern climate and streamflow. Climatic Change. 55 (3): 315–338.

Dee D. P., Uppala S. M., J. Simmons A., Berrisford P., Poli P., S. Kobayashi, U. Andrae, M. A. Balmaseda, G. Balsamo, P. Bauer, P. Bechtolda A. C. M. Beljaars, L. van de Berg, J. Bidlot, N. Bormann, C. Delsol, R. Dragani, M. Fuentes, A. J. Geer, L. Haimberger, S. B. Healy, H. Hersbach, E. V. Holm, L. Isaksen, P. K°allberg, M. Kohler, M. Matricardi, A. P. McNally, B. M. Monge-Sanz, J.-J. Morcrette, B.-K. Park, C. Peubey, P. de Rosnay, C. Tavolato, J.-N. Thepaut and F. Vitart, 2011. The ERA-Interim reanalysis: configuration and performance of the data assimilation system.

Dai, Trenberth, and T. Qian, 2004. A global data set of Palmer Drought Severity Index for 1870–2002: Relationship with soil moisture and effects of surface warming. *J. Hydrometeor.,* 5, 1117–1130.

Delgado, J., Garcia-Lafuente, j., Vargas, M.J., 2001. A simple model for submaximal exchange through the Strait of Gibraltar. Sci. Mar. 65 (4), 313—322.

Dubois, C., Somot, S., Calmanti, S., Carillo, A., Déqué, M., Dell' Aquilla, A., Elizalde, A., Gualdi, S., Jacob, D., L'Hévéder, B., Li, L., Oddo, P., Sannino, G., Scoccimarro, E., Sevault, F., 2012. Future projections of the surface heat and water budgets of the Mediterranean Sea in an ensemble of coupled atmosphere-ocean regional climate models. Clim.Dyn. 39, 1859—1884.

Dünkeloh, A., Jacobeit, J., 2003. Circulation dynamics of Mediterranean precipitation variability 1948–98. Int. J. Climatol. 23, 1843–1866.

Eshel, G., and B. F. Farrel, 2000. Mechanisms of Eastern Mediterranean rainfall variability. *J. Atmos. Sci.,* 57, 3219–3232.

Fasullo, J., and D. Z. Sun, 2001. Radiative sensitivity to water vapor under all-sky conditions. *J. Climate,* 14, 2798–2807.

Ferguson, B. K., 1996. Estimation of Direct Runoff in the Thornthwaite Water Balance, The Professional Geographer, 48:3, 263-271.

Ferguson, B. K., 1992. Landscape hydrology, a component of landscape ecology. Journal of Environmental Systems, 2 l(3), 193-205.

Fleury, P., Bakalowicz, M. and de Marsily, G., 2007. Submarine springs and coastal karst aquifers: A review. *Journal of Hydrology* 339, 79–92.

Fleury, P., 2005. Sources sous-marines et aquiferes karstiques cττiers Mediterraneens. Fonctionnement et caracterisation. Ph.D. thesis, Universite Pierre et Marie Curie, Paris.

Furlani, S., Pappalardo, M., Gómez-Pujol, L., Chelli, A., 2014. The rock coast of the Mediterranean and Black seas: Geological Society, London, Memoirs, 40(1), 89-123.

García Lafuente, J., Delgado, J., Criado, F., 2002. Inflow interruption by meteorological forcing in the Strait of Gibraltar. Geophys. Res. Lett. 29 (19), 1914.

Garcva-Ruiz, J. M., Lopez-Moreno, J. I., Vicente-Serrano, S. M., Lasanta–Martvnez, T. & Beguerva, S., 2011. Mediterranean water resources in a global change scenario. *Earth-Science Reviews* 105, 121–139.

Garzoli, S. and Maillard, C., 1979. Winter circulation in the Sicily and Sardinia straits region. *Deep-Sea Research* 26A: 933–54.

Gascard, J. C. and Richez, C., 1985. Water mass and circulation in the western Alboran Sea and in the Strait of Gibraltar. *Progress in Oceanography* 15: 157–216.

Geiger, R., 1961. Überarbeitete Neuausgabe von Geiger, R.: Köppen-Geiger / Klima der Erde. (Wandkarte 1:16 Mill.)– KlettPerthes, Gotha– KlettPerthes, Gotha.

Gibelin A. L. and Deque M., 2003. Anthropogenic climate change over the Mediterranean region simulated by a global variable resolution model *Climate Dynamics.* 20 237–339.

Gilli, E., 2015. Deep speleological salt contamination in Mediterranean karst aquifers: perspectives for water supply. Environmental Earth Sciences 74, 101–113.

Gilman, C., and C. Garrett, 1994. Heat flux parametrizations for the Mediterranean Sea: The role of atmospheric aerosols and constraints from the water budget. *J. Geophys. Res.,* 99 (C3), 5119– 5134.

Giorgi, F., Lionello, P., 2008. Climate change projections for the Mediterranean region. Global and planetary change, 63(2-3), 90-104.

Giorgi, F. 2006. Climate change hot-spots. *Geophysical research letters,* 33 L08707.

Gordon, N., 2012. Connecting Earth's water cycle to climate change. *Atmos News*.

Gualdi, S., Somot, S., Li, L., Artale, V., Adani, M., Bellucci, A., Braun, A., Calmanti, S., Carillo, A. & Dell'aquila, A. 2013. The CIRCE simulations: regional climate change projections with

realistic representation of the Mediterranean Sea. *Bulletin of the American Meteorological Society,* 94**,** 65-81.

Gualdi, S., Somot, S., May, W., Castellari, S., Déqué, M., Adani, M., Artale, V., Bellucci, A., Breitgand, J.S., Carillo, A., Cornes, R., Dell'Aquila, A., Dubois, C., Efthymiadis, D., Elizalde, A., Gimeno, L., Goodess, C.M., Harzallah, A., Krichak, S.O., Kuglitsch, F.G., Leckebusch, G.C., L'Heveder, B., Li, L., Lionello, P., Luterbacher, J., Mariotti, A., Navarra, A., Nieto, R., Nissen, K.M., Oddo, P., Ruti, P., Sanna, A., Sannino, G., Scoccimarro, E., Sevault, F., Struglia, M.V., Toreti, A., Ulbrich, U., Xoplaki, E., 2013. Future climate projections. In: Navarra, A., Tubiana, L. (Eds.), Regional Assessment of Climate Change in the Mediterranean, Vol. 1. Springer, Dordrecht, The Netherlands, pp. 53–118.

Harzallah, A., D. L. Cadet, and M. Crepon, 1993. Possible forcing effects of net evaporation, atmospheric pressure and transients on water transports in the Mediterranean Sea. *J. Geophys. Res.,* 98 (C7), 12 341–12 350.

Hecht, M. W., W. Holland, V. Artale, and N. Pinardi, 1997. North Atlantic model sensitivity to Mediterranean waters. *Assessing Climate Change, Results from the Model Evaluation Consortium for Climate Assessment,* W. Howe and A. Henderson-Sellers, Eds., Gordon and Breach Science, 169–191.

Hersbach H., Dee D., 2016. ERA5 reanalysis is in production. *ECMWF Newsletter No. 147, page 7 – Spring 2016*.

Hill, P.S., Fox, J. M., Crockett, J. S., Curran, K. J., Friedrichs, et al., 2007. Sediment delivery to the seabed on continental margins, Continental Margin Sedimentation: From Sediment Transport to Sequence Stratigraphy, p. 49-99, In: Continental Margin Sedimentation: Transport to Sequence, Nittrouer C.A., Austin, J.A., Jr., Field, M.E., Kravitz, J.H., Syvitski, J.P.M., Wiberg, P.L. (Eds), IAS Special Publication 37, Blackwell Publishing Ltd, Oxford.

Houghton, J. T., Y. Ding, D. J. Griggs, M. Noguer, P. J. van der Linden, X. Dai, K. Maskell, and C. A. Johnson, Eds., 2001. *Climate Change 2001: The Scientific Basis*. Cambridge University Press, 881 pp.

Hurrell, 1996. Influence of variations in extratropical wintertime teleconnections on Northern Hemisphere temperature. *Geophys. Res. Lett.,* 23, 665–668.

Hurrell, J. W., 1995. Decadal trends in the North Atlantic Oscillation: Regional temperatures and precipitation. *Science,* 269 (5224): 676–679.

IPCC, 2007. *Climate Change 2007: The Physical Science Basis. Contribution of Working Group I to the Fourth Assessment Report of the Intergovernmental Panel on Climate Change* (Cambridge: Cambridge University Press) p 996.

IUCN, 2008. How Does Climate Change Affect The Water Cycle? *ScienceDaily*.

Jaoshvilli, Sh., 2002. The rivers of the Black Sea, European Environmental Agency, Techn. report no. 71.

Johnson, R. G., 1997. Climate control requires a dam at the Strait of Gibraltar. *Eos, Trans. Amer. Geophys. Union,* 78, 277–281.

Jordà, G., Von Schuckmann, Josey, 2017. The Mediterranean Sea heat and mass budgets: Estimates, uncertainties and perspectives. *Progress in Oceanography* 156, 174–208.

Jordà, G., Gomis, D., 2013. On the interpretation of the steric and mass componentsof sea level variability: the case of the Mediterranean basin. J. Geophys. Res. Oceans 118.

Jordà, G., Gomis, D., Marcos, M., 2012. Comment on ‘‘Storm surge frequency reduction in Venice under climate change” by Troccoli et al. Clim. Change 113 (3), 1081–1087.

Kalnay, E., Kanamitsu M, Kirtler R, Collins W, Deaven D, Gandin L, IredellM, SahaS,WhiteG,WoollenJ, ZhuY,ChelliahM,EbisuzakiW, Higgins W, Janowiak J, Mo KC, Ropelewski C, Wang J, Leetma A, Reynolds R, Jenne R, Joseph D. 1996. The NCEP/NCAR 40-year reanalysis project. *Bull. Amer. Meteorol. Soc.* 77: 437–471.

Karl, T. R., and K. E. Trenberth, 2003. Modern global climate change. *Science,* 302, 1719–723.

Kiehl, J. T., and K. E. Trenberth, 1997. Earth’s annual global mean energy budget. *Bull. Amer. Meteor. Soc.,* 78, 197–208.

Knippertz, P., Ulbrich, U., Marques, F., Corte-Real, J., 2003. Decadal changes in the link El Niño, NAO and European/north African rainfall. Int. J. Climatol. 23, 1293–1311.

Konovalov, s.k., Murray, J.W., Luther III, G.W., 2005. Black Sea Biogeochemistry. Oceanography, 18(2), 24-35.

Köppen, W., 1900. Versuch einer klassifikation der klimate, vorzugsweise nach ihren beziehungen zur pflanzenwelt. Geogr. Z. 6, 593–611. 657–679.

Korotaev, G., 2003. Seasonal, interannual, and mesoscale variability of the Black Sea upper layer circulation derived from altimeter data. Journal of Geophysical Research. 108.

Krahmann, G. and Schott, F. 1998. Longterm increases in western Mediteranean salinities and temperatures: a mixture of anthropogenic and climate sources. *Geophysical Research Letters,* 25**,** 4209-4212.

LaMoreaux, P. E., Tanner, Judy T., 2001. Geologic/Hydrogeologic Setting and Classification of Springs. Springs and Bottled Waters of the World: Ancient History, Source, Occurrence, Quality and Use. Springer. p. 57. ISBN 978-3-540-61841-6.

Lamy, F., Arz, H. W., Bond, G. C., Barh, A. and Pätzold, J., 2006. Multicentennial scale hydrological changes in the Black Sea and northern Red Sea during the Holocene and the Arctic/North Atlantic Oscillation.

Li Laurent Z. X., 2006. Atmospheric GCM response to an idealized anomaly of the Mediterranean sea surface temperature.

Lionello, P. & Scarascia, 2017 L. Linking the Mediterranean regional and the global climate change. EGU General Assembly Conference Abstracts, 2017. 3954.

Lionello P., Abrantes F., Congedi L., Dulac F., Gacic M., Gomis D., Goodess C., Hoff H., Kutiel H., Luterbacher Jürg, Planton S., Reale M., Schröder K., Struglia M. V., Toreti A., Tsimplis M., Ulbrich U., Xoplaki E., 2012. Introduction: Mediterranean Climate-Background Information.

Lionello, P., Galati, M.B., 2008. Links of the significant wave height distribution in the Mediterranean Sea with the north hemisphere teleconnection patterns. Adv. Geo. 17, 13-18.

Lionello, P., Malanotte-Rizzoli, P., Boscolo, R., Alpert, P., Artale, V., Li, L., et al., 2006a. The Mediterranean climate: an overview of the main characteristics and issues. Dev. Earth Environ. Sci. 4 (C), 1–26.

Ludwig, W., Bouwman, A. F., Dumont, E. and Lespinas, F., 2010. Water and nutrient fluxes from major Mediterranean and Black Sea rivers: Past and future trends and their implications for the basin-scale budgets. *Global Biogeochemical Cycles* 24, 1–14.

Ludwig W., Dumont E., Meybeck M., Heussner S., 2009. River discharges of water and nutrients to the Mediterranean and Black Sea: Major drivers for ecosystem changes during past and future decades. Progress in Oceanography, 80, 199–217.

Ludwig, W., Meybeck, M., Abousamra, F., 2003. Riverine transport of water, sediments, and pollutants to the Mediterranean Sea. UNEP MAP Technical report Series 141, UNEP/MAP Athens, 111 p.

Macias, D.M., Garcia-Gorriz, E., Stips, A., 2015. Productivity changes in the Mediterranean Sea for the twenty-first century in response to changes in the regional atmospheric forcing. Front. Mar. Sci. 2, 79. fmars.2015.00079.

Malanotte-Rizzoli, P., Manca, B., d'Alcala, M., Theocharis, A., Brenner, S., Budillon, G., Ozsoy, E., 1999. The Eastern Mediterranean in the 80s and in the 90s: the big transition in the intermediate and deep circulations. Dyn. Atmos. Oceans 29 (2—4), 365—395.

Malanotte-Rizzoli, P. and Bergamasco, A., 1989. The circulation of the eastern Mediterranean, Part I. *Oceanologica Acta* 12: 335–51.

Malanotte-Rizzoli, P. and Hecht, A., 1988. Large-scale properties of the eastern Mediterranean: a review. *Oceanologica Acta* 11: 323–35.

Margat, J., 2008. L'eau des Méditerranéens. Situation et Perspectives; L'Harmattan: Paris, France.

Margat, J., Treyer, S., 2004. L'eau des Mediterranens: situation et perspectives. MAP Technical Report Series No. 158, 366 p.

Mariotti, A., Pan, Y., Zeng, N., Alessandri, A., 2015. Long-term climate change in the Mediterranean region in the midst of decadal variability. Clim. Dyn.

Mariotti, A. 2010. Recent changes in the Mediterranean water cycle: a pathway toward long-term regional hydroclimatic change? *Journal of Climate,* 23**,** 1513-1525.

Mariotti A., Zeng N., Yoon Jin-Ho, Artale V., Navarra A., Alpert P. and Li Laurent Z X, 2008. Mediterranean water cycle changes: transition to drier 21st century conditions in observations and CMIP3 simulations.

Mariotti, A., Struglia, M. V., Zeng, N. & Lau, K. 2002. The hydrological cycle in the Mediterranean region and implications for the water budget of the Mediterranean Sea. *Journal of climate,* 15**,** 1674-1690.

Mariotti, A., Zeng, N., Lau, K.M., 2002a. Euro-Mediterranean rainfall and ENSO—a seasonally varying relationship. Geophys. Res. Lett. 29, 1621.

Mather J. R., 1978. The Chaotic Water Balance in Environmental Analysis, Lexington: Lexington Books.

McClusky, S.; S. Balassanian; et al., 2000. "Global Positioning System constraints on plate kinematics and dynamics in the eastern Mediterranean and Caucasus". Journal of Geophysical Research. 105 (B3): 5695–5719.

McKenzie, DP., 1970. "Plate tectonics of the Mediterranean region". Nature. 226 (5242): 239–43. Bibcode: 1970 Natur.226..239M.

Menemenlis, D., Fukumori, I., Lee, T., 2007. Atlantic to Mediterra-nean Sea level difference driven by winds near Gibraltar Strait. J. Phys. Oceanogr. 37 (2), 359—376.

Mertens, C., Schott, F., 1997. Interannual variability of deep-water formation in the northwestern Mediterranean. J. Phys. Oceanogr. 28, 1410—1424.

Milly, P.C.D., Dunne, K.A., Vecchia, A.V., 2005. Global Pattern of trends in streamflow water availability in a changing climate. Nature 438, 347–350.

Molcard, A., Gervasio, L., Griffa, A., Gasparini, G., Mortier, L., Özgökmen, T., 2002. Numerical investigation of the Sicily Channel dynamics: density currents and water mass advection. J. Mar. Syst. 36, 219—238.

Moore Willard S., 2009. The Effect of Submarine Groundwater Discharge on the Ocean.

Murray J. W., H. W. Jannasch, S. Honjo, R. F. Anderson, W. S. Reeburgh, Z. Top, G. E. Friederich, L. A. Codispoti, E. Izdar , 1989. Unexpected changes in the oxic/anoxic interface in the Black Sea.

New, M.G., Hulme, M., Jones, P.D., 2000. Representing twentieth century space time climate fields. Part II: development of a 1901–1996 mean monthly terrestrial climatology. J. Clim. 13, 2217–2238.

Nikishin, A, 2003. The Black Sea basin: tectonic history and Neogene–Quaternary rapid subsidence modelling". Sedimentary Geology. 156: 149–168.

NOAA, 2013. Hydrological Cycle (evaporation and precipitation) Impacts. *Global Warming*.

Norrant, C., Douguıdroit, A., 2005. Monthly and daily precipitation trends in the Mediterranean (1950–2000). Theoretical and Applied Climatology 20.

Onogi K., Tsutsui J., Koide H., Sakamoto M., Kobayashi S., Hatsushika H., Matsumoto T., Yamazaki N., Kamahori H., Takahashi K., Kadokura S., Wada K., Kato K., Oyama R., Ose T., Mannoji N., Taira R. 2007. The JRA-25 Reanalysis. *J. Meteor. Soc. Japan* 85: 369–432.

Ozay M. 1999. Water Balances In The Eastern Mediterranean: Summary Of A Workshop No. 18,

Ozsoy, E. and U. Unluata, 1997. Oceanography of the Black Sea: A review of some recent results. Earth-Science Reviews. 42 (4): 231–272.

Panin, N., 2007. The Black Sea Coastal Zone: Present-day state and threats arising from global change and from regional variability. Rapport Communicacion international Mer Méditerranee, Instabul 2007, 38, 21-22.

Peixoto, J. P., M. De Almeida, R. D. Rosen, and D. A. Salstein, 1982. Atmospheric moisture transport and the water balance of the Mediterranean Sea. *Water Resour. Res.,* 18, 83–90.

Pierini, S., Rubino, A., 2001. Modeling the oceanic circulation in the area of the Strait of Sicily: the remotely forced dynamics. J. Phys. Oceanogr. 31, 1397—1412.

Pinardi, N. and Masetti, E., 2000. Variability of the large scale general circulation of the Mediterranean Sea from observations and modelling: a review. *Palaeogeography, Palaeoclimatology, Palaeoecology* 158: 153–73.

PNUE/PAM/PLAN BLEU, 2004. L'eau des Méditerranéens: situation et perspectives. No. 158 de la Série des rapports techniques du PAM, PNUE/PAM, Athènes.

Poulos, S. E., 2019. River systems and their water and sediment fluxes towards the marine regions of the Mediterranean Sea and Black Sea earth system. An overview. *Mediterranean Marine Science*, 549-565.

Poulos, S. E., & Collins, M. B. (2002). Fluviatile sediment fluxes to the Mediterranean Sea: a quantitative approach and the influence of dams. *Geological Society, London, Special Publications*, *191*(1), 227-245.

Rasmusson, E. M., 1968. Atmospheric water vapor transport and the water balance of North America. Part II: Large-scale water balance investigation. *Mon. Wea. Rev.,* 96, 720–739.

Reale, O., and J. Shukla, 2000. Modeling the effects of vegetation on Mediterranean climate during the Roman classical period: Part II. Model simulation. *Global Planet. Change,* 25, 185–214.

Reid, J. L., 1979. On the contribution of the Mediterranean Sea outflow to the Norwegian–Greenland Sea. *Deep-Sea Res.,* 26, 1199– 1223.

Rekacewicz, 2001. Socio-economic indicators for the countries of the Black Sea basin. UNEP/GRID-Arendal Maps and Graphics Library.

Richard, G., 2010. Undersea river discovered flowing on sea bed.

Rienecker M.M., Suarez M.J., Gelaro R., Todling R., Bacmeister J, Liu E, Bosilovich MG, Schubert S.D., Takacs L, Kim G-K, Bloom S, Chen J, Collins D, Conaty A, da Silva A, Gu W, Joiner J., Koster RD., Lucchesi R, Molod A, Owens T, Pawson S, Pegion P, Redder CR, ReichleR, Robertson FR, Ruddick AG, Sienkiewicz M., Woollen J. 2011. MERRA – NASA's Modern-Era Retrospective Analysis for Research and Applications. *J. Climate*.

Roads, J. O., S. C. Chen, A. K. Guetter, and K. P. Georgakakos, 1994. Large-scale aspects of the United States hydrologic cycle. *Bull. Amer. Meteor. Soc.,* 75, 1589–1610.

Robinson A. R., Leslie W. G., Theocharis A., Lascaratos A., 2001. Mediterranean Sea Circulation.

Rodellas, V., Garcia-Orellana, J., Masque, P., Feldman, M. & Weinstein, Y., 2015. Submarine groundwater discharge as a major source of nutrients to the Mediterranean Sea. Proceedings of the National Academy of Sciences 112, 3926–3930.

Rodo, X., E. Baert, and F. A. Comin, 1997. Variations in seasonal rainfall in southern Europe during present century: Relationships with the North Atlantic Oscillation and the El Nin˜o Southern Oscillation. *Climate Dyn.,* 13, 275–284.

Rohling, E. & Bryden, H. L. 1992. Man-induced salinity and temperature increases in western Mediterranean deep water. *Journal of Geophysical Research: Oceans,* 97**,** 11191-11198.

Romanou, A. *et al*., 2010. Evaporation–Precipitation Variability over the Mediterranean and the Black Seas from Satellite and Reanalysis Estimates. *Journal of Climate* 23, 5268–5287.

Rowell D. P., 2003. The Impact of Mediterranean SSTs on the Sahelian Rainfall Season.

Saha S, Moorthi S, Pan H-L, Wu X, Wang J, Nadiga S, Tripp P, Kistler R, Woollen J, Behringer D, Liu H, Stokes D, Grumbine R, Gayno G, Hou Y-T, Chuang H-Y, JuangH-MH, Sela J, Iredell M, Treadon R, Kleist D, vanDelst P, Keyser D, Derber J, Ek M, Meng J, WeiH, YangR, Lord S, van den Dool H, Kumar A, Wang W, Long C, Chelliah M, Xue Y, Huang B, Schemm J-K, Ebisuzaki W, Lin R, Xie P, Chen M, Zhou S, Higgins W, Zou C-Z, Liu Q, Chen Y, Han Y, Cucurull L, Reynolds RW, Rutledge G, Goldberg M., 2010. The NCEP Climate Forecast System Reanalysis. *Bull. Amer.Meteorol. Soc.* 91: 1015–1057.

Salat, J., Font, J., 1987. Water mass structure near and offshore the Catalan coast during winters of 1982 and 1983. Ann. Geophys. 5B (1), 49—54.

Sánchez Román, A., Sannino, G., García Lafuente, J., Carillo, A., Criado Aldeanueva, F., 2009. Transport estimates at the western section of the Strait of Gibraltar: a combined experimental and numerical modeling study. J. Geophys. Res.: Oceans 114 (C6), C06002.

Sarigu, A. & Montaldo, N. A new eco-hydrological distributed model for the predictions of the climate change impact on water resources of Mediterranean water-limited basins: the Mulargia basin case study in Sardinia. EGU General Assembly Conference Abstracts, 2017. 9208.

Schanze, J. J., Schmitt, R. W. & Yu, L. 2010. The global oceanic freshwater cycle: A state-of-the-art quantification. *Journal of Marine Research,* 68**,** 569-595.

Schewe, J. *et al*., 2014. Multimodel assessment of water scarcity under climate change. *Proceedings of the National Academy of Sciences* 111, 3245–3250.

Schlesinger, W. H., 1997. *Biogeochemistry: An Analysis of Global Change*. 2d ed. Academic Press, 588 pp.

Schroeder, K., Josey, S., Herrmann, M., Grignon, L., Gasparini, G. & Bryden, H. 2010. Abrupt warming and salting of the Western Mediterranean Deep Water after 2005: atmospheric forcings and lateral advection. *Journal of Geophysical Research: Oceans,* 115.

Schubert M., Knöller K., Stollberg R., Mallast Ulf, Ruzsa G. and Melikadze G., 2017. Evidence for Submarine Groundwater Discharge into the Black Sea-Investigation of Two Dissimilar Geographical Settings.

Schubert S.D., Rood R, Pfaendtner J. 1993. An assimilated dataset for earth science applications. *Bull. Am. Meteorol. Soc.* 74: 2331–2342.

Shaltout, M., Omstedt, A., 2014. Modelling the water and heat balances of the Mediterranean Sea using a two-basin model and available meteorological, hydrological, and ocean data.

Shaltout, M., Omstedt, A., 2012. Calculating the water and heat balances of the Eastern Mediterranean Basin using ocean model-ling and available meteorological, hydrological and ocean data. Oceanologia 54 (2), 199—232.

Sheffield J. and Wood E. F., 2008. Projected changes in drought occurrence under future global warming from multi-model, multi scenario, IPCC AR4 simulations *Clim. Dyn.* 31 79–105. Shiklomanov I., chapter "World fresh water resources" in Peter H. Gleick (editor), 1993, Water in Crisis: A Guide to the World's Fresh Water Resources.

Shillington, Donna J.; White, Nicky; Minshull, Timothy A.; Edwards, Glyn R.H.; Jones, Stephen M.; Edwards, Rosemary A.; Scott, Caroline L., 2008. "Cenozoic evolution of the eastern Black Sea: A test of depth-dependent stretching models". Earth and Planetary Science Letters. 265 (3–4): 360–378.

Skliris, N., Sofianos, S., Gkanasos, A., Mantziafou, A., Vervatis, V., Axaopoulos, P. & Lascaratos, A. 2012. Decadal scale variability of sea surface temperature in the Mediterranean Sea in relation to atmospheric variability. *Ocean Dynamics,* 62, 13-30.

Skliris, N., Sofianos, S. & Lascaratos, A., 2007. Hydrological changes in the Mediterranean Sea in relation to changes in the freshwater budget: A numerical modelling study. *Journal of Marine Systems* 65, 400–416.

Skoulikidis, N.T., Sabater, S., Datry, T., Morais, M. M., Buffagni, A.,et al., 2017. Non-perennial Mediterranean rivers in Europe: status, pressures, and challenges for research and management. Science of the Total Environment, 577, 1-18.

Smith, K. and Darwall, W., 2006. *The Status and Distribution of Freshwater Fish Endemic to the Mediterranean Basin*., (The World Conservation Union (IUCN), Gland, Switzerland and Cambridge, UK).

Soden, B. J., D. L. Jackson, V. Ramaswamy, D. Schwarzkopf, and X. Huang, 2005. The radiative signature of upper tropospheric moistening. *Science,* 310, 841–844.

Somot, S., Sevault, F., Déqué, M., Crépon, M., 2008. 21st century climate change scenario for the Mediterranean using a coupled atmosphere-ocean regional climate model. Global Planet. Change 63 (2–3), 112–126.

Somot, S., Sevault, F., Déqué, M., 2006. Transient climate change scenario simulation of the Mediterranean Sea for the twenty-first century using a high-resolution ocean circulation model. Clim. Dyn. 27 (7–8), 851–879.

Soto-Navarro, J., Criado-Aldeanueva, F., García-Lafuente, J., Sán-chez-Román, A., 2010. Estimation of the Atlantic inflow through the Strait of Gibraltar from climatological and in situ data. J. Geophys. Res. 115, C10023.

Sparnocchia, S., Picco, P., Manzella, G.M.R., Ribotti, A., Copello, S., Brasey, P., 1995. Intermediate water formation in the Ligurian Sea. Oceanol. Acta 18 (2), 151—162.

Spiteri, C.; Slomp, C.P.; Charette, M.A.; Tuncay, K.; Meile, C., 2008. Flow and nutrient dynamics in a subterranean estuary (Waquoit Bay, MA, USA): Field data and reactive transport modeling. Geochim. Cosmochim. Acta, 72, 3398–3412.

Stansfield, K., Smeed, D.A., Gasparini, G.P., 2002. The path of the overflows from the sills in the Sicily Strait. In: The 2nd Meeting on the Physical Oceanography of Sea Straits, Villefranche, France, 15—19 April 2002, 211—215.

Syvitski, J.P.M., Vorosmarty, C.J., Kettner, A., Green, P., 2005. Impact of humans on the flux of terrestrial sediment to the global coastal ocean. Science, 308, 376–80.

Talley L.D., Pickard G.L., Emery W.J., Swift J.H., 2011. Descriptive Physical Oceanography: An Introduction (Sixth Edition), Elsevier, Boston, 560 pp.

Tanhua T., Hainbucher D., Schroeder K., Cardin V., ´Alvarez M., and Civitarese G., 2013. The Mediterranean Sea system: a review and an introduction to the special issue.

Tarek M., Brissette F. P., Arsenault R., 2019. Evaluation of the ERA5 reanalysis as a potential reference dataset for hydrological modeling over North-America.

Taupier-Letage, Isabelle and Millot Claude, 2010. Recent results and new ideas about the Eurafrican Mediterranean Sea. Outlook on the similarities and differences with the Asian Mediterranean Sea.

Trenberth K. E., Fasullo John T., Mackaro Jessica, 2011. Atmospheric Moisture Transports from Ocean to Land and Global Energy Flows in Reanalyses.

Trenberth, K. E., 2009. An imperative for climate change planning: Tracking Earth's global energy. Curr. Opinion Environ. Sustain., 1, 19–27.

Trenberth K. E., Smith Lesley, Qian Taotao, Dai Aiguo, Fasullo John, 2006. Estimates of the Global Water Budget and Its Annual Cycle Using Observational and Model Data.

Trenberth K. E., and L. Smith, 2005. The mass of the atmosphere: A constraint on global analyses. *J. Climate,* 18, 864–875.

Trenberth K. E., and D. J. Shea, 2005. Relationships between precipitation and surface temperature. *Geophys. Res. Lett.,* 32, L14703.

Trenberth K. E., and D. P. Stepaniak, 2003a. Co-variability of components of poleward atmospheric energy transports on seasonal and interannual timescales. *J. Climate,* 16, 3691–3705.

Trenberth K. E., and Stepaniak, 2003b. Seamless poleward atmospheric energy transports and implications for the Hadley circulation. *J. Climate,* 16, 3706–3722.

Trenberth K. E., 1999. Atmospheric moisture recycling: Role of advection and local evaporation. *J. Climate,* 12, 1368–1381.

Trenberth, K. E., 1998. Atmospheric moisture residence times and cycling: Implications for rainfall rates with climate change. *Climatic Change,* 39, 667–694.

Trigo, R., Xoplaki, E., Zorita, E., Luterbacher, J., Krichak, S.O., Alpert, P., et al., 2006. Chapter 3. Relations between variability in the Mediterranean region and mid-latitude variability. Dev. Earth Environ. Sci. 4 (C), 179–226.

Tsimplis, M.N., Calafat, F.M., Marcos, M., Jordà, G., Gomis, D., Fenoglio-Marc, L., Struglia, M.V., Josey, S.A., Chambers, D.P., 2013. The effect of the NAO on sea level and on mass changes in the Mediterranean Sea. J. Geophys. Res. Oceans 118.

Tsimplis, M.N. and Josey, S.A., 2001. Forcing of the Mediterranean sea by atmospheric oscillation over the north Atlantic. Geophys. Res. Lett. 28, 803—806.

Tsimplis, M.N. and T. F. Baker, 2000. Sea level drop in the Mediterranean Sea: An indicator of deep water salinity and temperature changes? *Geophys. Res. Lett.,* 27, 1731–1734.

Tsimplis, M.N. and Bryden, H.L., 2000. Estimating of the transport through the strait of Gibraltar. Deep Sea Res. 47, 2219—2242.

Türkeş, M., 1996. Spatial and temporal analysis of annual rainfall variations in Turkey". International Journal of Climatology. 16 (9): 1057–1076.

Ulbrich U. *et al.,* 2006. The Mediterranean climate change under global warming *Mediterranean Climate Variability and Predictability* ed P Lionello *et al* (Amsterdam: Elsevier) pp 398–415.

UNEP/MAP, 2012. State of the Mediterranean Marine and Coastal Environment, UNEP/MAP-Barcelona Convention, Athens, 2012, 92 p.

UNEP-MAP RAC/SPA, 2010. The Mediterranean Sea Biodiversity: state of the ecosystems, pressures, impacts and future priorities. In: Bazairi, H., Ben Haj, S., Boero, F., Cebrian, D., De Juan, S., Rais, C. (editors), RAC/SPA, Tunis, 100 p.

UNEP/MAP/MED POL, 2005. Transboundary Diagnostic Analysis (TDA) for the Mediterranean Sea. UNEP/MAP, Athens, 228 p.

UNESCO, 2017. *Wastewater: the untapped resource*, No. 2017 In The United Nations world water development report OCLC: 989085577, ISBN:978-92-3-100201-4 (UNESCO, Paris).

UNESCO, 2004. Submarine groundwater discharge: management implications, measurements and effects. No. 44 in Manuals and guides. OCLC: 249283770, (Paris).

Uppala S.M., Kallberg P.W., Simmons A.J., Andrae U, Da Costa Bechtold V, Fiorino M, Gibson JK., Haseler J., Hernandez A, Kelly GA, Li X, Onogi K, Saarinen S, Sokka N, Allan RP, Andersson E, Arpe K., Balmaseda MA., Beljaars ACM, Van De Berg L, Bidlot J, Bormann N, Caires S, Chevallier F, Dethof A, Dragosavac M, Fisher M, FuentesM, Hagemann S, Holm E, Hoskins BJ, Isaksen L, Janssen PAEM, Jenne R, McNally AP, Mahfouf JF, Morcrette J-J, Rayner NA, Saunders RW, Simon P, Sterl A, Trenberth KE, Untch A, Vasiljevic D, Viterbo P, Woollen J. 2005. The ERA-40 re-analysis. *Q. J. R. Meteorol. Soc.* 131: 2961–3012.

Vargas-Amelin, E. and Pindado, P., 2014. The challenge of climate change in Spain: Water resources, agriculture and land. *Journal of Hydrology* 518, 243–249.

Vella, Andrew P., 1985. "Mediterranean Malta". Hyphen. 4 (5): 469–472.

Verri, G., Pinardi, N., Oddo, P., Ciliberti, S. A. & Coppini, G., 2018. River runoff influences on the central mediterranean overturning circulation. *Climate Dynamics* 50, 1675–1703.

Vörösmarty, C.J., 1997. The storage and aging of continental runoff in large reservoir systems of the world. Ambio, 26, 210-219.

Wang F. and Polcher Jan., 2019. Assessing the freshwater flux from the continents to the Mediterranean Sea.

Ward, M. N., 1998. Diagnosis and short-lead predictions of summer rainfall in tropical North Africa at interannual and multidecadal timescales. *J. Climate,* 11, 3167–3191.

Woodward J., 2009. The Physical Geography of the Mediterranean.

Wust, G., 1961. On the vertical circulation of the Mediterranean Sea, *Journal of Geophysical Research* 66: 3261–71.

Wust, G., 1960. Die tiefenzirkulation des Mittellandischen Meeres in den Kernschichten des Zwischen-und des Tiefenwassers. *Deutsche Hydrographische Zeitschrift* 13: 105–31.

Xoplaki, E., Gonzalez-Rouco, J.F., Luterbacher, J.U., Wanner, H., 2004. Wet season Mediterranean precipitation variability: Influence of large-scale dynamics and trends: Climate dynamics, 23(1), 63-78.

Xoplaki, E., Gonzalez-Rouco, F. J., Luterbacher, J., Wanner, H., 2003. Mediterranean summer air temperature variability and its connection to the large-scale atmospheric circulation and SSTs. Clim. Dyn. 20, 723–739.

Xoplaki, E., 2002. Climate variability over the Mediterranean, Ph.D. Thesis, University of Bern, Switzerland.

Zektser, I. S., Džamalov, R. G. and Everett, L. G., 2007. Submarine groundwater.

Zektser, I. S. and Everett, L. G. (eds), 2004. Groundwater Resources of the World and Their Use. No. 6 in IHP-VI, SERIES ON GROUNDWATER (UNESCO, 7, place de Fontenoy, Paris 07SP).

Zeng, N., 1999. Seasonal cycle and interannual variability in the Amazon hydrologic cycle. *J. Geophys. Res.,* 104 (D8), 9097– 9106.

Zervakis, V., Georgopoulos, D., Drakopoulos, P., 2000. The role of the North Aegean in triggering the recent Eastern Mediterranean climatic changes. J. Geophys. Res. 105 (C11), 26103—26116.

Zika, J. D., Skliris, N., Nurser, A. G., Josey, S. A., Mudryk, L., Laliberté, F. & Marsh, R. 2015. Maintenance and broadening of the ocean's salinity distribution by the water cycle. *Journal of Climate,* 28, 9550-9560.

Žumer, Jože, 2004. "Odkritje podmorskih termalnih izvirov" [Discovery of submarine thermal springs]. Geografski Obzornik (in Slovenian). 51 (2): 11–17. ISSN 0016-7274.

APPENDIX

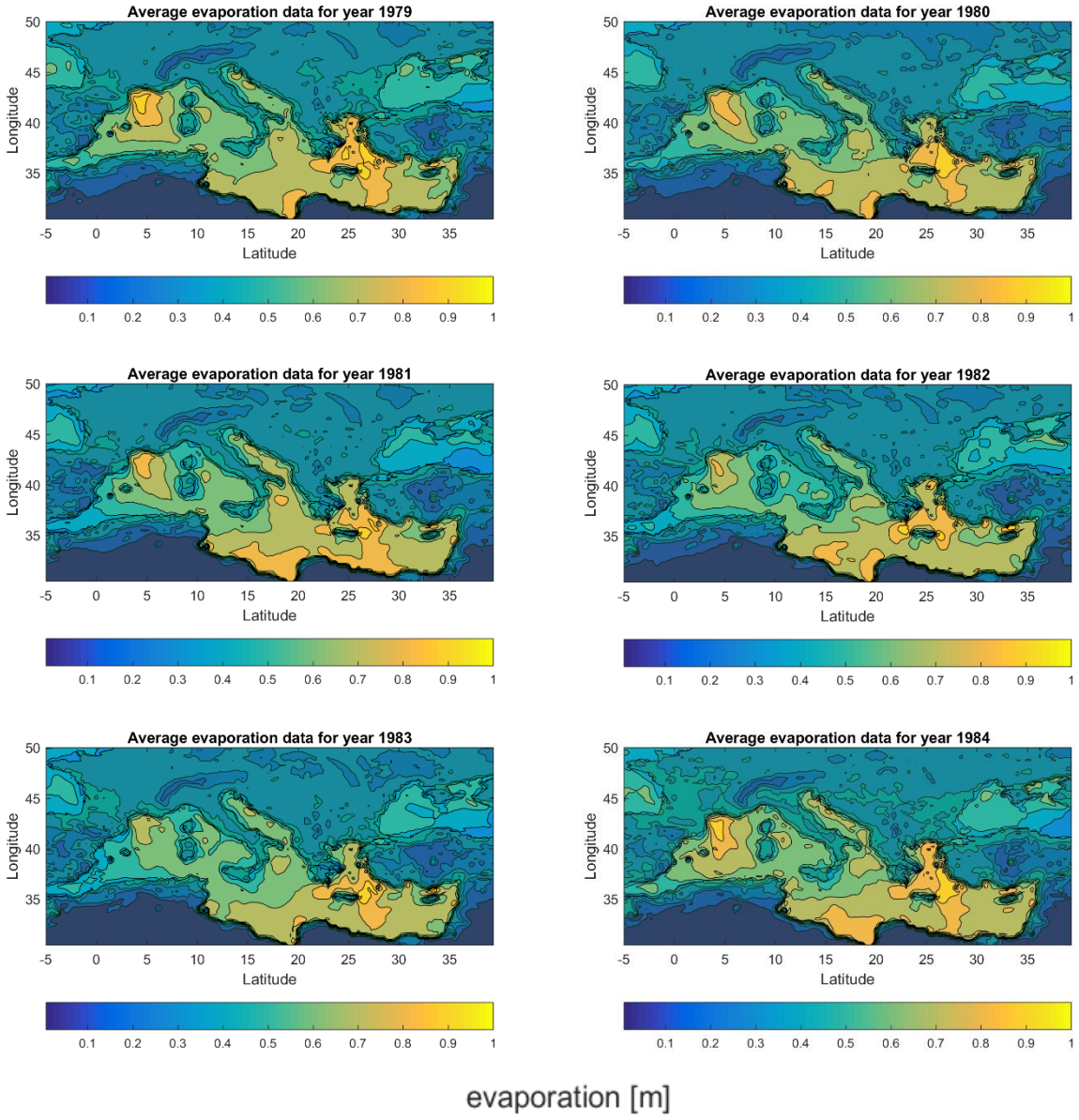

Figure A1. Evaporation in meters (m) per each year from 1979 to 2018.

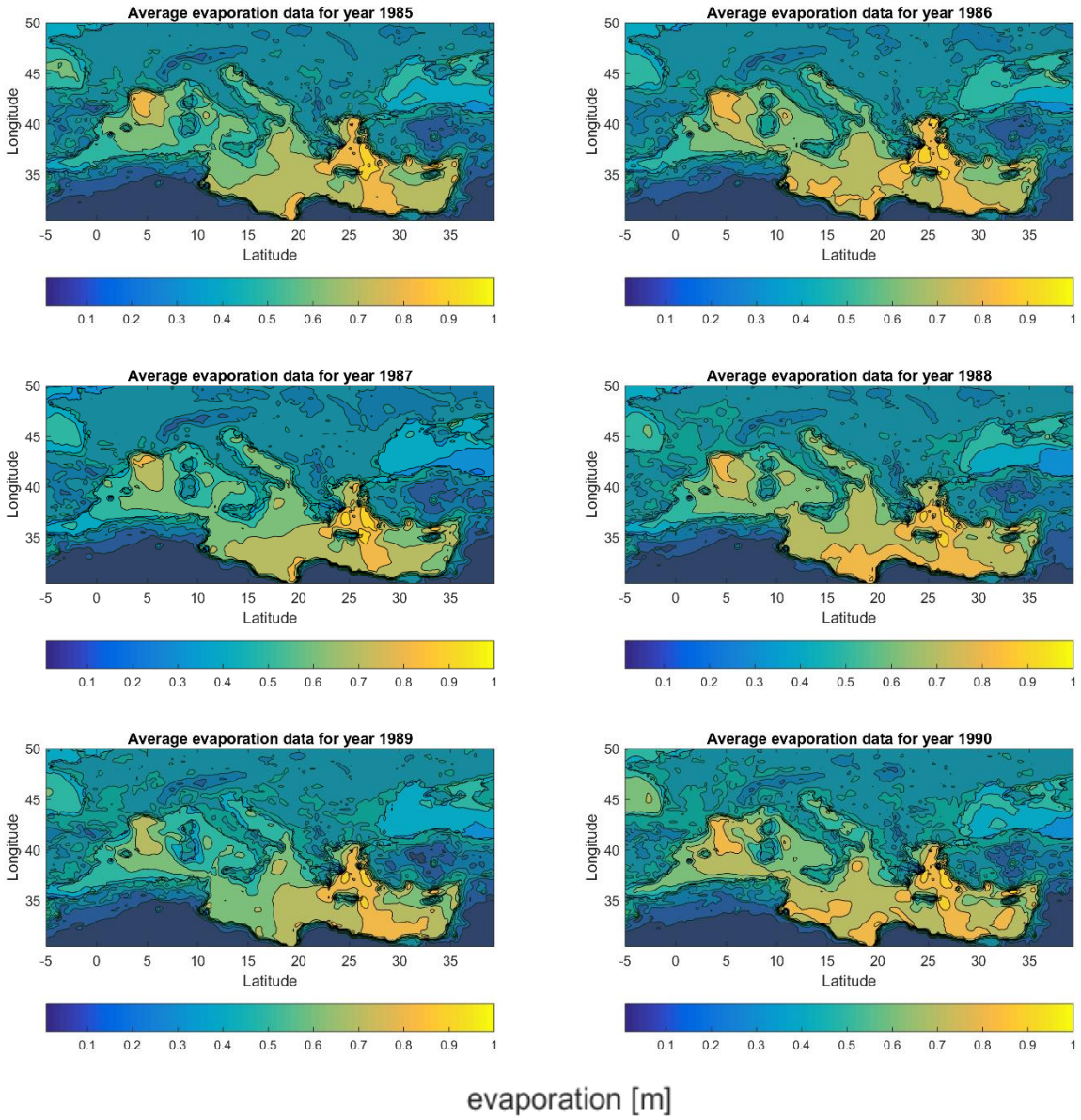

Figure A2. Evaporation in meters (m) per each year from 1979 to 2018.

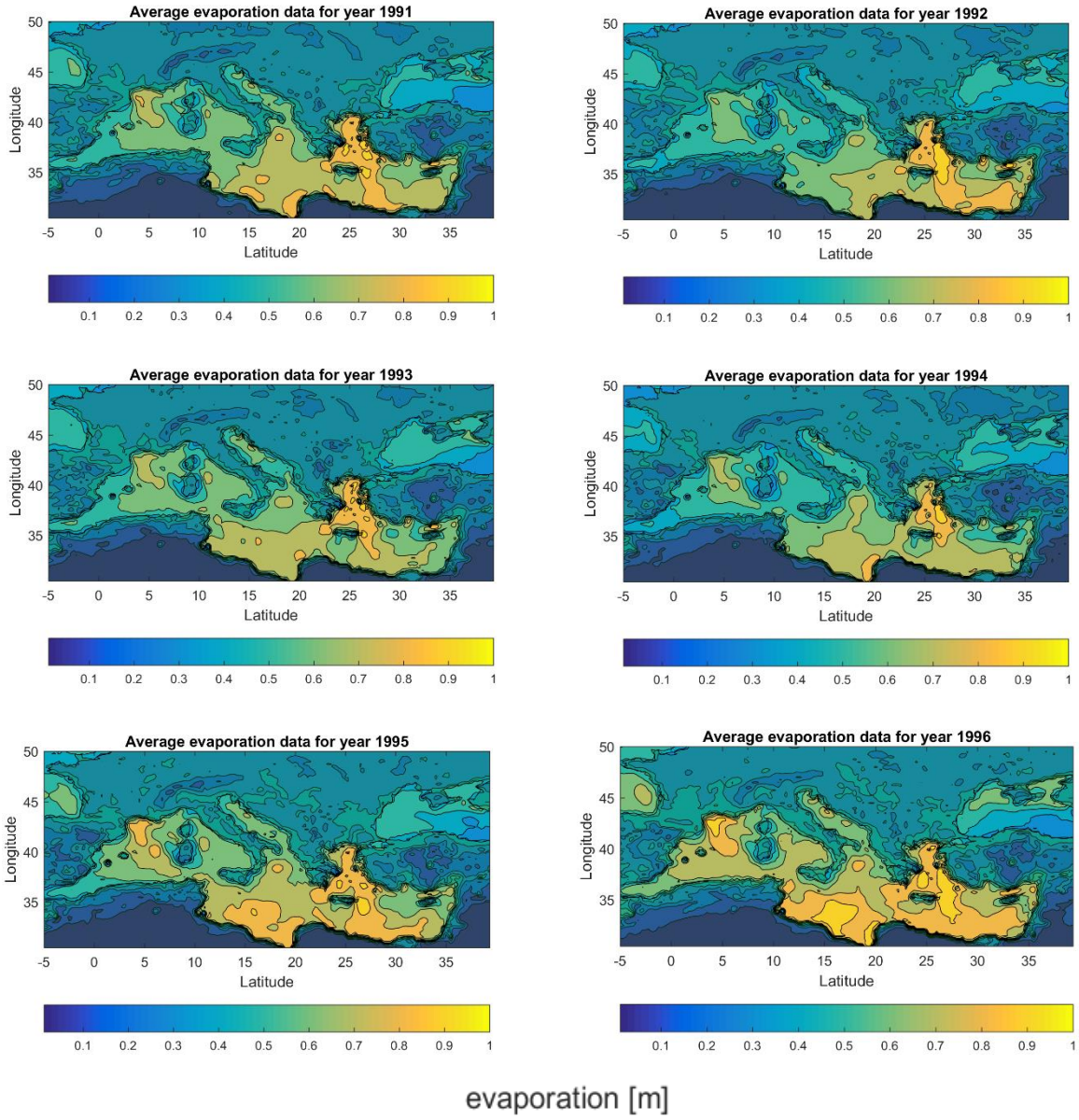

Figure A3. Evaporation in meters (m) per each year from 1979 to 2018.

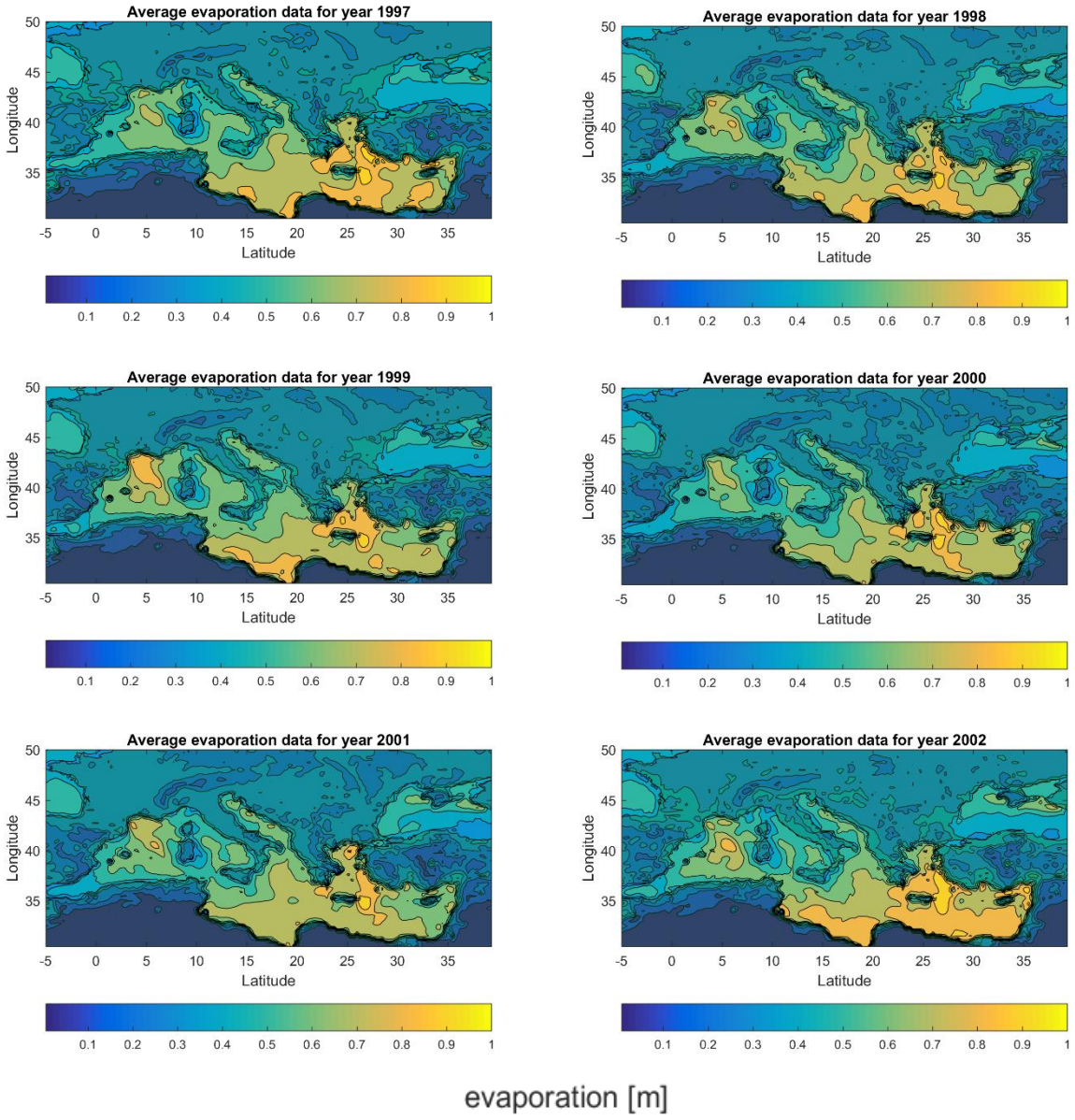

Figure A4. Evaporation in meters (m) per each year from 1979 to 2018.

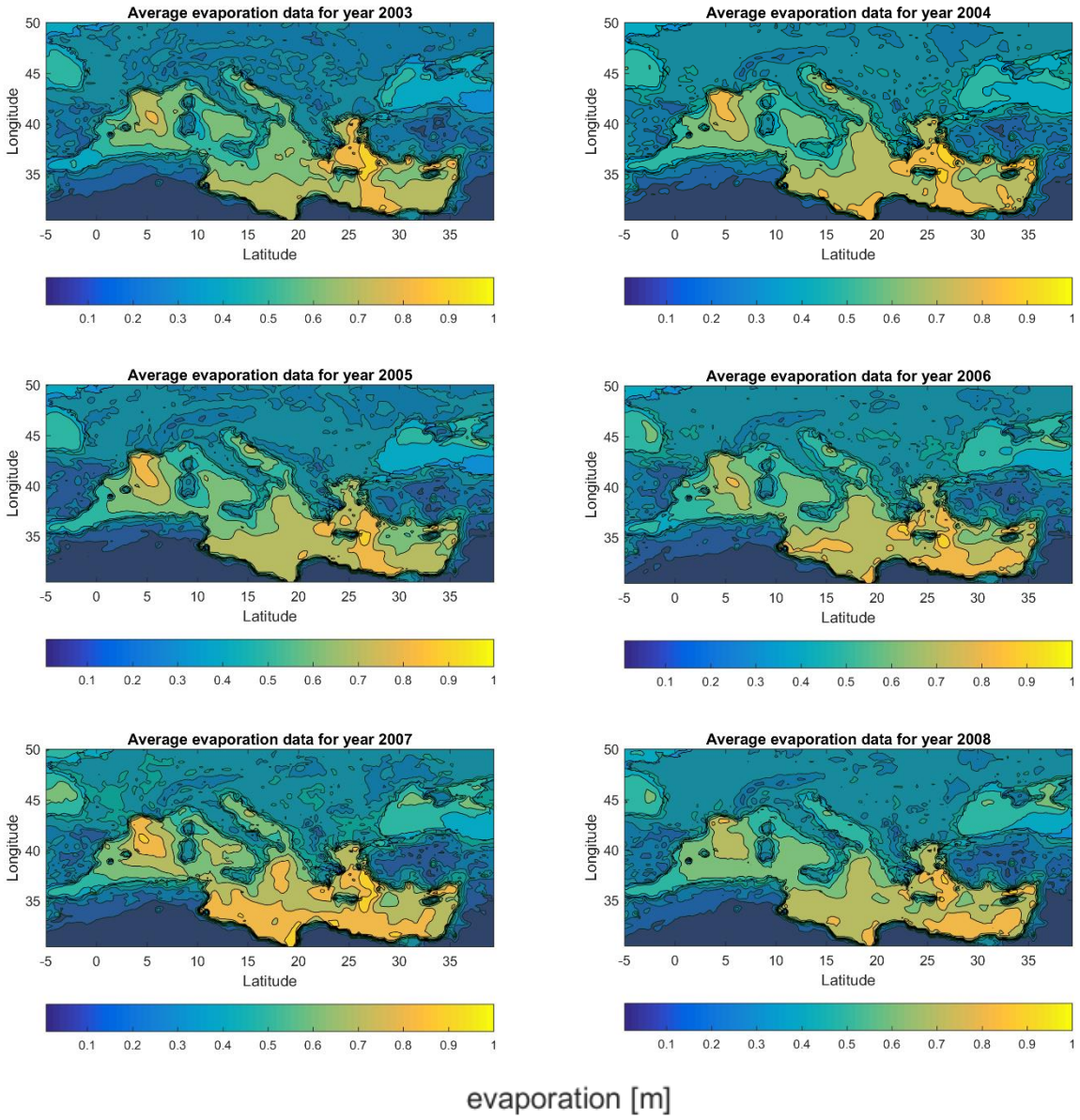

Figure A5. Evaporation in meters (m) per each year from 1979 to 2018.

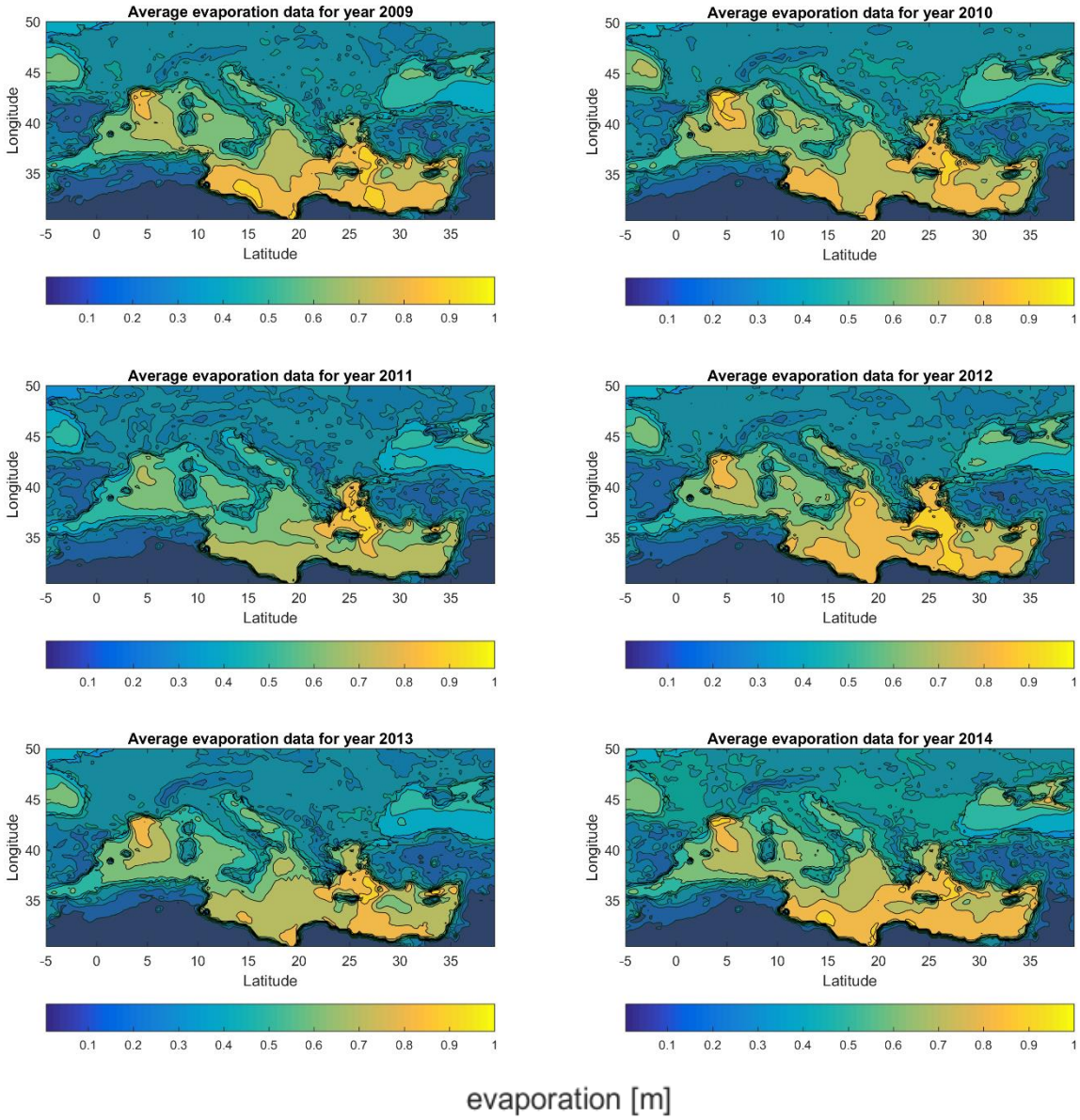

Figure A6. Evaporation in meters (m) per each year from 1979 to 2018.

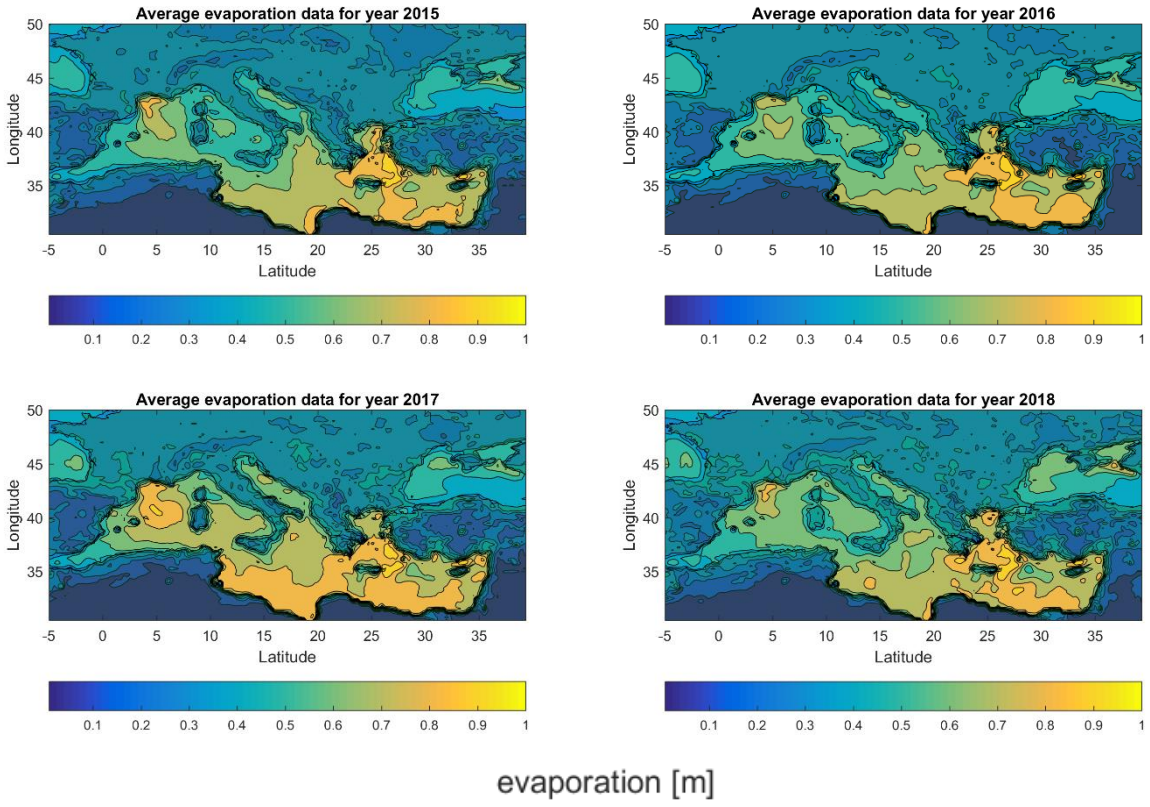

Figure A7. Evaporation in meters (m) per each year from 1979 to 2018.

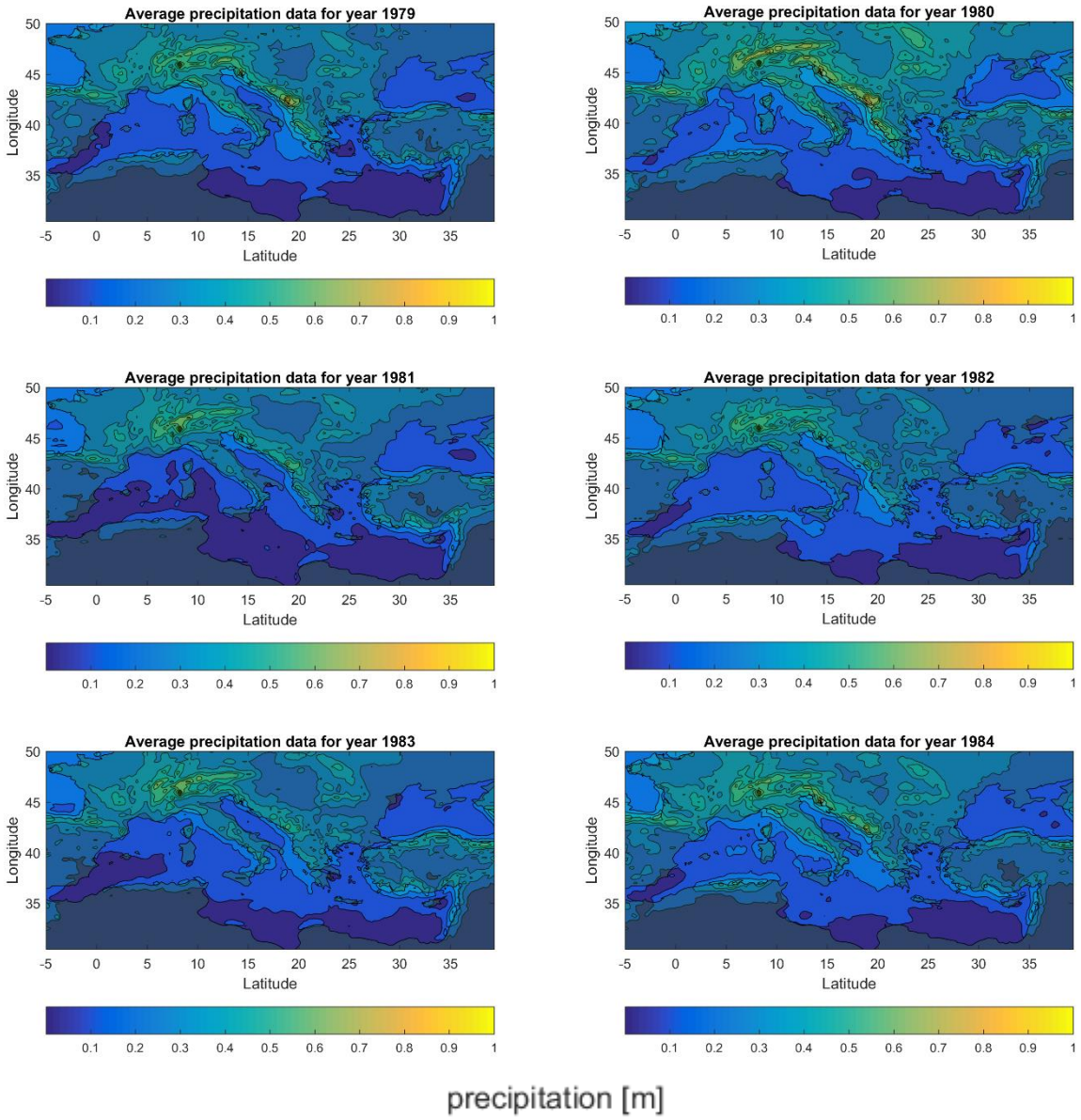

Figure A8. Total Precipitation in meters (m) per each year from 1979 to 2018.

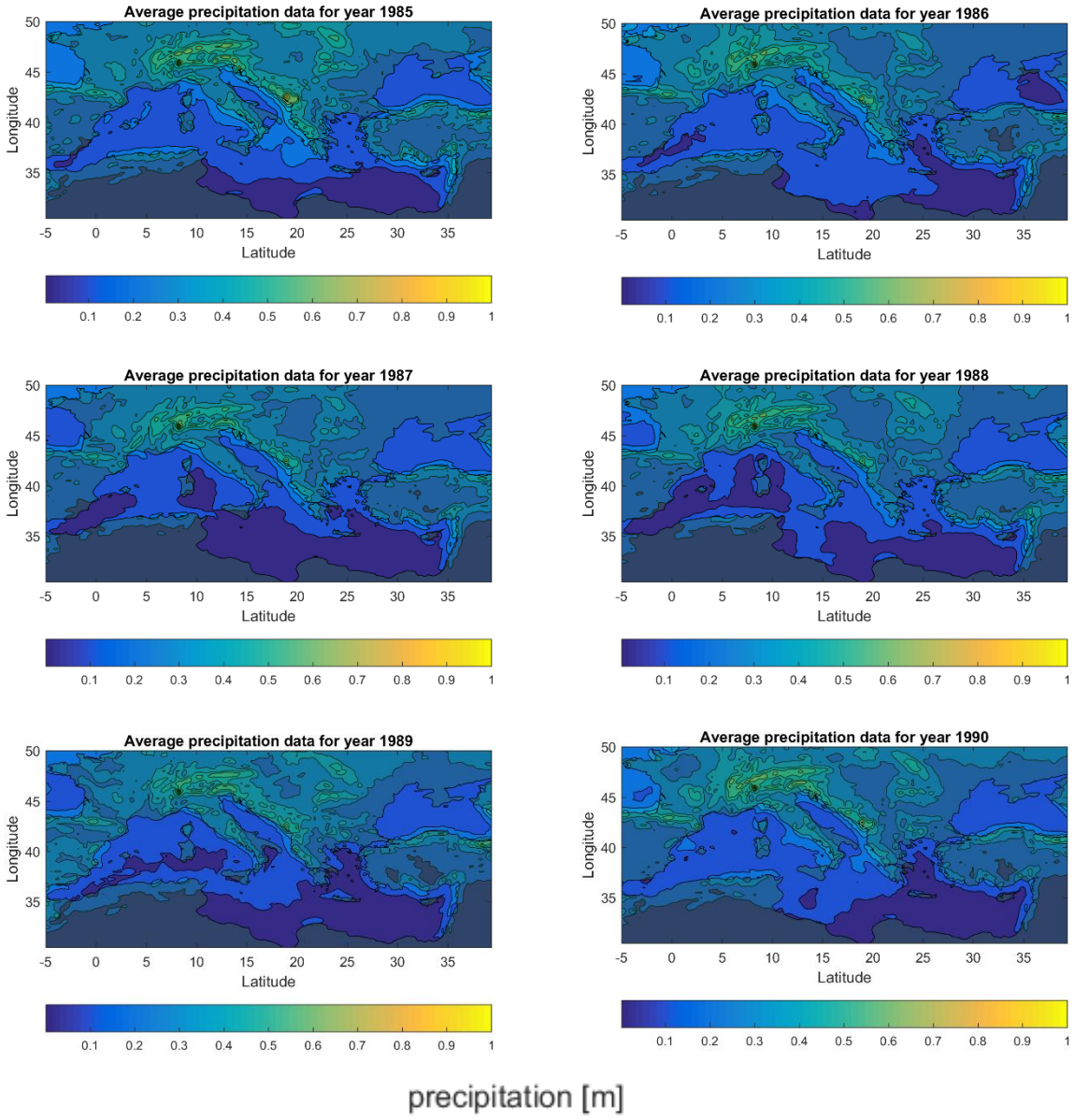

Figure A9. Total Precipitation in meters (m) per each year from 1979 to 2018.

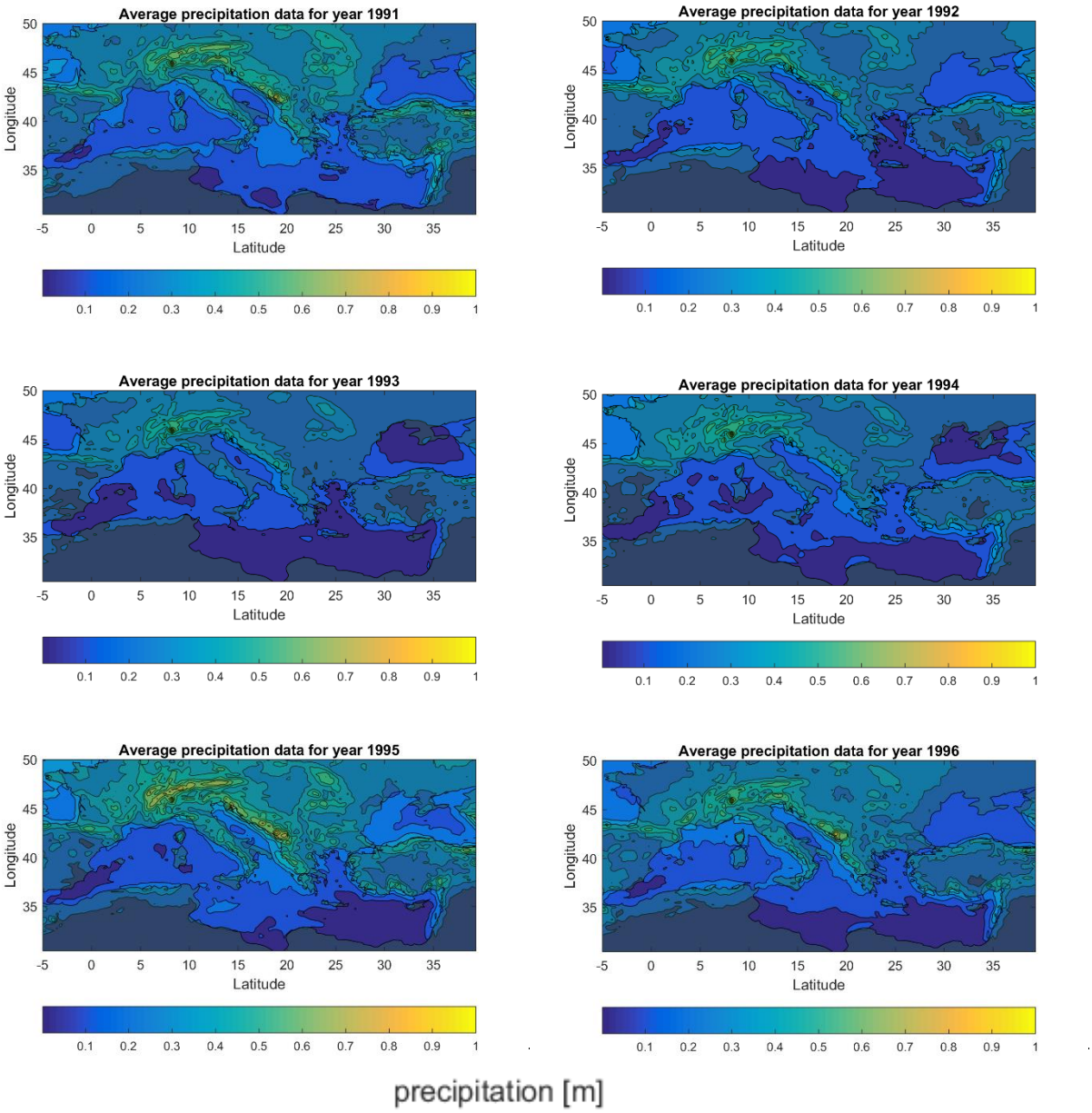

Figure A10. Total Precipitation in meters (m) per each year from 1979 to 2018.

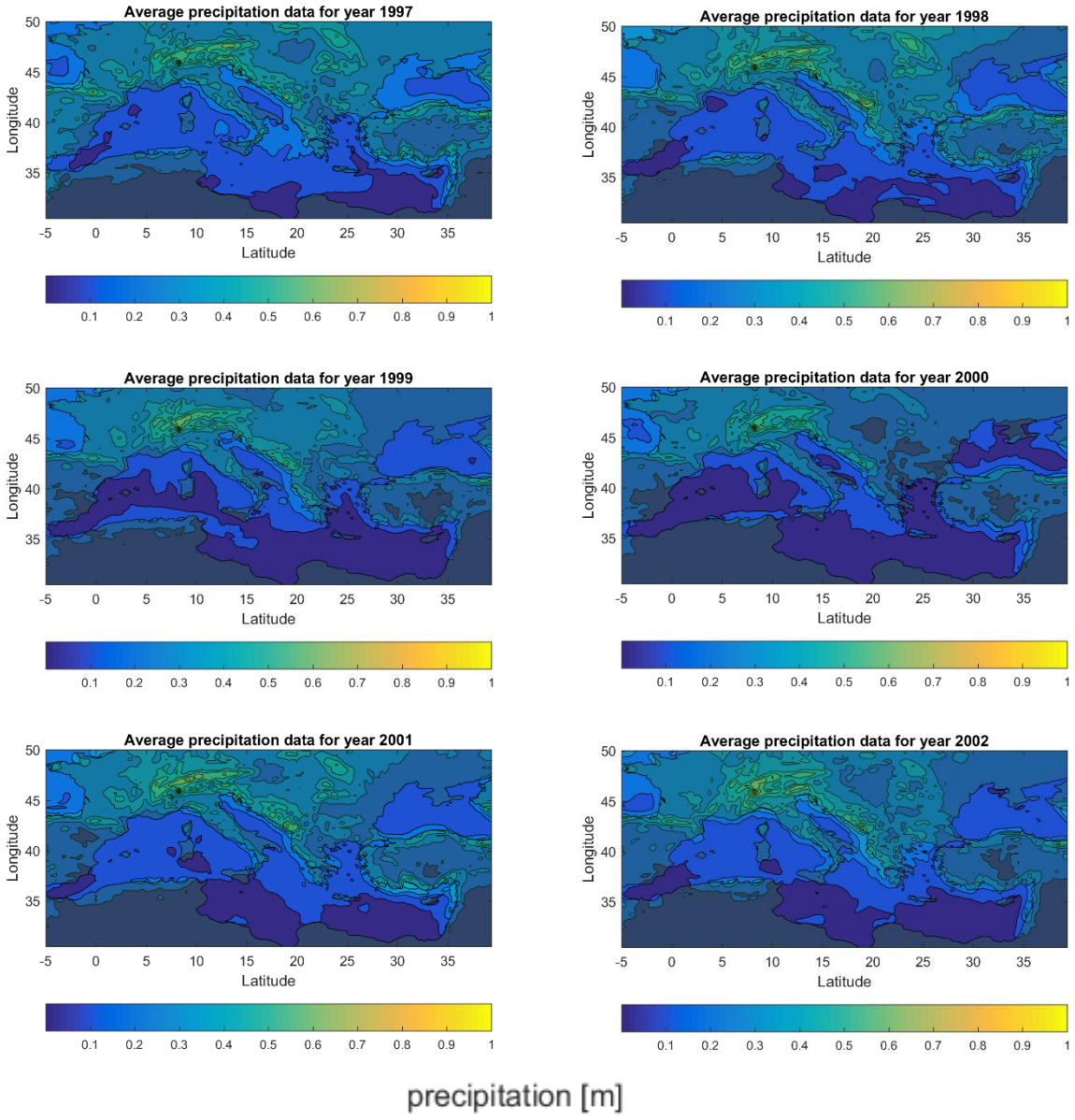

Figure A11. Total Precipitation in meters (m) per each year from 1979 to 2018.

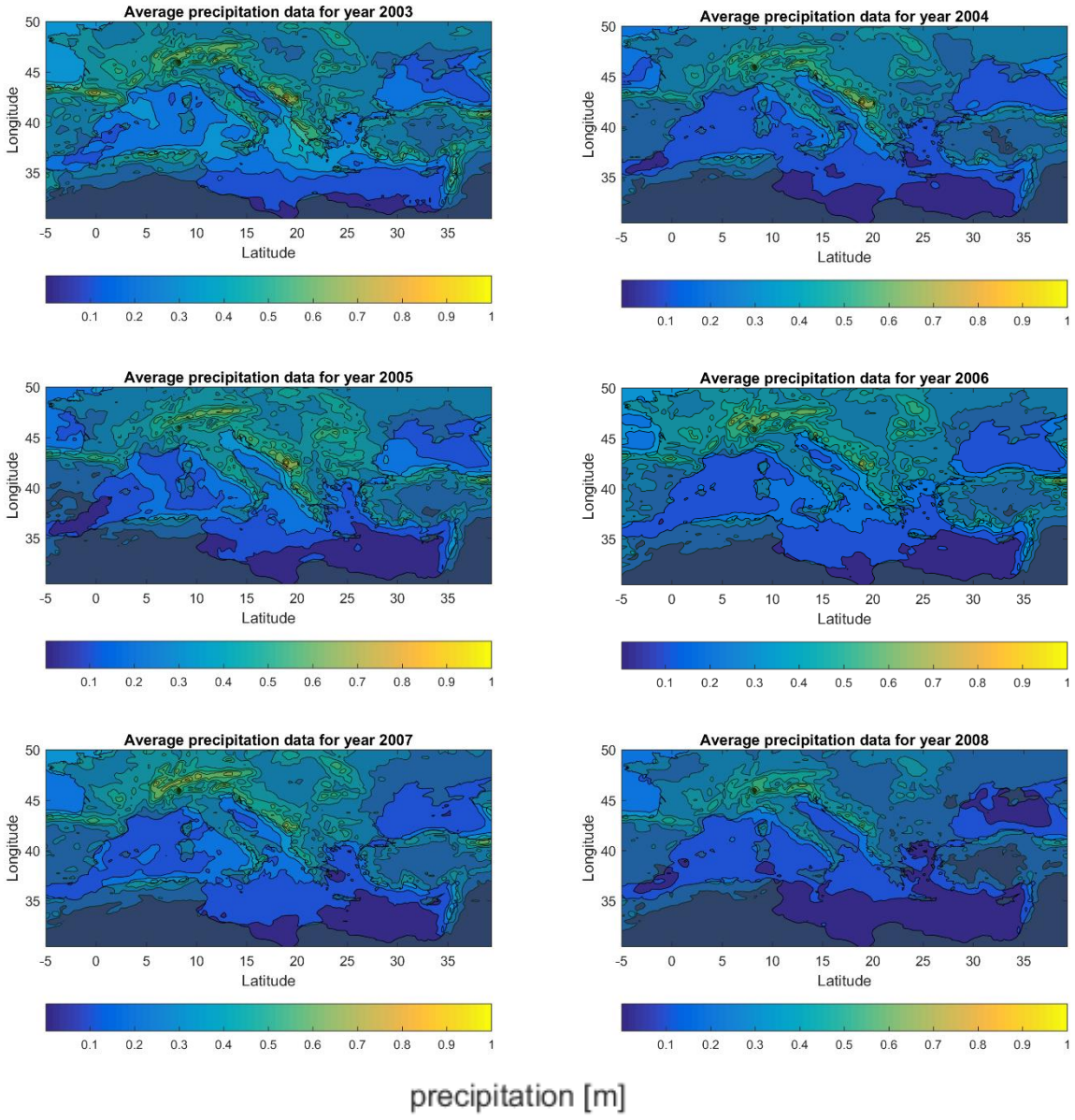

Figure A12. Total Precipitation in meters (m) per each year from 1979 to 2018.

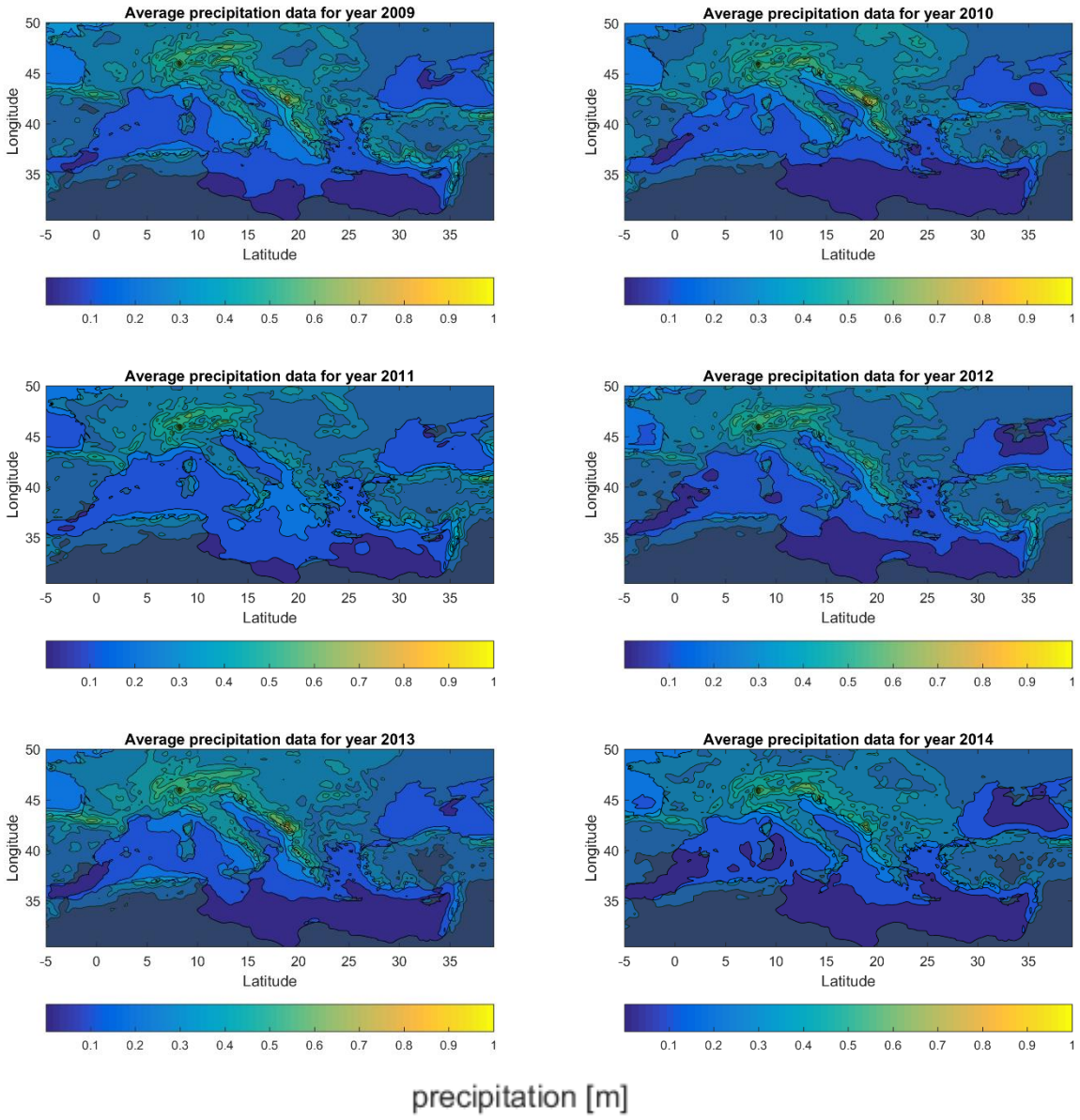

Figure A13. Total Precipitation in meters (m) per each year from 1979 to 2018.

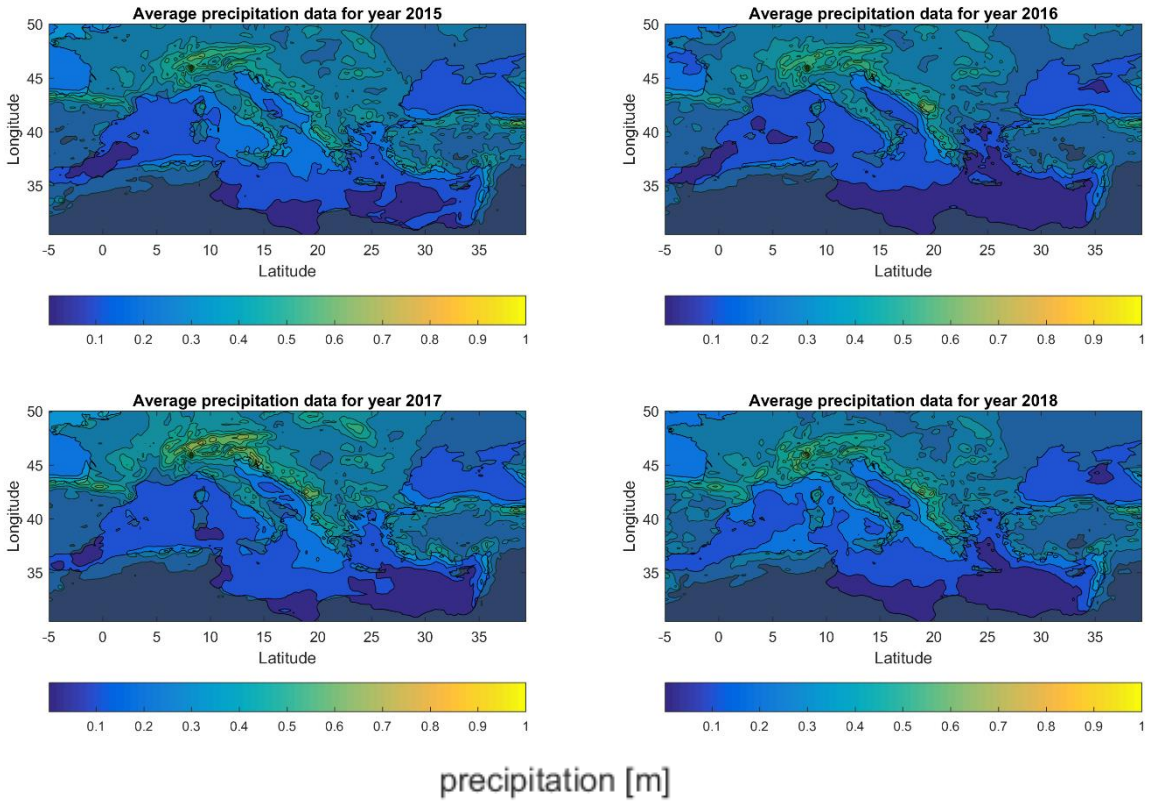

Figure A14. Total Precipitation in meters (m) per each year from 1979 to 2018.

Table A1. Mean annual values of water discharge (RD) in km^3 for rivers with catchment areas (CA) >250 km^2 for the watersheds of the MBS marine regions (from Poulos 2019 and references herein).

River (country)	CA	RD
ALB		
Guadiaro (ES)	1,500	0.3
Guadalhorce (ES)	3,200	0.2
Guadalfeo (ES)	1,300	0.02
Adra Adria (ES)	750	0.03
Andarax (ES)	2,200	0.01
Tafna (DZ)	8,800	0.28
Moulouya (MA)	51,000	1.6
Kerte (MA)	3,100	0.25
Nekor (MA)	790	0.9
WEST_N		
Jucar (Xïquer) (ES)	22,084	4.5
Turia (ES)	6,400	0.46
Mijares (ES)	4,028	0.2
Ebro (ES)	85,835	50
Llobregat (ES)	5,200	0.69
Besos (ES)	1,000	0.13
Ter (ES)	3,000	0.84
Fluvia (ES)	1,124	0.31
Tet (FR)	1,600	0.3
Orb (FR)	1,800	1.3
Aude (FR)	5,900	1.31
Herault (FR)	2,900	1.5
Rhone (FR)	96,000	54
Argens (FR)	2,600	0.6
Var (FR)	2,800	1.3
Coghinas (IT, Sar)	2,551	0.6
Magra (IT)	1,200	1.3
Arno (IT)	8,183	3.2
WEST_S		
Segura (ES)	19,525	3.1
Tirso (IT-Sar)	3,375	0.14
Miliane (TN)	2,000	0.02
Medherda (TN)	22,000	0.94
B. Namoussa (DZ)	570	0.15
Seybousse (DZ)	5,500	0.43
Kebir O. (DZ)	1,100	0.23
Saf-Saf (DZ)	300	0.07
Agriun (DZ)	660	0.17

Soummam (DZ)	8,500	0.79
Sebau (DZ)	2,500	0.51
Isser (DZ)	4,200	0.36
El Harrach (DZ)	390	0.13
Mazafran (DZ)	1,900	0.44
Cheliff (DZ)	44,000	1.3

TYR

Ombrone (IT)	3,200	0.79
Tevere (Tiber) (IT)	17,000	7.4
Liri (Gorigliano) (IT)	5,000	3.15
Volturno (IT)	5,500	3.1
Sele (IT)	3,400	2.84
Flumendosa (IT)	1,775	0.69
Cixerri (IT)	500	0.63

CEN

Gela (IT, Sic)	569	0.02
PlatanI (IT, Sic)	1,785	0.24

ION

Alcantara (IT, Sic)	573	0.08
Simeto (IT, Sic)	4,186	0.8
Agri (IT)	278	0.25
Basento (IT)	1,400	0.11
radano (IT)	2,743	0.2
Thiamis (Kalamas) (GR)	1,899	1.22
Louros (GR)	931	0.38
Arachthos (Arakhthos) (GR)	2,443	2.25/1.22
Acheloos (Akheloos) (GR)	5,688	7.78/5.67
Evinos (GR)	1,070	1.47
Mornos (GR)	1,010	1.13
Selinountas (GR)	245	0.01
Pinios Pel. (GR)	913	0.51
Alfios (Alpheios) (GR)	3,501	1.71/1.21
Evrotas (GR)	1,738	0.76

ADR

Ofanto (IT)	2,716	0.37
Fortore (IT)	1,126	0.42
Biferno (IT)	1,290	0.66
Trigno (IT)	1,200	0.1
Sangro (IT)	1,900	1.42
Pescara (IT)	3,300	1.7
Tavo (IT)	250	0.06

Tronto (IT)	1,200	0.5
Tenna (IT)	490	
Aso (IT)	280	
Tena (IT)	490	
Chienti (IT)	1,300	0.3
Potenza (IT)	770	0.2
Misa (IT)	380	0.2
Esino (IT)	1,200	0.35
Musona (IT)	1,200	0.35
Metauro (IT)	1,045	0.43
Foglia (IT)	700	0.25
Marrechia (IT)	357	0.31
Savio (IT)	597	0.33
Lamone (IT)	710	0.28
Reno (IT)	3,410	0.9
Po (IT)	54,290	46
Adige (IT)	17,000	7.3
Brenta (IT)	1,563	2.3
Piave (IT)	4,100	3.2
Tagliamento (IT)	3,600	2.7
Mirna (HR)	500	0.3
Zrmanja (HR)	900	1.39
Krka (HR)	2,200	2.01
Cetina (HR)	1,500	1.31
Neretva (HR)	13,000	12
Buna (AL)	5,200	10.1
Drin (AL)	19,582	21.44
Mati (AL)	2,300	3.4
Ishem (AL)	670	0.66
Erzen (AL)	760	0.57
Shkumbin (AL)	2,444	1.94
Semani (AL)	5,649	3.02
Osum (AL)	2,000	
Vijose (Aoos)(AL)	6,800	5.5

AEG

Asopos (GR)	1,100	0.7
Sperchios (GR)	1,662	1.14/0.4
Pinios –Th (GR)	10,850	3.8/2.4
Aliakmon (GR)	9,455	3.6/2.3
Axios (Vardar) (GR)	24,398	5.3/7.7
Gallikos(GR)	930	0.79
Strymon (GR)	16,816	5.2/2.8
Nestos (Mesta) (GR)	6,213	3.5
Evros (Meric) (GR-TR)	53,025	8.12

Karamenderes (TR)	1,569.4	0.42
Bakir / Bakircay TR)	3,400	0.56
Cediz-Nehri (TR)	18,000	2.3
Kujuk Menderes (TR)	6,900	1.00
Buyukmenderes (TR)	25,000	4.7

MAR

Gonen(TR)	1,451	0.46
Biga(TR)	2,096	0.6
Simav (TR)	23,765	4.55

LEV_N

Dalaman (TR)	4,481	1.52
Eşen (TR)	2,458	1.32
Aksu(TR)	1,579	0.96
Kopru (Köprücay)(TR)	1,974	2.67
Manavgat (TR)	1,300	4.1
Goksu (TR)	10,561	3.9
Lamas (TR)	2,200	0,154
Tarsus (TR)	1,400	0.1
Seyhan (TR)	22,000	8
Efrenk (Muftu) (TR)	480	0.16
Ceyhan(TR)	21,000	7
Asi (Orontes)(TR)	23,000	2.7
Serrachis(CY)	735	0.04
Pediaios(CY)	870	0.024
Gialias(CY)	600	0.018
Kouris(CY)	340	0.02
Diarizos(CY)	280	0.016
Xeros(CY)	255	0.014
Ezousas(CY)	250	0.013
Litani(LB)	2,500	0.125

LEV_S

Qishon (IL)	1,100	0.06
Yarcon (IL)	1,800	0.2
Lachish (IL)	1,000	0.013
Qama (IL)	800	0.04
Besor (IL)	3,700	0.01
Nile (EG)	2,880,000	90

BLA_W

Rezovska (BG)	183.4	0.025
Veleka (BG)	995	0.296
Ropotamo (BG)	248.7	0.037
Khadjiska (BG)	355.8	1.53

Dvoinitsa (BG)	478.8	0.065
Kamchea (BG)	5,358	0.61
Batova (BG)	338.8	0.023
Danube (RO)	817,000	200
Dniester(UA)	72,100	10.2
South Bug(UA)	63,700	2.2
Ingul(UA)	9,700	0.6
Dnieper(UA)	516,300	53
Alma(UA)	633	0.044
Salhir (RU/UA)	3,750	0.063
Kokozka(RU/UA)	840	0.037
Belbek (RU/UA)	270	0.068
Bolamani (TR)	1,063	0.57
Yeshil Irmak (TR)	36,100	5.3
Kizil Irmak (TR)	78,600	5.9
Kure (Inebolu) (TR)	425	0.13
Kojachai (Devrekani) (TR)	2,254	0.22
Filios (TR)	13,100	2.9
Melen cayi (TR)	2,174	1.51
Sakaria (TR)	56,500	5.6
Sarisu deresi (TR)	2,000	0.4

AZOV

Don (RU)	442,500	28
Kuban (RU)	63,500	12.8
Salhir (RU)	3,750	0.63

BLA_E

Pshada(RU)	360	0.31
Vulan(RU)	280	0.2
Shapsukho(RU)	300	0.222
Tuapse(RU)	350	0.404
Ashe(RU)	280	0.39
Psesuapse (RU)	290	0.486
Shakhe(RU)	550	1.161
Sochi(RU)	300	0.508
Mzymta(GE)	885	1.562
Psou(GE)	420	0.606
Bzyb(GE)	1,510	3.79
Aapsta(GE)	250	0.341
Gumista(GE)	580	1.051
Kodori(GE)	2,030	4.17
Mokva(GE)	336	0.571
Galidzga(GE)	483	0.928
Okumi(GE)	265	0.458
Inguri(GE)	4,060	5.207

Khobi(GE)	1,340	1.895
Rioni(GE)	13,400	9.62
Supsa(GE)	1,130	1.581
Natanebi(GE)	657	0.773
Kintrishi(GE)	291	0.527
Chorokhi (Goruh) (GE)	22,100	8.71
Firtina(TR)	1,149	0.9
Iyidere(TR)	1,047	0.895
Deghir menderes(TR)	730	0.377
Kharshit(TR)	3,500	1.1
Melet cayi(TR)	1,024.4	0.34

Country's abbreviation: Albania (AL), Algeria (DZ), Bulgaria (BG), Croatia/Hrvatska (HR), Cyprus (CY), Egypt (EG), France (FR), Georgia (GE), Greece (GR), Israel (IL), Italy (IT), Lebanon (LB), Morocco (MA), Romania (RO), Russian Federation (RU), Spain (ES), Tunisia (TN), Turkey (TR), Ukraine (UA).